SINGLE CHIRALITY THROUGH CRYSTAL GRINDING

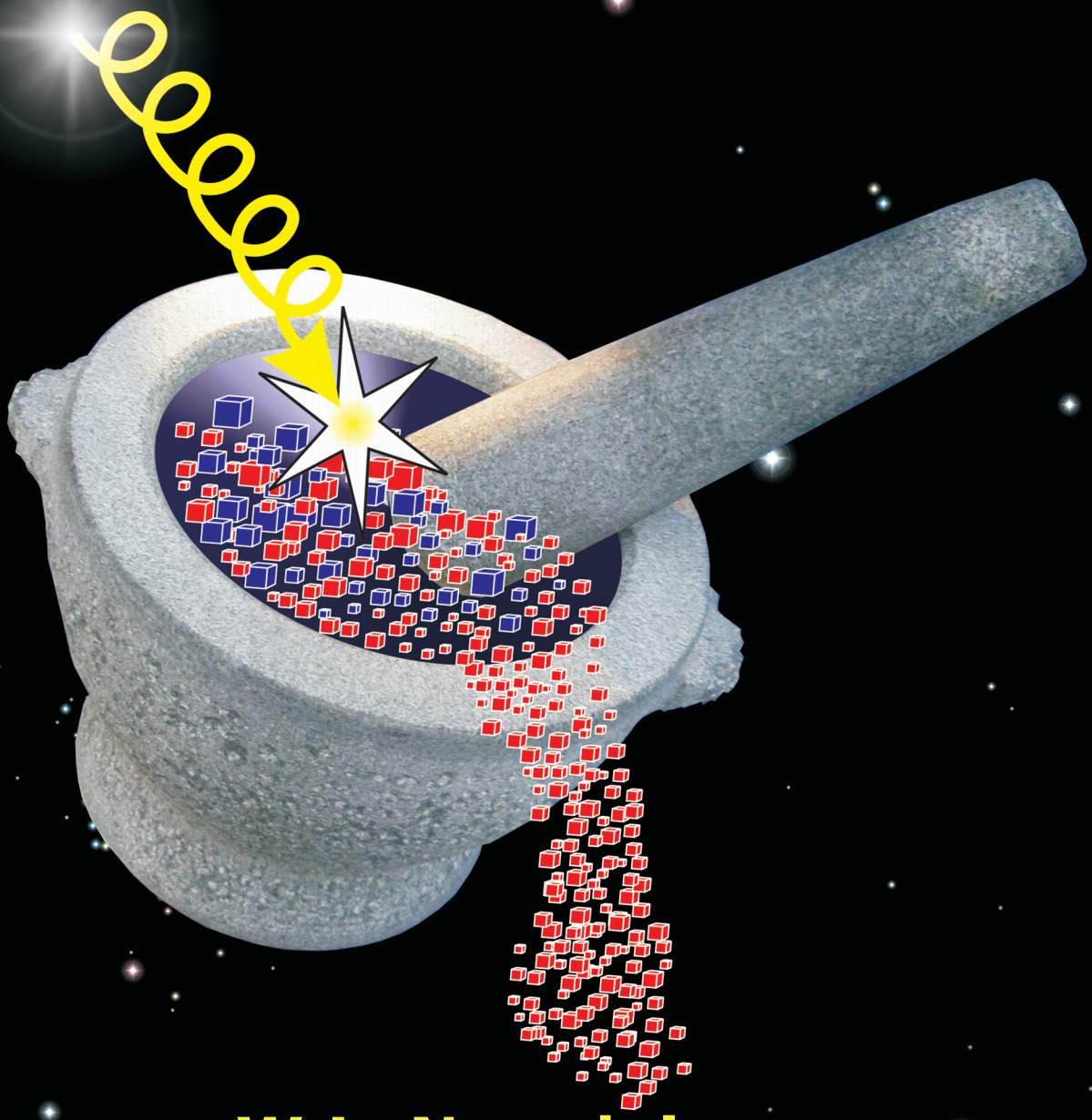

W.L. Noorduin

This research project, named Ultimate Chiral Technology (UCT), was partially financially supported by Samenwerkingsverband Noord-Nederland (Cooperation Northern Netherlands) and the European Fund for Regional Development (EFRO).

ISBN: 978-90-9024812-7

Single Chirality through Crystal Grinding

Een wetenschappelijke proeve op het gebied van de
Natuurwetenschappen, Wiskunde en Informatica

Proefschrift

ter verkrijging van de graad van doctor
aan de Radboud Universiteit Nijmegen,
op gezag van rector magnificus
prof. mr. S.C.J.J. Kortmann,
volgens besluit van het College van Decanen
in het openbaar te verdedigen op
woensdag 13 januari 2010
om 15.30 uur precies

door

Willem Lieuwe Noorduin

geboren op 31 december 1980
te Amersfoort

Promotor:
Prof. dr. E. Vlieg

Copromotores:
Dr. H. Meekes
Dr. W.J.P. van Enckevort

Manuscriptcommissie:
Prof. dr. R.J.M. Nolte
Prof. dr. F.P.J.T. Rutjes
Dr. C. Viedma (Universidad Complutense, Madrid, Spanje)

Contents

Chapter 1

Introduction to Chirality and Crystallization

1.1 Chirality

Our two hands are mirror images, implying that they cannot be superimposed on each other by pure rotations or translations. This property is called *chirality* from the Greek word for hand "chier" (χειρ). Chirality also plays an important role in chemistry. In 1874 Van 't Hoff and Le Bel independently postulated the tetrahedral arrangement of groups around a saturated carbon atom.[1] When four different groups are attached to a carbon atom, the molecule is chiral as it can not be superimposed on its mirror image (Figure 1.1). The two molecules of such a chiral pair are called *enantiomers*.

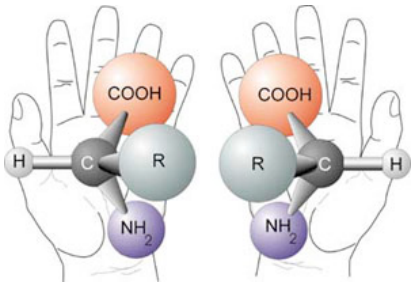

Figure 1.1. Schematic representation of the two enantiomers of a chiral molecule.

Synthesis of chiral molecules from achiral substrates in the absence of directing chiral agents results in the formation of equal amounts of both enantiomers (a so-called *racemic mixture,* or *racemate*). Interestingly, molecules that form the building blocks of life such as amino acids and sugars only exist as a single enantiomer. This raises the fundamental question how these molecules were directed to this asymmetry in the evolution of biological systems. In the artificial synthesis experiments of Miller, for example, only racemates of amino acids were formed.[2]

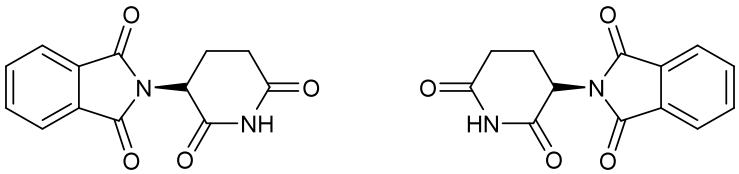

Figure 1.2. Structure of the enantiomers of the pharmaceutical compound thalidomide. The (*S*) enantiomer causes severe birth defects whereas the (*R*) enantiomer is an effective tranquilizer and painkiller.

The asymmetry in nature has vital implications for the interaction of chiral substances in living objects. Just like your right hand only fits in a right glove, the activity of the two enantiomers of a molecule can be different in the human body as was tragically exemplified

by the fetal abnormalities caused by the (*S*) enantiomer of thalidomide, also known as Softenon (Figure 1.2).[3] Therefore, routes to obtain molecules of single handedness are of paramount importance, especially for pharmaceutical compounds, but also in e.g. the food industry. A major complication in the separation of enantiomers is that the two mirror image molecules have the same physical properties, for instance solubility and boiling point. Pure enantiomers are obtained mainly via three routes (Figure 1.3):

1. Asymmetric synthesis: enantiopure molecules can be synthesized from achiral substrates using an enantiopure agent or auxiliary.
2. Prochiral pool: readily available enantiopure molecules that can be extracted from nature such as amino acids and sugars.
3. Resolution of racemates: the separation of enantiomers from a racemic mixture.

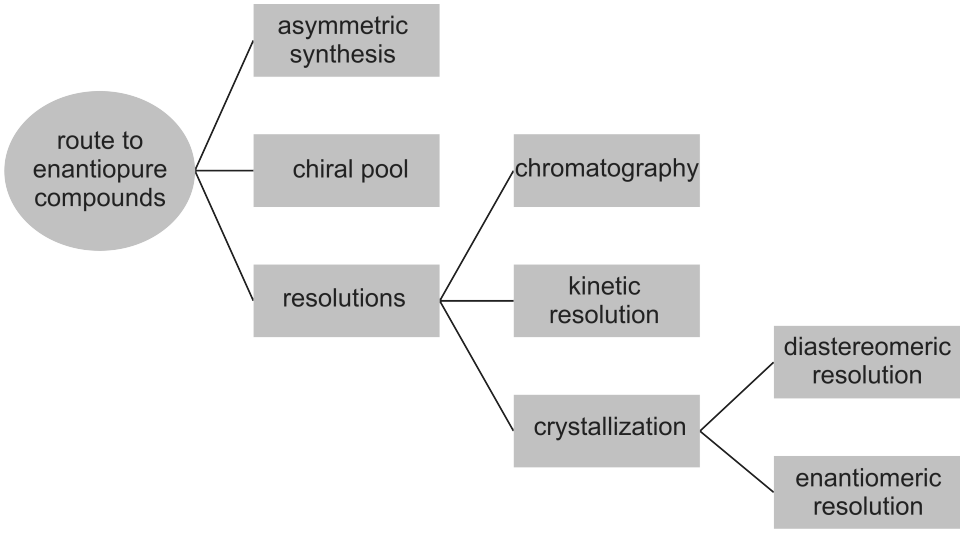

Figure 1.3. Routes to obtain enantiomerically pure compounds.

Focussing on the third route, the resolution of racemates can be performed in several ways. Chiral chromatography uses a stationary phase that is attached to a column wall of single handedness. A kinetic resolution takes advantage of different reaction rates in the presence of an enantiomerically pure reagent. And finally, enantioselective crystallization can be employed to yield enantiopure compounds.[4] This approach can be subdivided in enantiomeric and diastereomeric resolutions. In a diastereomeric resolution an extra enantiomerically pure chiral centre is introduced, for instance using an enantiopure reagent that forms a salt. In this way two compounds can be formed with different physical properties, unlike enantiomers. These diastereomeric compounds can then be separated based on their difference in solubility. After the fractional crystallization, filtration can be used to isolate the optically pure crystals. Furthermore, in the so-called 'Dutch resolution' additive molecules may be used to further optimize the diastereomeric resolution process.[5] It should be noted that finding a suitable resolving agent is not always trivial. The enantiomeric resolution and the so-called crystallization induced enantiomeric transformation will be addressed next.[6]

1.2 Crystallization Induced Enantiomeric Separation

Crystallization forms an attractive starting point for the separation of enantiomers as the organization of growth units within a crystal allows an efficient molecular recognition. Racemic mixtures can crystallize in three different ways: as racemic compounds, racemic

conglomerates and solid solutions (Figure 1.4).[4] In a *racemic compound* the unit cell of the crystals contains both enantiomers in equal amounts. In case a racemic mixture crystallizes as a *racemic conglomerate* the unit cell contains only one enantiomer and the solid phase consists of a mechanical mixture of crystals of the two pure enantiomers. Such crystals are called *enantiomorphs*. *Solid solution* behaviour is observed when the two enantiomers coexist in the solid phase in an unordered fashion; the crystal is not selective to either enantiomer. Racemic conglomerates occur in approximately 10 % of all cases; full solid solutions are rare.[4]

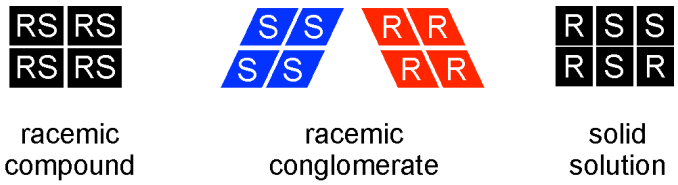

Figure 1.4. Schematic representation of three possible arrangements of chiral molecules in a crystal structure.

Of these three types of crystallization behaviour, only racemic conglomerates are suitable for a separation of the enantiomers into enantiopure solid phases, i.e. a resolution, as was already demonstrated by Louis Pasteur in 1848.[7] In that time he was studying the crystallization of the chiral molecule tartaric acid. He noticed that the sodium salt of this molecule formed crystals that could be separated into two groups with a mirror image crystal shape. After dividing the crystals based on their shape, he observed that one group of dissolved crystals rotated the polarized light clockwise, whereas the mirror image group rotated the light counter clockwise. From this experiment he concluded that the solutions that rotated the light consisted of enantiomerically pure molecules. Thus, because the enantiomers crystallized in separate crystals, Pasteur was able to separate the two mirror images of the molecule. Later, the technique of crystallization for resolutions was refined by starting from a clear supersaturated solution that was seeded with crystals of the desired handedness.[6] These enantiopure seeds could grow further, thereby leaving the other enantiomer in solution.

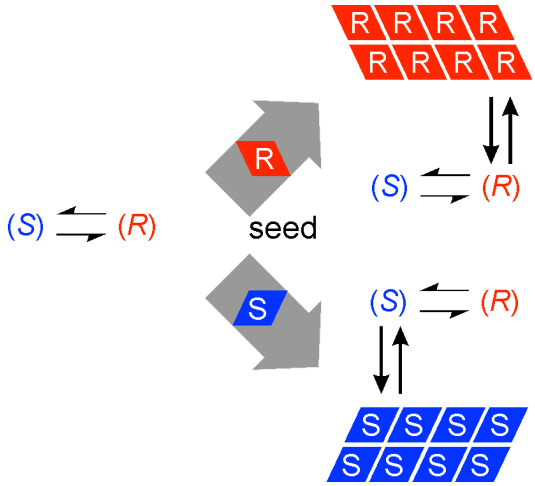

Figure 1.5. Schematic representation of the physical and chemical equilibria during a crystallization induced asymmetric transformation. Starting from a clear supersaturated solution in which racemization occurs (middle), enantioselective seeding results in a solid phase of single handedness.

However, as the solubilities of the two enantiomers for a racemic conglomerate are independent of each other, at least for ideal solutions, the solution is supersaturated for the undesired enantiomer as well and spontaneous nucleation of the latter may occur, thereby hampering the resolution. It is therefore crucial to carefully control the supersaturation during the process.
When only one enantiomer is desired, the maximum theoretical yield for a resolution of conglomerates is limited to 50%, as half of the starting material of the racemic mixture is composed of the opposite enantiomer. It is thus of interest to convert this unwanted enantiomer via a racemization reaction into the desired enantiomer. This racemization reaction may occur ex-situ by racemizing the undesired handedness in a separate step in the resolution. Alternatively, the reaction can be performed during the enantioselective crystallization (Figure 1.5). This so-called *crystallization induced asymmetric transformation* is restricted to compounds for which the racemization is compatible with the crystallization conditions. For such compounds, this execution form has the advantage over the ex-situ method that the supersaturation of the undesired handedness remains low as a result of the solution phase racemization reaction, thereby preventing the nucleation of this enantiomer. Pioneering experiments for this process were performed by the Dutch scientist Havinga using *N,N,N*-methylethylallylanilinium iodine.[8]

1.3 Grinding during Asymmetric Crystallizations

The Dutch version of Havinga's paper on the crystallization induced transformation of *N,N,N*-methylethylallylanilinium iodine contains an interesting footnote.[8a] In this footnote, he speculates that the breaking off of small fragments of an enantiomorphous crystal results in seeds of the same handedness that may further grow. This effect of secondary nucleation was observed by Kondepudi *et al.* by rapidly stirring a solution of sodium chlorate ($NaClO_3$) and was even mentioned in a popular textbook (Figure 1.6b).[9] Although this salt is not chiral in solution, in the crystal the atoms pack in a chiral fashion (like a sort of spiral). Therefore one can distinguish between left- and right-handed crystals of sodium chlorate. Crystallization of a clear solution of $NaClO_3$ in water results in the formation of both left- and right-handed crystals (Figure 1.6a). However, when the crystallization is performed under severe stirring, it was observed that the resulting solid phase in most experiments was dominated by crystals of one handedness (figure 1.6b). McBride *et al.* were able to videotape the process, showing that after a unique initial primary nucleation event, the secondary nucleation caused by the stirring resulted in many small crystallites of the same handedness.[10]
This theory was challenged by Viedma in 2004.[11] He reported that the symmetry breaking in $NaClO_3$ works even when the primary nucleation is very fast, resulting in the nucleation of many crystals of both enantiomers. As the subsequent secondary nucleation caused by the stirring would result in seed crystals of both enantiomorphs, secondary nucleation can not fully explain the observed symmetry breaking. This argumentation was further supported by the surprising observation that even starting from a prepared slurry with a mixture of racemic crystals still resulted in the emergence of a single chiral solid phase under abrasive grinding conditions (Figure 1.6c, 1.7).[12] Thus, even in the absence of primary nucleation, grinding still resulted in the transformation of a mixture of enantiomorphous crystals into crystals of single handedness. This remarkable result forms the starting point of this thesis.

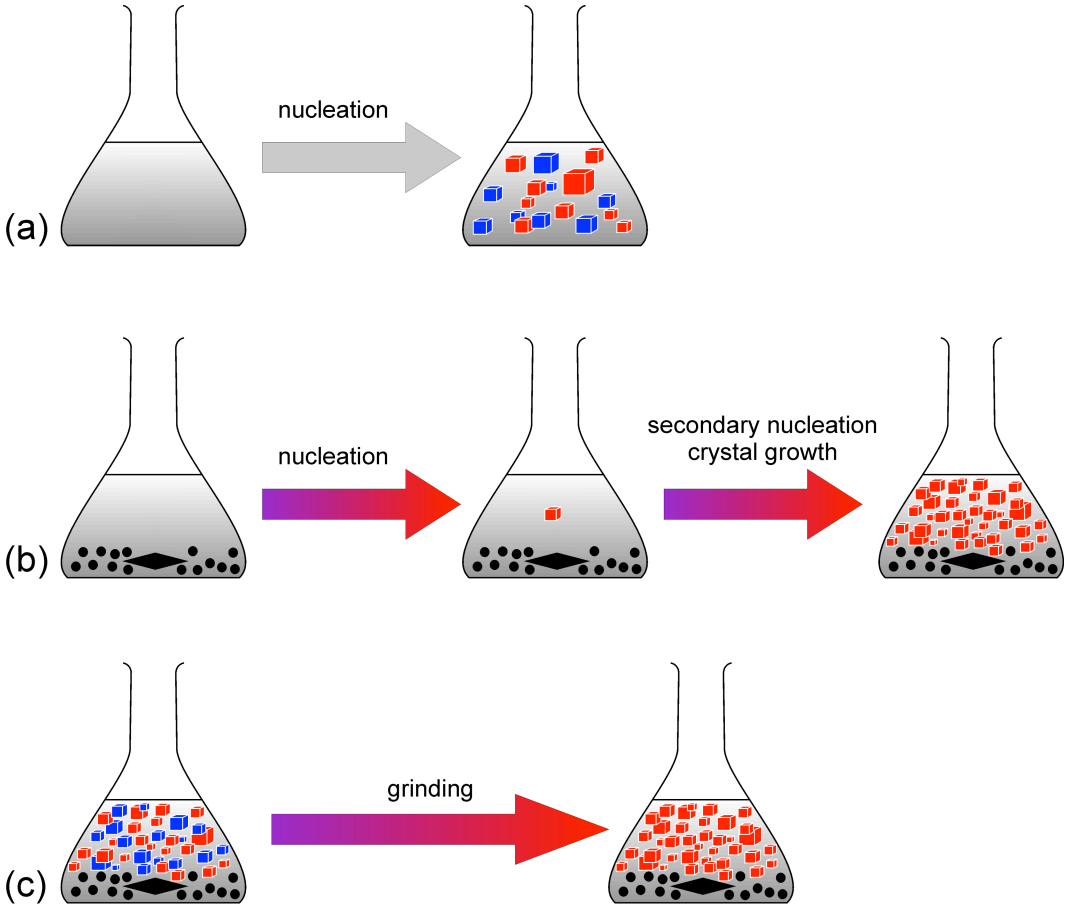

Figure 1.6. Schematic representations of the crystallization of sodium chlorate. If $NaClO_3$ is crystallized from a clear solution, a mixture of crystals of both enantiomorphs is obtained (a). If a clear solution is crystallizing under grinding conditions, a unique nucleation event of one crystal, which is thus of single handedness, can be amplified by the generation of secondary nuclei through grinding (b). The bottom figure (c) shows that even starting with solids of both enantiomorphs instead of a clear solution results in the emergence of a single chiral solid phase.

Figure 1.7. Experimental setup of Viedma. The reaction flask contains a slurry with a racemic mixture of $NaClO_3$ crystals. In the original experiment coloured glass marbles of a necklace were used for the abrasive grinding that resulted in the emergence of a single chiral solid state. Since many researchers have used $NaClO_3$, it is surprising that the transformation was not discovered before. [13-17]

1.4 Aim and Outline of the Thesis

We already mentioned that routes to molecules of single handedness are very important. So could we apply this grinding technique to real chiral molecules, such as those that can be used as enantiopure building blocks for pharmaceutical compounds? In the case of sodium chlorate, the process relies on the fact that the solids of different handedness can nurture each other via the achiral solution (Figure 1.8). For an intrinsically chiral molecule, the equivalent of this process is the separate crystallization of the enantiomers (like in the case of Pasteur) combined with a solution phase racemization reaction in which the two enantiomers can interconvert into each other.[18] In this way a chiral molecule that is built into a crystal can dissolve, racemize into the opposite handedness and then be incorporated in a crystal of this handedness.

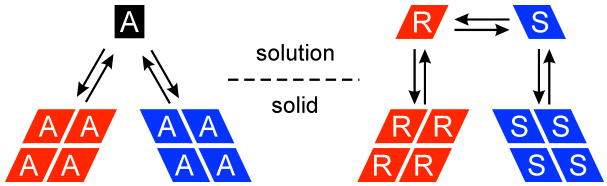

Figure 1.8. Analogy between solid-solution equilibrium for an intrinsically achiral molecule (left); and a chiral molecule undergoing solution-phase racemization (right).

In Chapter 2 we demonstrate the proof of principle for this method to achieve complete deracemization of a solid state phase initially consisting of a racemic mixture of conglomerate crystals, in contact with a saturated solution which is maintained racemic by a racemization agent. These results were triggered by the simulation studies, described in Chapter 3, that convinced us that deracemization of enantiomorphous crystals should be possible, both in the absence and presence of abrasive grinding. To validate this computer model, the critical experimental parameters were explored (Chapter 4). This investigation allowed us to optimize the deracemization method, thereby reducing the time needed to arrive at 100 % chiral purity on practical timescales.
We then moved on to demonstrate the general applicability of the method. In Chapter 5 a second example is presented by using grinding as a route to obtain the enantiopure phenyl alanine, a natural amino acid. Chapter 6 describes a practical and patentable route to obtain the enantiopure nonsteroidal anti-inflammatory drug Naproxen. Additionally, the technique of grinding was exploited to resolve racemic conglomerates even in the absence of racemization, by applying abrasive grinding in the presence of a suitable chiral additive that leads to an asymmetry in the crystal size distribution between the two enantiomorphs (Chapter 7).
Of course, we are also fascinated in the fundamental scientific issue of the origin of the single handedness of biomolecules in the prebiotic world. Various deterministic scenarios for the evolution of biological homochirality, as found in left-handed amino acids and right-handed sugars, have been proposed. Circularly polarized light (CPL), a phenomenon that is also observed during star formation, is one of the possible actors for such mechanisms. In Chapter 8 we therefore used circularly polarized light to direct the evolution of an amino acid derivative to a completely enantiomerically pure solid phase using abrasive grinding as a single-step asymmetric amplification mechanism.

Compared to other techniques to obtain single chirality, the grinding of crystals is a simple and robust way to make molecules of single handedness. Not only do we show the first proof-of-principle, we also demonstrated that this is a practical method by elucidating the rate

determining parameters of grinding as a route to enantiopure amino acids and pharmaceutical compounds. Also, we found many ways to steer the final outcome either to a left- or a right handed solid phase. From another perspective, the deracemization method outlines a pathway to create enantiomerically pure compounds starting from racemic components, thereby contributing to the discussion on the emergence of prebiotic chiral molecules.

1.5 References and Notes

[1] a) J. H. Van 't Hoff, *Bull. Soc. Chem. Fr.* **1875,** *23,* 295; b) J. A. Le Bel, *Bull. Soc. Chem. Fr.* **1874,** *22,* 337.

[2] a) S. L. Miller, *Science* **1953,** *117,* 528; b) S. L. Miller, H. C. Urey, *Science* **1959,** *130,* 245.

[3] E. L. Eliel, S. H. Wilen, *Stereochemistry of Organic Compounds* (John Wiley and Sons, New York, 1994). It should be noted that desired (*R*) enantiomer of thalidomide readily racemizes in the body in the harmful (*S*) enantiomer. Therefore, taking enantiomerically pure (*R*)-thalidomide may still result in birth defects.

[4] a) J. Jacques, A. Collet, S. H. Wilen, *Enantiomers, Racemates and Resolution* (Krieger, Florida, 1994); b) G. Coquerel, *Top. Curr. Chem.* **2007,** *269,*1.

[5] a) T. Vries, H. Wynberg, E. Van Echten, J. Koek, W. Ten Hoeve, R. M. Kellogg, *Angew. Chem. Int. Ed.* **1998,** *37,* 2349; b) J. W. Nieuwenhuijzen, R. F. P Grimbergen, C. Koopman, R. M. Kellogg, T. R. Vries, K. Pouwer, E. Van Echten, B. Kaptein, L. A. Hulshof, Q. B. Broxterman, *Angew. Chem. Int. Ed.* **2002,** *41,* 4281. see also: R. M. Kellogg, B. Kaptein, T. R. Vries, in *Topics in Current Chemistry*, Vol. 269, Eds. K. Sakai, N. Hirayama, R. Tamura (Springer-Verlag, Berlin, 2007) 83-132 .

[6] R. Yoshioka, in *Topics in Current Chemistry*, Vol. 269, Eds. K. Sakai, N. Hirayama, R. Tamura (Springer-Verlag, Berlin, 2007) 83-132 .

[7] L. Pasteur, *C.R. Hebd. Séanc. Acad. Sci. Paris* **1848**, *26,* 535.

[8] a) E. Havinga, *Chem. Weekblad* **1941**, *38*, 642; b) E. Havinga, *Biochem. Biophys. Acta* **1954**, *13*, 171.

[9] D. K. Kondepudi, R. J. Kaufman, N. Singh, *Science* **1990**, *250*, 975-977; see also: A. Holden, P. Singer *Crystals and Crystals growing* (Anchor Books Doubleday & Company, New York, 1960) 291: "The randomness with which right-handed and left-handed seeds of sodium chlorate form in a solution might be upset by suitable influences…. you must be careful that the seeds you finally examine are not all formed from a single seed which has been knocked about in the solution, producing more of its own type".

[10] J. M. McBride, R. L. Carter, *Angew. Chem.* **1991,** *103,* 298; *Angew. Chem. Int. Ed.* **1991,** *30,* 293.

[11] C. Viedma, *J. Cryst. Growth* **2004,** *261,*118–121.

[12] C. Viedma, *Phys. Rev. Lett.* **2005**, *94*, 065504.

[13] So why wasn't this stunningly simple method of grinding a slurry of sodium chlorate, the Adam and Eve example of chiral crystallization, not discovered before? The famous physical chemist Wilhelm Ostwald was probably the closest. The first experiments of 'Ostwald's rule of stages' were actually performed using $NaClO_3$, and during the experiments Ostwald observed the crystals through a polarized light microscope, not only to improve the contrast but also to enjoy the colorful images.[14] On the other hand, he also used the technique of prolonged grinding of slurries using 'Tariergranate' (metal balls used for weighing) to prove his crystal ripening theory. Ostwald worked with the right compound and ground slurries under conditions almost identical to those used by Viedma more than 100 years later.[15,16] What would have been the result had the careful experimentalist Ostwald performed his solubility experiments under grinding conditions using $NaClO_3$ instead of the mercury compounds that he later chose? See also the fascinating report by Kipping and Pope on the crystallization of $NaClO_3$.[17]

[14] W. Ostwald, *Z. Phys. Chem.* **1897,** *22,* 289-330.

[15] W. Ostwald, *Lehrbuch der Allgemeinen Chemie, vol. 2, part 1*. (Leipzig, Germany, 1896).

[16] W. Ostwald, *Z. Phys. Chem.* **1900,** *34,* 495-503.

[17] W.S. Kipping, W.J. Pope, *J. Chem. Soc. Trans.* **1898**, *73*, 606

[18] J. Crusats;, S. Veintemillas-Verdaguer, J. M. Ribó, *Chem. Eur. J.* **2006,** *12,* 7776-7781.

Chapter 2

Emergence of a Single Solid Chiral State from a Nearly Racemic Amino Acid Derivative

2.1 Introduction

Understanding how the single-handedness of biological molecules came about has been of intense interest since Pasteur first separated mirror-image crystals of a tartrate salt.[1] Several models have been proposed to address the question of how enantiomerically pure solutions or crystalline phases could have emerged from a presumably racemic prebiotic world.[2-9] Viedma recently demonstrated the inexorable and random emergence of solid phase single chirality for the intrinsically achiral inorganic compound $NaClO_3$ initially present as a racemic mixture of two enantiomorphic solid phases in equilibrium with the achiral aqueous phase (Scheme 2.1, left).[6] Grinding the slurry of crystals with glass beads promotes dynamic dissolution/crystallization processes that result in the conversion of one solid enantiomorph into the other. The conversion relies on the fact that the solid-phase chiral identity of the intrinsically achiral $NaClO_3$ is lost upon dissolution.
An intriguing analogy to this system is presented by a molecular system of true enantiomers that forms separate *R* and *S* solid phase crystals (known as a conglomerate), and that can be induced to undergo racemization in solution.[10-12] (Scheme 2.1, right). We report here the first experimental proof-of-concept for the emergence of a single solid-phase chiral state for an intrinsically chiral molecule starting from a nearly racemic mixture of enantiomorphic crystals. This finding extends Viedma's model to biologically relevant enantiomeric molecules, holding profound implications for our understanding of the origin of single chirality in living systems.

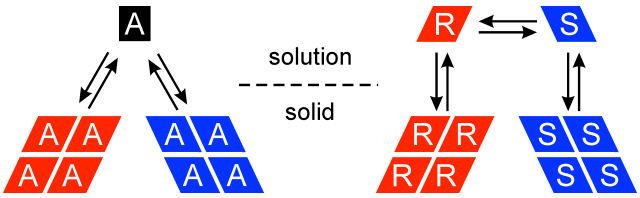

Scheme 2.1. Analogy between solid-solution equilibrium for an intrinsically achiral molecule (left); and a chiral molecule undergoing solution-phase racemization (right).

2.2 Results and Discussion

The imine of 2-methyl-benzaldehyde and phenylglycinamide **1** (Scheme 2.2) forms a conglomerate in the solid phase and racemizes rapidly in solution with added base ($t_{1/2}$ < 2 min at 25 °C with the organic base DBU in MeOH, pK_a = 12). Solution-solid mixtures of **1** (4 g) at varying overall *ee* were magnetically stirred (1250 rpm) at ambient temperature in MeOH or MeCN (36 g) in the absence and in the presence of 2.5 mm glass beads (10 g). After establishing solution-solid equilibrium, solution-phase racemization was initiated by adding DBU (5 mol%). Samples of the solid were collected over time and the enantiomeric purity was measured using two independent chiral HPLC methods. Experiments were carried out in

all participating laboratories. In the presence of glass beads, which induce continuous attrition of the crystals, we found that the *ee* of the solid rises inexorably over time, evolving to a single solid chiral state from initial small imbalance in crystal composition as low as 2-3% *ee* (see Figure 2.1 (left) and Experimental Section). The solid of single chirality thus obtained is stable over time in the presence of the racemizing solution. For a stirred slurry in the absence of glass beads, the solid phase *ee* remained unchanged from its initial value.

This result demonstrates that a slight enantioimbalance in **1** directs the trend to a single solid chiral state. We also observed that seeding a racemic system of crystals of **1** with chiral additives could also direct the establishment of a single chiral solid. For example, concentrations low as 0.1 mol% enantiopure phenylglycine (Phg) as an additive provide a sufficient chiral bias for achieving attrition-induced solid-phase single chirality (Figure 2.1, right).[13-16] (*S*)-Phg leads to an *R* chiral end state, (*R*)-Phg to *S* chirality, and with a resolution time that decreases for higher Phg concentrations.

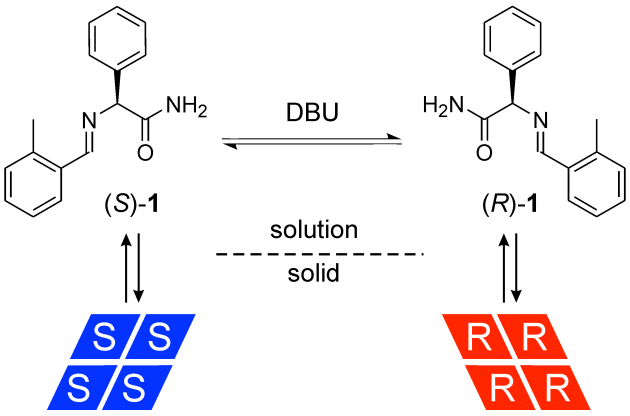

Scheme 2.2. Chemical and physical equilibria in the racemization and crystallization/ dissolution processes for **1**.

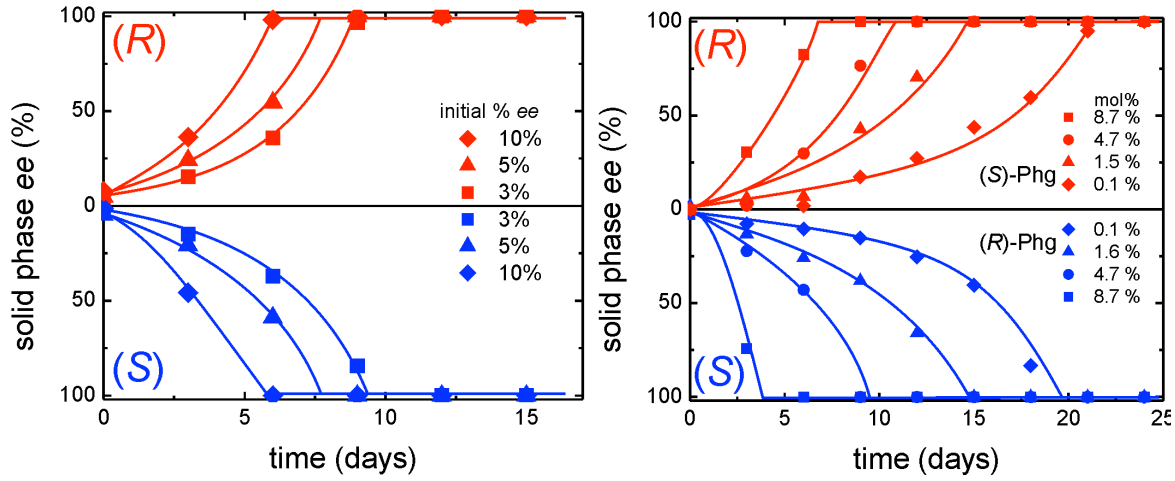

Figure 2.1. Attrition-enhanced evolution of solid-phase ee for **1** in MeCN. Left: starting from initial ee values of **1** as shown. Right: starting from racemic **1** with added Phg as shown. Lines are a guide to the eye.

These findings may be rationalized taking into account Viedma's model involving a dynamic process of crystal dissolution and growth enhanced by attrition, along with considerations of total surface area as a driving force for crystal growth.[6] According to the Gibbs-Thomson rule, smaller crystals produced by attrition dissolve more readily than larger ones.[17] In a saturated solution, this leads to Ostwald ripening in which large crystals grow at the cost of smaller ones regardless of their handedness. A small imbalance in the handedness of large compared to small crystals may occur due to a small initial enantiomeric excess or may be induced by minute amounts of chiral species present in the solution. In the latter case, Lahav's "rule of reversal" applies.[18,19] The continued fragmentation of crystals by attrition also provides a relative increase in the surface area of the hand that has established an excess. Although crystal growth and dissolution have approximately equal rates under near equilibrium conditions, the attrition-enhanced asymmetry described here coupled with solution-phase racemization produces a net flow of mass allowing depopulation of one chiral solid state towards the other via the solution phase. Paradoxically, the solution racemization provides the driving force for the evolution of solid-phase single chirality.
Crystallization-induced transformations of conglomerates as a route to chiral purification is practiced extensively for diastereomers that racemize in solution,[20] taking advantage of a difference in solubility. Our results stand in striking contrast to Dimroth's Principle,[20] which although applied today primarily to separation of diastereomers, was originally formulated for the general case of coupled physical and chemical equilibria. According to this principle, a general system as shown in Scheme 2.1 of two solid enantiomorphs in equilibrium with a solution in which racemization occurs represents a balance such that solid phase enrichment should not occur.[21,22] In our example, the continuous grinding of the solid enantiomorphs creates the essential solubility gradient for the dissolution and recrystallization processes that drive the system until all the solid material of one enantiomer is converted to the solid of the opposite hand. Once a state of single chirality is achieved, the system is „locked", because primary nucleation to form and sustain new crystals from the opposite enantiomer in the racemizing solution is kinetically prohibited under the conditions of the experiment. This provides a stable, irreversible route to extremely enantiopure compounds in high yield and with productivity limited only by the amount of solid material present at the outset. These concepts may readily be extended to other chiral systems.

2.3 Conclusions

Thus the emergence of a state of solid-phase single chirality for true enantiomers may be achieved in a near equilibrium process through an interplay between attrition-catalyzed dissolution and Ostwald ripening of crystals. This route to single chirality may be compared with physical models invoking, on the one hand, thermodynamic control for solution-phase enantioenrichment,[7,23] and on the other hand, "far-from-equilibrium" crystallization processes.[2a,5,24,25]
The state of solid-phase single chirality for an enantiomeric compound that forms a conglomerate is not more stable than the racemic state for the same size and number of crystals but simply represents a kinetic trap accessible on our time scale due to acceleration of both crystal dissolution/growth and racemization. Thermodynamics dictates that single chirality may ultimately be achieved over eons of time, as in a prebiotic scenario, even in the absence of accelerating influences. Our results demonstrate for the first time that the concept of attrition-enhanced solid-phase enantioenrichment may be extended from simple achiral salts to include biologically relevant enantiomeric molecules such as those responsible for recognition, replication and ultimately for the chemical basis of life.

2.4 References and Notes

[1] L. Pasteur, C.R. *Hebd. Séanc. Acad. Sci. Paris* **1848**, *26*, 535.
[2] a) E. Havinga, *Chem. Weekblad* **1941,** *38*, 642-644; b) E. Havinga, *Biochem. Biophys. Acta* **1954**, *13*, 171-174.
[3] a) F. C. Frank, *Biochim. Biophys. Acta* **1953,** *11*, 459-463; b) M. Calvin, *Molecular Evolution.* Oxford Univ. Press, Oxford, UK, 1969.
[4] K.Soai, T. Shibata, H. Morioka, K. Choji, *Nature* **1995**, *378*, 767-768.
[5] D. K. Kondepudi,; R. J. Kaufman, N. Singh, *Science* **1990**, *250*, 975-977.
[6] a) C. Viedma, *Phys. Rev. Lett.* **2005**, *94*, 065504; b) C. Viedma, *Astrobiol.* **2007**, *7*, 312-319.
[7] M. Klussmann, H. Iwamura, S.P. Mathew, D.H. Wells Jr., U. Pandya, A. Armstrong, D.G. Blackmond, *Nature* **2006**, *441*, 621-623.
[8] I. Weissbuch, L. Leiserowitz, M. Lahav, *Top. Curr. Chem.* **2005**, *253*, 123–165.
[9] W. A. Bonner, *Orig. Life Evol. Biosph.* **1994**, *24*, 63-78.
[10] J. Jacques, A. Collet,; S. H. Wilen, *Enantiomers, Racemates and Resolution* Krieger, Florida, 1994.
[11] a) J. Crusats;, S. Veintemillas-Verdaguer, J. M. Ribó, *Chem. Eur. J.* **2006,** *12,* 7776-7781. b) J. Crusats, S. Veintemillas-Verdaguer, J. M. Ribó, *Chem. Eur. J.* **2007**, DOI: 10.1002/chem.200700538.
[12] a) D. G. Blackmond, *Chem. Eur. J.* **2007**, *13*, 3290-3295; b) D. G. Blackmond, *Chem. Eur. J.* **2007**, *13*, 10306..
[13] We observed that an initially racemic mixture of crystals of **1** evolved to the *R* solid in all experiments, suggesting that minute levels of chiral impurities can interfere with the expected randomness (see Refs. 14-16). Phg is a starting material and conceivable impurity in the synthesis of **1**.
[14] G. Wald, *Ann. NY Acad. Sci.* **1957**, *69*, 352.
[15] D. W. Armstrong, J. P. Kullman, X. Chen, M. Rowe, *Chirality* **2001**, *13*, 153-158.
[16] M. Lahav, I.Weissbuch, E. Shavit, C. Reiner, G. J. Nicholson, V. Schurig, *Orig. Life Evol. Biosph.* **2006**, *36*, 151-170.
[17] W. Ostwald, *Lehrbuch der Allgemeinen Chemie, vol. 2, part 1*. Leipzig, Germany, 1896.
[18] L. Addadi, Z. Berkovitch-Yellin, N. Domb, E. Gati, M. Lahav, L. Leiserowitz, *Nature* **1982**, *296*, 21-26.
[19] L. Addadi, S. Weinstein, E. Gati, I. Weissbuch, M. Lahav, *J. Am. Chem. Soc.* **1982**, *104*, 4610-4617.
[20] K. M. J. Brands, A. Davies, *J. Chem. Rev.* **2006**, *106*, 2711-2733.
[21] O. Dimroth, *Justus Liebigs Ann. Chem.,* **1910**, *377*, 127-163.
[22] N. A. Hassan, E. Bayer, J. C. Jochims, *J. Chem. Soc. Perkin 1*, **1998**, 3747-3757.
[23] H. J. Morowitz, *J. Theoret. Biol.* **1969**, *25*, 491-494.
[24] D. K. Kondepudi, K. L. Bullock, J. A. Digits, P. D. Yarborough, *J. Am. Chem. Soc.* **1995**, *117*, 401-404.
[25] a) J. H. E. Cartwright, J. M. García-Ruiz, O. Piro, C. I. Sainz-Díaz, I. Tuval, *Phys. Rev. Lett.* **2004**, *93*, 035502; b) D. H. R. Barton, G. W. Kirby, *J. Chem. Soc*., **1962**, 806-817; c) R. E. Pincock, R. R. Perkins, A. S. Ma, K. R. Wilson, *Science* **1971**, *174*, 1018-1020.

Chapter 3

Explanation for the Emergence of a Single Chiral Solid State during Attrition Enhanced Ostwald Ripening -Survival of the Fittest-

3.1 Introduction

The single handedness of chiral molecules like sugars and amino acids, as evolved from a (presumably) racemic prebiotic world, has intrigued scientists ever since Louis Pasteur separated enantiomorphic sodium ammonium tartrate crystals.[1] Several mechanisms that lead to an imbalance between enantiomers have been proposed together with an amplification mechanism as an explanation for the origin of biomolecular single handedness. One class consists of autocatalytic reactions in which a small initial asymmetry is amplified, as was outlined by Frank and by Calvin and experimentally confirmed by Soai in a solution phase reaction.[2-5] Crystallization is an alternative route to chiral purification if the system behaves as a conglomerate.[6-8] This has been explored for racemizing systems under far from equilibrium conditions, for which the hard to control process of primary nucleation dictates the resolution outcome.[9-19]

In an intriguing experiment, Viedma demonstrated for $NaClO_3$,[7] which is intrinsically achiral but crystallizes in the chiral space group $P2_13$, that starting from a mixture of enantiomorphic crystals in contact with an achiral saturated solution, abrasive grinding can lead to a solid state of single chirality. This near-equilibrium technique is not only applicable to conglomerate forming salts, but also to racemic conglomerates of intrinsically chiral compounds that racemize in solution.[20,21] Experimental demonstration of the latter process was recently reported for an amino acid derivative (**1**) (Scheme 3.1).[8] In both the experiments with $NaClO_3$ and the amino acid derivative **1**, small enantioimbalances in the solid phase inexorably result in a complete solution mediated conversion of the minor chirality into the originally more abundant crystal phase.

In this chapter we give insight into the underlying principle of this complete symmetry breaking. So far, computational models designed to explain Viedma's results rely on the presence of primary nucleation,[22,23] but this is both unlikely and not necessary as we will show. As a starting point we use Viedma's suggestion that this process is driven by the counteracting combination of Ostwald ripening and attrition.[24] Such a process implies near equilibrium conditions, a situation in which primary nucleation is unlikely to occur. Using computational modeling we show that the combined processes of attrition and Ostwald ripening indeed result in the evolution of a single chiral solid phase. The model leads to both the breaking of the initial symmetry and the further enantiomeric enrichment, which is maintained once a solid phase of single chirality is reached. We derive a simple first order kinetics description of the process, which is in excellent agreement with experimental observations and provides further insight for process optimization.[8] The results are quite insensitive to the details of the model and its parameters, suggesting that attrition enhanced Ostwald ripening offers a robust pathway to single chirality.

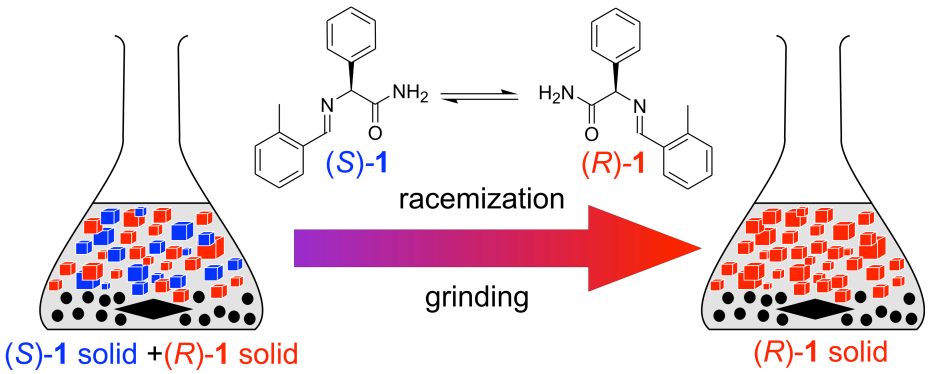

Scheme 3.1. The evolution of a single chiral solid phase during the process of abrasive grinding for N-(2-methylbenzylidene)-phenylglycine amide **1**. The compound **1** racemizes in solution in the presence of 5 mol% of DBU.

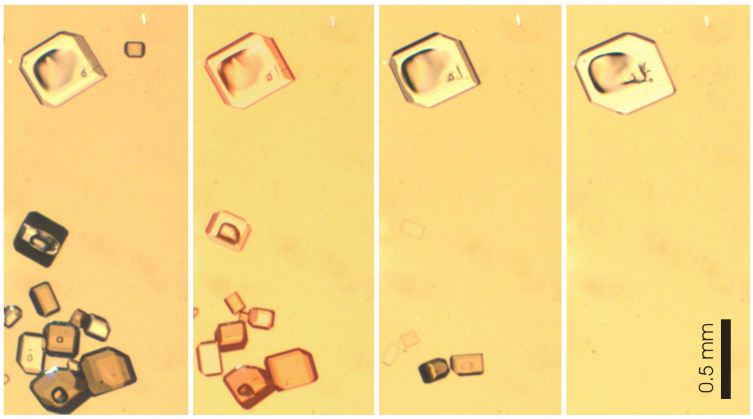

Figure 3.1. Polarized light microscope images showing the process of Ostwald ripening of $NaClO_3$ leading to a single chiral solid phase. A racemic mixture of $NaClO_3$ crystals in equilibrium with a saturated solution was studied. Under temperature controlled conditions no significant deracemization was observed in two months. Under conditions with temperature fluctuations of ±2 °C, the process of crystallization and dissolution is enhanced leading to one single crystal in two months in the observed region. The chirality of the crystals can be determined by rotating one of the crossed polarizers slightly either clockwise or anticlockwise. As a result, the l or d crystals, respectively, become dark.

3.1.1 Ostwald Ripening

According to the Gibbs-Thomson effect small particles have a higher solubility than large ones.[25] This is a direct consequence of the surface to volume ratio of the particles as the system minimizes its total surface free energy. In a saturated solution in contact with crystals, this leads to a process called Ostwald ripening: large crystals grow at the cost of smaller ones.[26] The thermodynamic ground state is therefore one single crystal. As shown in Figure 3.1, this has an interesting consequence for a system of chiral crystals in contact with an achiral or racemizing solution: the thermodynamic stable state is one single, and therefore enantiopure, crystal. In other words, Ostwald ripening always leads to complete chiral deracemization in these systems. Reaching a single crystal end state for macroscopic crystals through Ostwald ripening takes a long time, typically months or even longer, depending on the system volume, the solubility, the rate of racemization in the solution and the surface free energy.[27] For an initial crystal size distribution (CSD) with a large number of small crystals Ostwald ripening is fast, but its rate decreases rapidly as the CSD evolves towards large crystals. Because the final CSD is of no importance for the chiral purity, the advantage of

small crystals speeding up the Ostwald ripening can be exploited in the deracemization process. A way to arrive at a CSD with many small crystals is to induce attrition by stirring or milling. This attrition also creates rough surfaces and stress, which further enhances the ripening process.

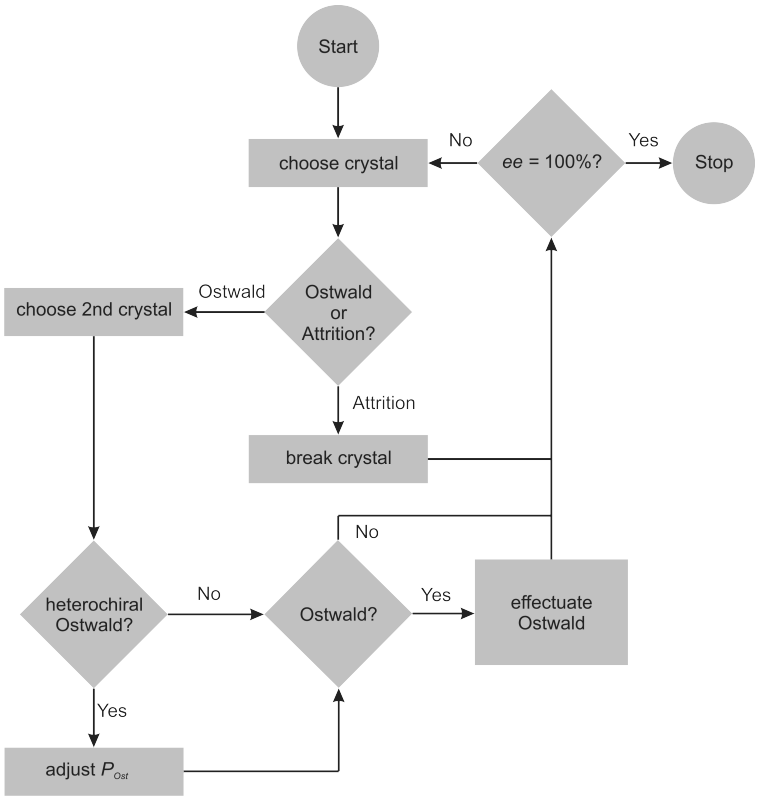

Figure 3.2. Flow diagram of the Monte Carlo simulation modeling the combined processes of Ostwald ripening and attrition.

3.1.2 Computational Method

In order to better understand how the interplay between Ostwald ripening, leading to larger crystals, and attrition, leading to smaller crystals, can yield a single chiral state with many small crystals, a computer model containing the essential features of these two processes was developed. A system consisting of a saturated solution, a reservoir with a constant number of achiral or racemizing molecules, in contact with the two CSDs of the enantiomers was subjected to a Monte Carlo simulation. The Monte Carlo process involves changes in the CSDs. The system has a constant total number, N, of molecules. With every Monte Carlo move, which mimicks a given time interval in a real experiment, for a randomly chosen crystal either attrition or Ostwald ripening occurs (Figure 3.2). The attrition-ripening ratio, ξ, is parameterized as the ratio between the probability of an attrition event, P_{attr}, and the probability of an Ostwald event, P_{Ost},

$$\xi = \frac{P_{attr}}{P_{Ost}} . \qquad (3.1)$$

The attrition-ripening ratio, to be interpreted as a measure for the stirring intensity, can also be regarded as a reciprocal measure for the exchange rate of solute, which, among others, is determined by solubility. The higher this rate, the more effective the Ostwald ripening, and

the smaller the attrition-ripening ratio. In an attrition event the crystal is broken into two pieces of arbitrary size. The only restriction is that the total number of molecules remains constant. Because in practice grinding is effective down to a minimal crystal size, attrition is only allowed above a minimal size in terms of the number of molecules n_{min}. Throughout this paper n_{min} is set to 10. For an Ostwald ripening event a second crystal is randomly selected. The largest of the two crystals may gain a single molecule at the cost of the other crystal. The probability that this event occurs, for a crystal with n_i molecules to a crystal with n_j molecules is:

$$P_{Ost}(n_i, n_j) = P_{Ost}\left(\frac{1}{\sqrt[3]{n_i}} - \frac{1}{\sqrt[3]{n_j}}\right). \tag{3.2}$$

In this equation linear growth/dissolution kinetics are assumed as the crystal surfaces are roughened by the grinding process. In a Monte Carlo process the events occur consecutively, whereas in a real experiment events take place simultaneously. The simulation time is therefore scaled with the number of crystals present in the CSD on each event.
The chiral identity of $NaClO_3$ molecules is instantaneously lost upon dissolution. In the experiment in which chiral molecules racemize in solution, the situation is more complex as the time scales of racemization and Ostwald ripening differ. The exchange rate of molecules between the solution and the crystals is high compared to the process of racemization in solution. We therefore need to distinguish between a homochiral and a heterochiral event for Ostwald ripening. For a heterochiral event a molecule will attach to a crystal of the opposite handedness, only after having attained the correct handedness as a result of racemization. The probability for 'heterochiral Ostwald ripening' is therefore reduced compared to a homochiral event, for which a dissolved molecule preserves its chirality and attaches to a crystal of the same handedness. To take account of this difference in the model, we reduce the chance for Ostwald ripening if the chosen crystal pair is of opposite chirality, using a racemization efficiency parameter χ according to:

$$P_{Ost} = \begin{cases} P_{Ost} & \text{(homochiral)} \\ \chi P_{Ost} & \text{(heterochiral)} \end{cases} \tag{3.3}$$

For a system in which the racemization is instantaneous $\chi = 1$, whereas in the absence of solution racemization $\chi = 0$.
The enantiomeric excess *ee* of the solid phase during a simulation run is computed from $ee = (N_D - N_L)/(N_D + N_L)$, where N_D and N_L are the number of D and L molecules, respectively, in the solid phase. Note that primary nucleation is not included in the model, as the actual solution is nearly saturated during the whole process. Even if the formation of primary nuclei would be included and a nucleus with the minority chirality should form, it would rapidly dissolve because of its large undersaturation with respect to the larger crystals.

3.2. Results and Discussion

3.2.1 Initial Racemic Conglomerates

Figure 3.3 presents the typical development of the CSDs of the two opposite chiral solids during a Monte Carlo run for $\xi = 0.01$ and $\chi = 0.1$. The simulations start with equal Gaussian shaped CSDs, although the exact shape is not important as the initial CSDs are rapidly

broadened around small average crystal sizes. The system *always* evolves into a single chiral end state. Once the last minority enantiomer crystal is dissolved, the single chiral solid phase remains in a steady state consisting of many small crystals of one enantiomer as long as the attrition is sustained. When the attrition is stopped (no stirring) the single chiral state persists as primary nucleation is not allowed, and Ostwald ripening will lead to a CSD with increasingly large crystals (not shown in Figure 3.3). By performing many such simulations we find that the final single chiral end state is randomly D or L for these conditions.

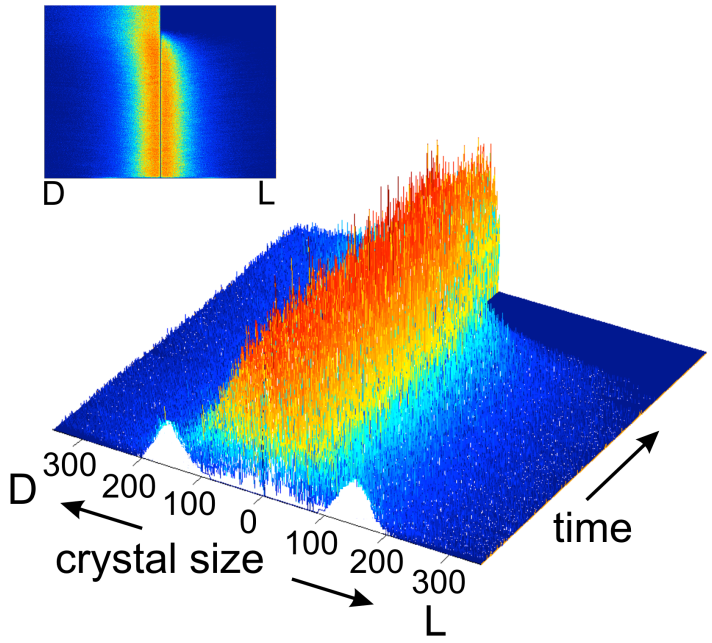

Figure 3.3. A typical example of the crystal size distribution of D and L crystals during a Monte Carlo run simulating the combined process of attrition and Ostwald ripening for a compound racemizing in solution. The initial CSD is set to a racemic mixture of two Gaussian distributions each containing 10^5 molecules centered around a crystal size of 150 molecules. The attrition-ripening ratio is set to $\xi = 0.01$; and the racemization efficiency to $\chi = 0.1$. The graph shows the evolution of the CSD during $1.8 \cdot 10^8$ Monte Carlo events. The inset shows a top view of the graph.

The time to reach a single chiral end state depends on the simulation parameters. Figure 3.4 presents the deracemization time t_{derac}, as a function of the attrition-ripening ratio ξ for $\chi = 0.1$. As expected, the deracemization times for either the L or the D state are equal. For small attrition-ripening ratios, t_{derac} is large as the system consists of only a few large crystals, a situation that is similar to Figure 3.1. This leads to long deracemization times. For intermediate values of the attrition-ripening ratio the crystals stay sufficiently small for the Ostwald process to be effective, resulting in a reduction of t_{derac} by several orders of magnitude. When applying very intense stirring, the CSDs narrow as they move to many crystals with sizes close to the minimal size for attrition, n_{min}, and Ostwald ripening becomes less effective as the differences in driving force become small and the attrition destroys large crystals. Figure 3.4 also shows that the deracemization time is independent of the size N of the system for intermediate and high values of the attrition-ripening ratio. This is in good agreement with experimental results for an amino acid derivative.[8] In the case of instantaneous racemization in solution ($\chi = 1$), the deracemization process evolves in a comparable fashion. There is, however, one essential difference. For $\chi = 1$ the system behaves more stochastically and the deracemization time scales linearly with the system size.

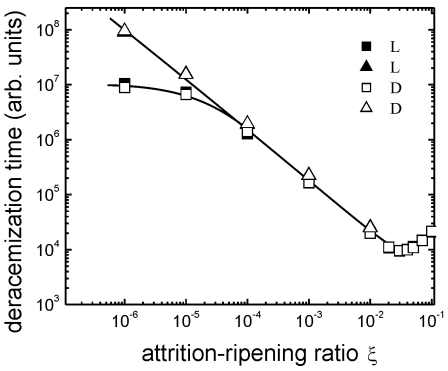

Figure 3.4. The average deracemization time t_{derac} as a function of the attrition-ripening ratio ξ for a compound racemizing in solution (χ = 0.1), with either D (open symbols) or L (full symbols) final state. The initial ee = 0. Results are averaged over 100 simulation runs and are shown for two system sizes: $N = 2 \cdot 10^4$ (square symbols), $N = 2 \cdot 10^5$ (triangle symbols). The line is drawn as a guide to the eye.

3.2.2 Initial Enantiomeric Excess

In the discussion so far, we have started with equal initial CSDs and therefore an *ee* of zero. To compare the model with the experimental results obtained with an initial enantioimbalance,[7,8] we simulated the effect of an excess amount in one enantiomer, while at the same time keeping the initial mean crystal sizes and variances equal for both distributions. For a racemization efficiency of χ = 0.1 and various initial values of the enantiomeric excess we determined the *ee* for 1600 simulation runs as a function of time. An initial enantiomeric excess of merely 2.5% caused *all* runs to evolve irreversibly and completely towards this enantiomer in excess. In Figure 3.5, the *ee* as a function of time is presented for nine individual simulation runs with different starting *ee*'s. As the figure shows, even small imbalances in the initial *ee* are effectively amplified to an enantiomeric pure end state, which is in good agreement with the experimentally observed results.[7,8] However, performing these simulation runs for instantaneous racemization in solution, i.e. χ = 1, we find no chiral amplification but only stochastic behavior towards a single chiral end state. This seems to be in contradiction with the amplification observed in $NaClO_3$,[7] which promptly loses its chiral identity upon dissolution. Therefore, we studied another form of initial asymmetry, namely that caused by a relative shift of the CSD of one of the enantiomers.

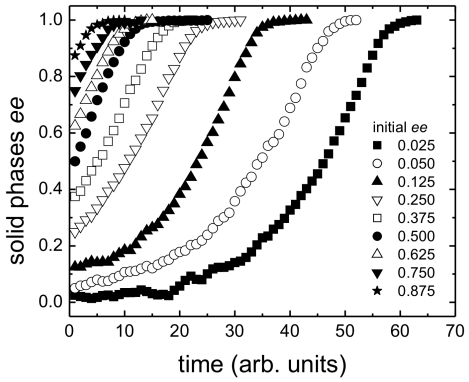

Figure 3.5. The enantiomeric excess versus time for the racemizing system (χ = 0.1) for small imbalances in the initial ee. N = 8000; ξ = 0.04.

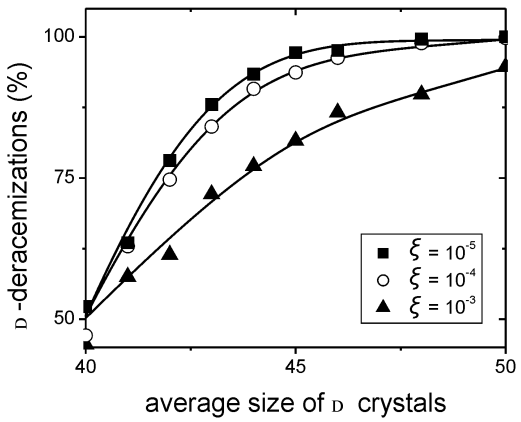

Figure 3.6. The influence of shifted CSDs on the deracemization outcome for an intrinsically racemic solution (χ = 1). Shown is the percentage of runs ending in pure d averaged over 1000 simulations as a function of the shift of the initial CSDs of the D enantiomer while keeping the ee equal to zero. for the two enantiomers. The initial CSD of the L crystals was kept constant around 40 molecules. The curves represent various attrition-ripening ratios ξ. N = 10^4. The lines are a guide to the eye.

3.2.3 Shifted CSDs

The size of the crystals plays an important role. In practice, the initial CSDs of both enantiomers of the conglomerate will never be completely equal, in contrast to our simulations so far. Therefore, we modeled the deracemization process for $\chi = 1$ with slightly shifted starting CSDs, while keeping the initial *ee* zero. The results are shown in Figure 3.6. Shifting one of the CSDs results in a higher probability of reaching the end state corresponding to the initially larger crystals. This amplification is strongest at low values of the attrition-ripening ratio. For these low values of ξ, the CSD 'memory' will exist long enough to induce a sufficient increase in overall *ee*, and to direct the system towards the correct single chiral state, whereas this memory is rapidly lost if very small crystals are formed by strong attrition. In the latter case, the outcome of the deracemization is more stochastic.

These results might explain the earlier mentioned experiments performed by Viedma,[7] in which he studied the effect of an initial excess in one of the enantiomers. Small imbalances in the initial CSD may have been amplified effectively to a deterministic end state of single chirality of the handedness of the initially larger crystals. Another mechanism that may play a role in the case of $NaClO_3$ is that in addition to single molecules, also small clusters that are still chiral are exchanged in the Ostwald process. For such clusters heterochiral events are not possible. This corresponds to a situation for which $\chi < 1$, i.e., a situation for which an initial enantiomeric excess will be amplified.

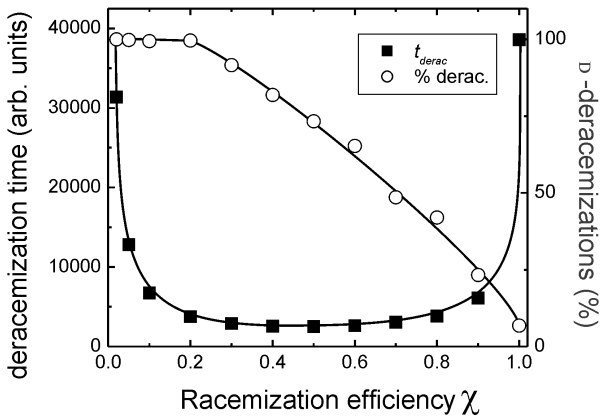

Figure 3.7. The deracemization time as well as the percentage of the deracemizations ending in pure d averaged over 1600 simulations as a function of the racemization efficiency χ for ξ = 0.04 and an initial ee = 5% in D. Lines are a guide to the eye.

3.2.4 The Racemization Efficiency

In order to understand the influence of the racemization efficiency on the enantiomeric enrichment, Figure 3.7 presents the deracemization time versus the racemization efficiency χ for ξ = 0.04, starting with *ee* = 5%. The bathtub shaped graph shows that a minimal deracemization time is accessible for a wide range of χ values. The graph also shows the chance that the system evolves to the enantiomer initially in excess. For $\chi < 0.2$ this chance is virtually 100% and it decreases almost linearly for higher values of χ up to the level that stochasticity completely dominates the deracemization outcome for $\chi = 1$.

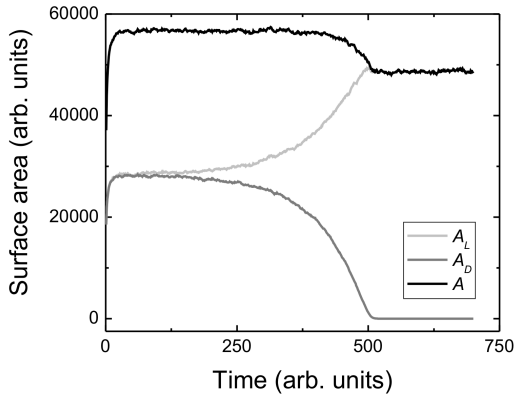

Figure 3.8. The total crystal surface area during the deracemization process shown in Figure 3.3 with A_D and A_L the total crystal surface areas of the D and L crystals, respectively, and A sum of these two.

3.2.5 Time Dependence of the Deracemization Process

The deracemization described here is a near equilibrium process in which the combined processes of dissolution and crystallization in the absence of attrition would result in a slowing down of enantiomeric purification as a result of the CSDs evolving to larger crystals. The crystals are, however, continuously broken by grinding which leads to quasi steady state

CSDs as can be seen in Figure 3.3. The CSDs only change appreciably at the very beginning of the deracemization process and at the end, where the *ee* approaches unity. Figure 3.8 shows that the corresponding total crystal surface area, A, remains approximately constant during the major part of the process. Therefore, we can write:

$$A_D(t) + A_L(t) \approx A \,, \tag{3.4}$$

with A_D and A_L the total crystal surface areas of the solids of D and L, respectively. We observe that a small initial *ee* of one enantiomer results in the emergence of a single chiral solid phase of the initially most abundant enantiomer. This deracemization is driven by the process of Ostwald ripening. During the major part of the deracemization, the Ostwald process leads to a transfer of crystal surface area from one enantiomer to the other as can be seen in Figure 3.8. Overall, the number of successful Ostwald events per time interval, corresponding to the attachment of a molecule to the crystal surface of the increasing population and the detachment of a molecule from the surface of the decreasing population, is linearly dependent on the difference in available crystal surface area of the two populations. Therefore, one can write the conversion of the solids in time as:

$$-\frac{dA_L}{dt} = \frac{dA_D}{dt} = k(A_D - A_L) = k(2A_D - A) \tag{3.5}$$

with k the rate constant for a given attrition-ripening ratio. After integration this results in:

$$\ln\left[\frac{2A_D(t) - A}{2A_D(0) - A}\right] = kt \tag{3.6}$$

for solid D. This equation can be expressed as a function of the enantiomeric excess in the solid phase assuming steady state normalized CSDs for both populations:

$$ee = \frac{N_D - N_L}{N_D + N_L} \approx \frac{A_D - A_L}{A_D + A_L} = \frac{2A_D - A}{A} \tag{3.7}$$

resulting in:

$$ee(t) = ee(0)\exp(kt) \,. \tag{3.8}$$

The initial *ee* is thus amplified exponentially. This first order kinetics expression can now be used to fit the simulated as well as the experimental results. Figure 3.9 shows a plot of ln(*ee*) versus time for the deracemizations of Figure 3.5. Clearly an exponential behavior is observed for the major part of the deracemization process. The experimental results for compound **1** are plotted in Figure 3.10 for various values of the initial *ee*.[8] In both figures the deracemization rate constant k turns out to have approximately the same value for all initial enantioimbalances. The rate constant k does depend, however, on the attrition-ripening ratio ξ (Figure 3.4) and the racemization efficiency χ (Figure 3.7). This was recently confirmed experimentally by the observation that adding more base, which catalyses racemization, to the system of compound **1** shortens the deracemization times considerably.[28]

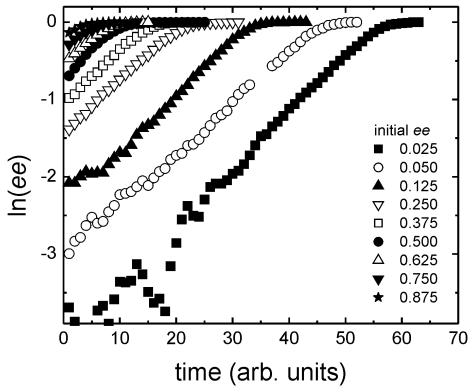

Figure 3.9. ln(ee) versus time for the experiments with small initial imbalances in the ee (Figure 3.5).

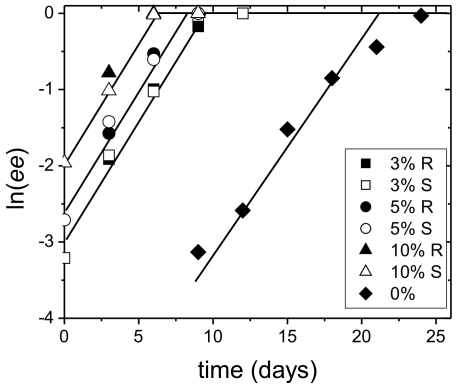

Figure 3.10. The logarithm of the ee versus time for various initial ee's of an amino acid derivative in acetonitril. The data are obtained from Figure 2.1 in Chapter 2. All ee values have been determined using chiral HPLC, except for the values at $t = 0$ which were calculated from the initial solid ee values and corrected for the solubility. The HPLC detection limit is estimated to be ee ≈ 5%. The lines are drawn as a guide to the eye.

3.2.6 Mechanism

In the deracemization process an imbalance in the populations of the two enantiomers, caused either by an initial enantioimbalance or stochastically by attrition, leads to a single chiral end state. Two mechanisms play a crucial role. The stochastic process of attrition leads to a non-deterministic evolution of the system. On the other hand, if the racemization mechanism is not instantaneous, the homochiral Ostwald ripening is more effective than the heterochiral. This drives the system deterministically to an end state corresponding to the larger crystals (Figure 3.3). To understand the interplay of the two mechanisms, we consider a system with initially isomorphous CSDs for various values of χ and ξ (Figure 3.11).

- We first consider the case for which $\chi = 0$ and $\xi = 0$, that is, a stagnant solution in which no racemization is involved. In that case, Ostwald ripening eventually leads to two single crystals of either handedness. This process will be very slow. An initial imbalance in the population of the solids of the two enantiomers, with isomorphous CSDs, leads to the lowest Gibbs free energy for the enantiomer in excess as a result of smaller surface to volume ratio.
- In case $0 < \chi << 1$ and $\xi = 0$, that is, a stagnant solution in which the racemization rate is small compared to the rate of Ostwald ripening, the end state will eventually be a single

crystal. The handedness of this crystal is still determined by the enantiomer initially in excess as a result of the slow racemization. Achieving the end state will take a very long time.

- If in addition attrition is applied ($\xi > 0$), the racemization rate will hardly be affected, but the rate of Ostwald ripening increases. The end state will therefore again be of single chirality consisting of many crystals of the enantiomer initially in excess (Figure 3.5). More importantly, the deracemization time will be smaller (Figure 3.4). The evolution to the end state will become less deterministic for values of the racemization efficiency approaching unity.
- In the limiting case of instantaneous racemization in solution ($\chi = 1$) the racemization rate and the Ostwald ripening rate are no longer distinguishable. As a result, the chance of finding either enantiomer as the end state equals the initial enantiomeric excess. This is clear for a stagnant solution ($\xi = 0$). In case of attrition, the model shows that this still holds.

In other words, the deracemization process is stochastic for instantaneous racemization in solution ($\chi = 1$). In case of a stagnant solution the end state will have a lower Gibbs free energy. When attrition is applied the CSDs rapidly reach a steady state situation. In this steady state, the relatively slow process of deracemization leads to a single chiral end state, without a further change in Gibbs free energy. This can be seen in the total crystal surface area which remains constant. Thus, there is no overall thermodynamic driving force in the case of instantaneous racemization and the single chiral end state is a trap from which the system will not escape as long as there is no primary nucleation. The situation is different for non-instantaneous racemization in solution ($\chi < 1$). During the deracemization the increasing imbalance in the populations of the two enantiomers leads to an increasing frequency for the homochiral Ostwald ripening events for the enantiomer in excess. Therefore, the overall Ostwald ripening process becomes increasingly efficient for this enantiomer. The resulting decreasing total crystal surface area offers the overall driving force towards a lower Gibbs free energy which can be seen in Figure 3.8.

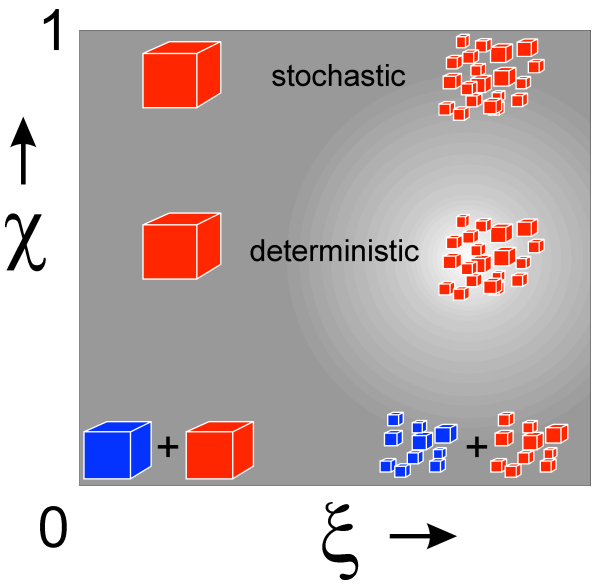

Figure 3.11. Schematic drawing of the end states of attrition enhanced Ostwald ripening as a function of the racemization efficiency χ and the attrition-ripening ratio ξ starting from a racemic mixture of enantiomorphic crystals. For values of $\chi \approx 1$ the process is stochastic. For intermediate values of χ the end state is reached in a deterministic way, amplifying small initial imbalances. The background brightness is an indication for the minimal deracemization time.

Our explanation for the deracemization process is also relevant for a discussion in the recent literature on the driving mechanism behind the process.[20-21] Setting aside the dispute, which was a main item in that discussion, on how to interpret Gibbs' phase rule and Meyerhoffer's double solubility rule in such systems, we will address the most relevant points one-by-one.

(i) As we have shown, primary nucleation does not play an essential role in the process.

(ii) The arguments used in the discussion to determine the most stable state of the system overlook the fact that in a stagnant solution the only stable state is that of one single crystal, which obviously is enantiopure. Lowering the total surface free energy provides the driving force to that stable state.

(iii) A distinction between homochiral and heterochiral events is important in order to parameterize the racemization efficiency in the solution. Chiral clusters could play a role but are not needed to explain the deracemization process.

(iv) The distinction between non-instantaneously and instantaneously racemizing solutions is essential. It does not arise from Gibbs' phase rule, but from the effect it has on the way the system evolves to single chirality as described by the racemization efficiency parameter χ.

3.3 Conclusions

We have developed a model that explains the complex behavior of enantiomorphic crystals in contact with a solution in which racemization occurs, continuously perturbed by attrition. Simulations based on the model show that Ostwald ripening drives such a system to a single chiral end state for the solid phase. The deracemization time for the solid phase is determined by two parameters, namely the attrition-ripening ratio ξ and the solution racemization efficiency χ. By choosing a moderate racemization efficiency, the handedness of the end state can be dictated by a small initial imbalance in the crystal size distributions (CSDs), either as an enantiomeric excess, or as a relative shift in the size of the crystals. The evolution to the single chiral end state can, in that case, be described by first order kinetics. The same behavior was found experimentally. The deracemization rate constant k can be increased by increasing the solution racemization efficiency χ. Paradoxically, the deracemization time for instantaneous racemization in solution ($\chi = 1$) is longer when compared with the case of relatively slow racemization ($\chi = 0.1$) (Figure 3.7). The reason for this is the stochastic behavior for $\chi = 1$, which is suppressed for smaller values of χ.

Thus, the model offers the ability to control and optimize this deracemization process under near equilibrium conditions.[28] The absence of the need for primary nucleation circumvents two drawbacks otherwise encountered.[29,30] The outcome of a process involving primary nucleation is difficult to control with a yield limited by the solubility of the compound. Therefore, the near equilibrium deracemization process is a promising and robust tool of industrial importance for the production of enantiopure pharmaceuticals.

In a broader perspective, the combination of stochastic attrition and Ostwald ripening is a selection process based on the principle of survival of the fittest, the fittest group consisting of more and/or larger crystals. The results presented elucidate a suggested route to enantiopure molecules that form the building blocks for the evolution of life.

3.4 References

[1] L. Pasteur, *C.R. Hebd. Séanc. Acad. Sci. Paris* **1848**, *26*, 535.
[2] F. C. Frank, *Biochim. Biophys. Acta* **1953**, *11*, 459.
[3] M. Calvin, *Molecular Evolution.* (Oxford Univ. Press, Oxford, UK, 1969).
[4] R. Plasson, D. K. Kondepudi, H. Bersini, A. Commeyras, K. Asakura, *Chirality* **2007**, *19*, 589.
[5] K. Soai, T. Shibata, H. Morioka, K. Choji, *Nature* **1995**, *387*, 767.

[6] J. Jacques, A. Collet, S. H. Wilen, *Enantiomers, Racemates and Resolution* (Krieger, Florida, 1994).
[7] C. Viedma, *Phys Rev. Lett.* **2005**, *94*, 065504.
[8] W. L. Noorduin, T. Izumi, A. Millemaggi, M. Leeman, H. Meekes, W. J. P. van Enckevort, R. M. Kellogg, B. Kaptein, E. Vlieg, D. G. Blackmond, *J. Am. Chem. Soc.* **2008**, *130*, 1158.
[9] E. Havinga, *Chem. Weekblad* **1941**, *38*, 642.
[10] E. Havinga, *Biochem. Biophys. Acta* **1954**, *13*, 171.
[11] D. H. R. Barton, G. W. Kirby, *J. Chem Soc.* **1962**, 806.
[12] R. E. Pincock, R. R. Perkins, A. S. Ma, K. R. Wilson, *Science* **1971**, *174*, 1018.
[13] L.Addadi, L. Z. Berkovitch-Yellin, N. Domb, E. Gati, M. Lahav; L. Leiserowitz, *Nature* **1982**, *296*, 21.
[14] J. Van Mil, L. Addadi, M. Lahav, *Tetrahedron* **1987**, *43*, 1281.
[15] D. K. Kondepudi, R. J. Kaufman, N. Singh, *Science* **1990**, *250*, 975.
[16] D. K. Kondepudi, K. L. Bullock, J. A. Digits, P. D. Yarborough, *J. Am. Chem. Soc.* **1995**, *117*, 401.
[17] J. H. E. Cartwright, J. M. García-Ruiz, O. Piro, C. I. Sainz-Díaz, I. Tuval, *Phys. Rev. Lett.* **2004**, *93*, 035502.
[18] R. Plasson, D. K. Kundepudi, K. Asakura, *J. Phys. Chem. B* **2006**, *110*, 8481.
[19] R.-Y. Qian, G. D. Botsaris, *Chem. Eng. Science* **1998,** *53*, 1745.
[20] (a) J. Crusats, S. Veintemillas-Verdaguer, J. M. Ribó, *Chem. Eur. J.* **2006**, *12***,** 7776. (b) J. Crusats, S. Veintemillas-Verdaguer, J. M. Ribó, *Chem. Eur. J.* **2007**, *13***,** 10303.
[21] (a) D. G. Blackmond, *Chem. Eur. J.* **2007**, *13*, 3290. (b) D. G. Blackmond, *Chem. Eur. J.* **2007**, *13*, 10306.
[22] M. Uwaha, *J. Phys. Soc. Jpn.* **2004**, *73*, 2601.
[23] Y. Saito, H. Hyuga, *J. Phys. Soc. Jpn.* **2005**, *74*, 2.
[24] C. Viedma, *Astrobiol.* **2007**, *7*, 312.
[25] J. W. Gibbs, *Collected works Vol. I, Thermodynamics.* (Yale University Press, New Haven, USA, 1948).
[26] W. Ostwald, *Lehrbuch der Allgemeinen Chemie, vol. 2, part 1*. (Leipzig, Germany, 1896).
[27] M. Beinfait, R. Kern, *Bull. Soc. Fran. Mineral. Crys.* **1964**, *87*, 604.
[28] W. L. Noorduin, H. Meekes, W. J. P. van Enckevort, A. Millemaggi, M. Leeman, B. Kaptein, R. M. Kellogg, E. Vlieg, *Angew. Chem.* **2008,** *120,* 6545.
[29] K. M. J. Brands, A. J. Davies, *Chem. Rev.* **2006,** *106,* 2711.
[30] D. A.Chaplin, N. B. Johnson, J. M. Paul, G. A. Potter, *Tetrahedron Lett.* **1998,** *39*, 6777.

Chapter 4

Complete Deracemization by Attrition Enhanced Ostwald Ripening Elucidated

4.1 Introduction

Direct resolution by crystallization of racemic mixtures, induced by seeding or by adding tailor-made additives, forms an attractive alternative to separation using diastereomeric salts.[1-4] Unfortunately, the yield of such resolutions is limited as a result of the maximum attainable supersaturation. Combination of a direct resolution with racemization in the solution permits a total enantiomeric transformation.[5-14] Such a complete resolution in a single operation would be of great practical use but, examples have been limited to achiral molecules.[15,16]

Recently, inspired by the work of Viedma, proof of principle was given by means of a novel deracemization method in which a racemic solid phase consisting of conglomerate crystals in contact with a solution in which racemization occurs evolves smoothly to a single chiral solid end state on application of abrasive grinding.[17] This was demonstrated for the racemic conglomerate *N*-(2-methylbenzylidene)-phenylglycine amide **1** (Figure 4.1), which is used in the synthesis of semi-synthetic antibiotics like ampicillin, cefalexin and cefaclor. If the process is carried out starting with a mixture slightly enriched in one enantiomer in the solid phase, the solid phase is completely converted into the major enantiomer via the solution phase racemization reaction. Within a few weeks either solid enantiomer can be obtained at will quantitatively and with an enantiomeric excess *ee* > 99.9%.

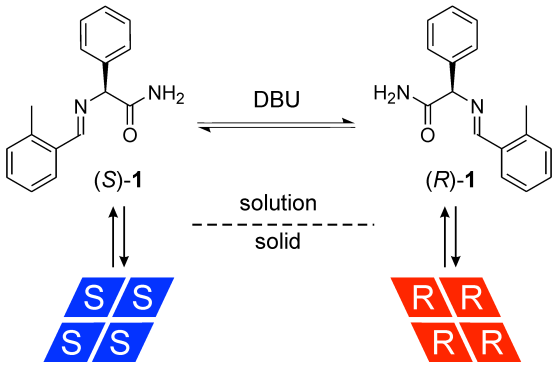

Figure 4.1. Chemical and physical equilibria in the process of attrition enhanced crystallization/dissolution for compound **1**.

In Chapter 3 Monte Carlo simulations led to a model that showed that two processes are responsible for the deracemization: continuous attrition of crystals and Ostwald ripening, which leads to growth of large crystals at the cost of smaller ones.[18-20] Here we explore the essential parameters of this deracemization process as derived from theory by varying the experimental conditions. The insight obtained into the underlying process of attrition enhanced Ostwald ripening also allows definition of suitable conditions to increase the deracemization rate drastically.

4.2 Results and Discussion

First, we express the Monte Carlo simulation model in terms of the experimental parameters. In the model three parameters are crucial. First, the rate at which molecules racemize in solution is described by the racemization efficiency χ. Second, the continuous ablation of crystals is determined by an attrition probability ζ, and, third, the growth of larger crystals at the cost of smaller crystals proceeds according to the Ostwald ripening probability κ. The simulation results confirmed the experimentally observed exponential behavior typical for asymmetric autocatalysis, of the time evolution of the enantiomeric excess *ee* in the solid state according to:[20]

$$ee(t) = ee(0)\exp(kt)\,, \tag{4.1}$$

for not too small values of the initial enantiomeric excess *ee*(0).[21] The deracemization rate constant *k* (see appendix) can be expressed in terms of the three parameters according to:

$$k = \frac{\nu_0}{b_{solid}}\chi\kappa\zeta\,, \tag{4.2}$$

where the proportionality parameter v_0 is an event frequency and b_{solid} the amount of solid material written as a molality.[22] The racemization efficiency via the solution, χ, depends on the amount of the racemization catalyst, b_{rc}. Assuming a linear relationship we can write $\chi = \alpha_{\chi,solv}\, b_{rc}$, where the proportionality constant $\alpha_{\chi,solv}$ depends on the solvent used. The Ostwald ripening probability κ is determined by the solute exchange frequency between the solution and the crystallites, which in turn depends on the surface free energy of the crystallites in the solution. Nielsen and Söhnel have shown that a logarithmic relation exists between the surface free energy and the solubility.[23] Using this relation, the Ostwald ripening probability κ can be shown to be proportional to the solubility b_{solute}, according to $\kappa = \alpha_{Ost}\, b_{solute}$ (see appendix). The attrition probability ζ is not further specified in experimental terms, as this depends on complicated parameters like the stirring speed, the grinding agents used and the crystal hardness.[24] Combination of all the relations leads to the following expression for the deracemization rate constant *k*:

$$k = \frac{\nu_0}{b_{solid}}\alpha_{\chi,solv} b_{rc} \alpha_{Ost} b_{solute} \zeta\,. \tag{4.3}$$

Using this equation we have studied the dependencies of the deracemization rate experimentally.

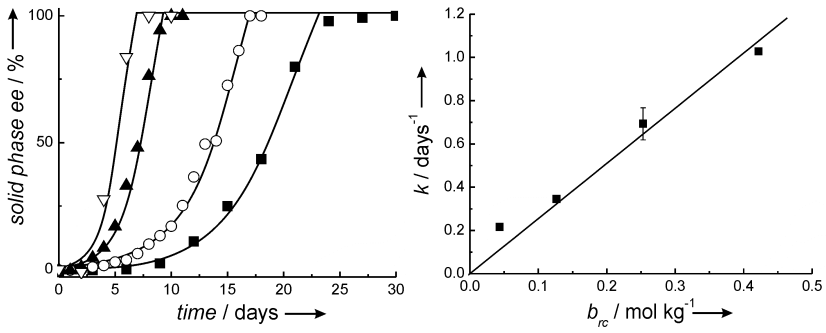

Figure 4.2. The evolution of the solid phase *ee* in MeCN for different amounts of DBU: 0.42 (▽), 0.25 (▲), 0.13 (○) and 0.04 mol kg^{-1} (■) (Lines are provided as a guide to the eye) (left). From these data, the rate constant *k* is obtained according to Equation (4.1) (right).

To determine the effect of the amount of racemization catalyst, we performed deracemization experiments for various DBU molalities b_{rc} using MeCN as a solvent (Figure 4.2, left).[25] Fitting the data to Equation (4.1) shows that the rate constant k increases linearly with increasing b_{rc} (Figure 4.2, right).
Figure 4.3 shows the dependence of the deracemization rate on the amount of solid material, b_{solid}, in MeCN with all other parameters fixed. As expected, the rate constant k is inversely proportional to the amount of solid material b_{solid}.

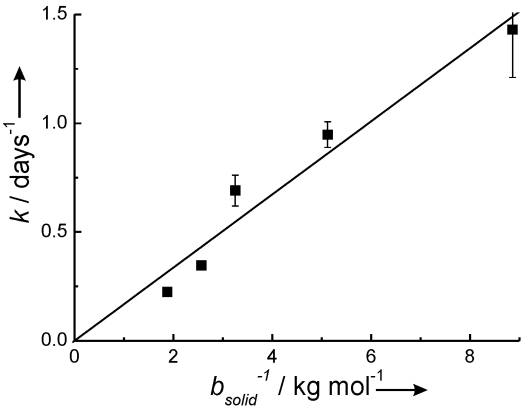

Figure 4.3. The deracemization constant k as a function of b_{solid}^{-1} in MeCN (35 g) with 0.13 mol kg^{-1} DBU.

To study the effect of the solvent toluene was used as a low solubility solvent (0.4 wt% at 25 °C) and tetrahydrofuran (THF) as a good solvent (6.8 wt%), as compared to acetonitrile (MeCN) (2.2 wt%). In toluene, after 30 days the enantiomeric excess in the solid phase was merely 10% (Figure 4.4). As expected, for the solvents with a higher solubility, MeCN and THF, the deracemization is faster and complete chiral purity is reached after 21-24 days.
The measured solubilities b_{solute}, the solvent dependent racemization parameters $\alpha_{\chi,solv}$, the amount of solid material b_{solid} and the normalized deracemization rate constant k_{theo}, calculated using Equation (4.3), are given in Table 4.1; ζ is kept constant. The decreasing trend in the experimental rate constants for the three solvents is also found for the theoretical values. These results show that for practical applications the efficiency increases on use of a good solvent but that the solution racemization rate must be considered as well. On comparison of MeCN and THF, the latter has the higher solubility but the former has a higher racemization rate constant (appendix) resulting in the highest deracemization rate in MeCN.

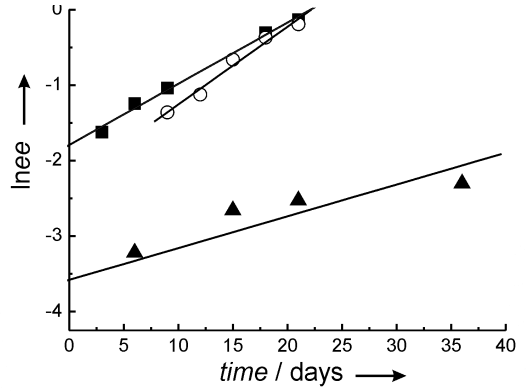

Figure 4.4. The evolution of ln *ee* in the solid phase for the deracemization experiments in THF (■),MeCN (○) and toluene (▲) .

Table 4.1. Comparison of the theoretical deracemization rate k_{theo} and the experimentally observed deracemization rate k_{exp}.

	b_{solute}	b_{solid}	b_{rc}	$\alpha_{\chi,solv}$ [a,b]	k_{theo} [a,c]	k_{exp} [a,d]
MeCN	0.088	0.387	0.0573	1.00	1.00	1.00
THF	0.287	0.390	0.0409	0.23	0.53	0.77
Toluene	0.018	0.204	0.0177	0.31	0.04	0.16

[a] Normalized for MeCN. [b] The solution racemization rates were determined in saturated solutions for the three different solvents without any solid present (appendix). [c] Calculated using Equation (4.3). [d] Determined from the data in Figure 4.4.

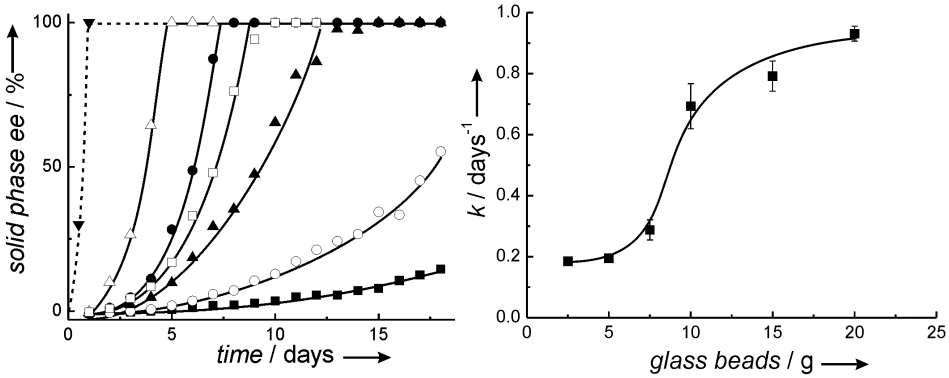

Figure 4.5. The evolution of the *ee* as a function of the amount of glass beads in grams, 2.5 (■), 5.0 (○), 7.5 (▲), 10.0 (□), 15.0 (•), 20.0 g (Δ), for a constant amount of DBU (0.25 mol kg^{-1}) and 4 g of **1** in MeCN (35 g) (left). Additionally the deracemization was perfomed under these conditions with 15.0 g glass beads using an ultrasonic bath (▼). From these results, the rate constant *k* as a function of the amount of glass beads is obtained using Equation (4.1) for a constant amount of DBU (0.25 mol kg^{-1}) in MeCN (right). The lines are provided as a guide to the eye.

All experiments described thus far were performed at constant stirring rates and amounts of glass beads. This results in an approximately constant crystal size distribution (CSD) during the process. The computer simulations, however, predict that the deracemization process can be enhanced by applying intense attrition conditions leading to a CSD of smaller crystals.[20] Therefore, the influence of the attrition on the deracemization time was explored by varying the amount of glass beads. As expected, the deracemization time decreases for increasing amounts of glass beads as the crystals are ground to smaller sizes (Figure 4.5).[26] The shape of the curve shows that the relation between the amount of glass beads and *k* in Equation (4.3) is rather complicated. Note that even in the absence of glass beads, the magnetic stirrer will cause attrition of crystals. To intensify the grinding even more, we repeated the experiment with 15 g glass beads (see Figure 4.5), now using a thermostated standard ultrasonic bath instead of magnetic stirring. These experiments led to an approximately five times higher rate, reducing the deracemization time to one single day (Figure 4.5). As predicted from Equation (4.1) a further decrease in the deracemization time can be realized by starting with a solid state that is already enriched, instead of beginning with almost racemic material.[27]

4.3 Conclusions

The rate of the emergence of a single chiral solid state during grinding of a slurry has been studied. The insight obtained into the underlying process of attrition enhanced Ostwald

ripening also allows definition of suitable conditions to increase the deracemization rate drastically, making this a practical route to enantiopure compounds.

4.4 References and Notes

[1] H. Murakami, *Top. Curr. Chem.* **2007**, *269*, 273.
[2] J. Jacques, A. Collet, S. H. Wilen, *Enantiomers, Racemates and Resolution* (Krieger, Florida, **1994**).
[3] L. Addadi, Z. Berkovitch-Yellin, N. Domb, E. Gati, M. Lahav, L. Leiserowitz, *Nature* **1982**, *296*, 21.
[4] L. Addadi, S. Weinstein, E. Gati, I. Weissbuch, M. Lahav, *J. Am. Chem. Soc.* **1982**, *104*, 4610.
[5] a) E. Havinga, *Chem. Weekblad* **1941**, *38*, 642; b) E. Havinga, *Biochem. Biophys. Acta* **1954**, *13*, 171.
[6] D. H. R. Barton, G. W. Kirby, *J. Chem. Soc.* **1962**, 806.
[7] R. E. Pincock, R. R. Perkins, A. S. Ma, K. R. Wilson, *Science* **1971**, *174*, 1018.
[8] J. Van Mil, L. Addadi, M. Lahav, *Tetrahedron* **1987**, *43*, 1281.
[9] S. N. Black, L. J. Williams, R. J. Davey, F. Moffatt, R. V. H. Jones, D. M. McEwan, D. E. Sadler, *Tetrahedron* **1989,** *45*, 2677.
[10] D. K. Kondepudi, R. J. Kaufman, N. Singh, *Science* **1990**, *250*, 975.
[11] B. Kaptein, T. R. Vries, J. W. Nieuwenhuijzen, R. M. Kellogg, R. F. P. Grimbergen, Q. B. Broxterman, *Handbook of Chiral Chemicals* (CRC Press-Taylor & Francis Group, New York, **2006**) 97-116.
[12] R. Yoshioka, *Top. Curr. Chem.* **2007**, *269*, 83.
[13] K. M. J. Brands, A. J. Davies, *Chem. Rev.* **2006,** *106,* 2711.
[14] D. A. Chaplin, N. B. Johnson, J. M. Paul, G. A. Potter, *Tetrahedron Lett.* **1998,** *39*, 6777.
[15] C. Viedma, *Phys. Rev. Lett.* **2005**, *94*, 065504.
[16] P. S. M. Cheung, J. Gagnon, J. Surprenant, Y. Tao, H. Xu, L. A. Cuccia, *Chem. Comm.* **2008,** 987.
[17] W. L. Noorduin, T. Izumi, A. Millemaggi, M. Leeman, H. Meekes, W. J. P. van Enckevort, R. M. Kellogg, B. Kaptein, E.Vlieg, D. G. Blackmond, *J. Am. Chem. Soc.* **2008**, *130*, 1158.
[18] Viedma, C. *Astrobiol.* **2007**, *7*, 312.
[19] J. H. E. Cartwright, O. Piro, I. Tuval *Phys Rev. Lett.* **2007,** *98,* 165501.
[20] W. L. Noorduin, H. Meekes, A. A. C. Bode, W. J. P. van Enckevort, B. Kaptein, R. M. Kellogg, E. Vlieg, *Cryst. Growth Des.* **2008**, *8*, 1675.
[21] The simulations show that in the case of instantaneous racemization in the solution the deracemization process becomes stochastic. Here, we limit the discussion to relatively low racemization efficiencies ($\chi \leq 0.1$, SI) and nonzero values for *ee*(0), for which the process becomes deterministic.
[22] Throughout this chapter we express amounts in terms of molalities *b* (mol per kg solvent).
[23] A. E. Nielsen, O. Söhnel, *J. Cryst. Growth* **1971**, *11*, 233.
[24] H. Briesen, *Powder Technol.* **2007**, *178,* 87-98.
[25] The linearity of the relationship between the solution racemization time and the DBU concentration was also checked (appendix).
[26] The computer simulations show a minimum in the deracemization time as a function of the attrition probability ζ, which was found at high attrition rates, for which the CSD is dominated by the minimal crystal size that can be obtained by attrition (appendix).
[27] Starting with $ee(t=0) \neq 0$ also suppresses stochastic behavior at low *ee* values.[20]
[28] As expected from Equation (3), scaling up of all parameters in the experiment has no influence on the deracemization rate. This was verified by performing experiments at a 5 times larger scale (ca. 20 g (*RS*)-**1**, 0.25 mol kg^{-1} DBU, 50 g glass beads, 175 g MeCN). The enantiopure end state was reached in 7 days, which shows that the deracemization rate indeed is independent of the system size (cf. Figure 4.2).

Chapter 5

Attrition Enhanced Deracemization of a Natural Amino Acid Derivative that forms an Epitaxial Racemic Conglomerate

5.1 Introduction

Unravelling of the origins of single chirality as found in Nature is a fundamental scientific goal. Such understanding has practical ramifications for the preparation of enantiopure compounds including pharmaceutical components. Separate *R* and *S* solid phases (known as racemic conglomerates) were the starting point for obtaining enantiopure compounds from racemic mixtures, when Pasteur manually sorted the mirror-image crystals of a tartrate salt.[1] In the direct resolution of conglomerates the desired handedness can be obtained more efficiently using preferential crystallization through stereoselective seeding or by using enantiomerically pure tailor-made additives.[2-5] Although applied nowadays on an industrial scale, the crystallization yields are limited and often this type of resolution is hampered by mutual epitaxial growth of the enantiomers.[6] In such cases, enantioselective seeding is of no use.

In this perspective, the recently reported attrition enhanced complete deracemization of $NaClO_3$ and other achiral salts is of interest as it works under near-equilibrium conditions.[7,8] On application of this abrasive grinding technique to the solid phase of a nearly racemic nonproteogenic amino acid derivative, in contact with a saturated solution in which racemization takes place, the solid phase smoothly evolved to a single chiral end state.[9,10] An explanation for this deracemization process was given in terms of attrition enhanced Ostwald ripening.[11-13] In this Chapter we describe the attrition enhanced total resolution of a conglomerate derivative of the natural racemic amino acid phenylalanine, but with the complication of epitaxial behavior. Furthermore we provide support for the role of Ostwald ripening in this process.

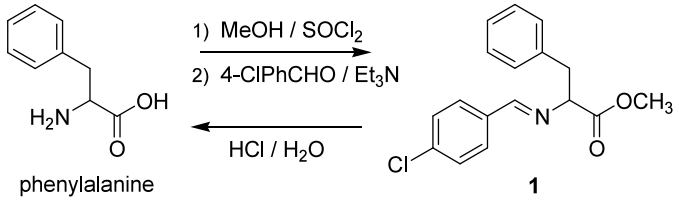

Scheme 5.1. Synthesis of **1** from phenylalanine.

5.2 Results and Discussion

The compound (*RS*)-*N*-(4-chlorobenzylidene)phenylalanine methyl ester **1** was chosen as the starting material for the attrition enhanced deracemization method as the compound crystallizes as a conglomerate (Scheme 5.1).[14] Because of the relatively acidic proton at the

α-carbon of **1** this compound can be readily racemized under basic conditions (pKa = 19.0).[15] The X-ray crystal structure determination of single crystals grown from an isopropanol solution of (*S*)-**1** revealed that this compound crystallizes in space group $P2_12_12_1$ (Figure 5.1, see appendix). The relatively heavy chloride atom permits assignment of the absolute configuration using anomalous dispersion.[16] Crystals grown both from racemic and enantiomerically pure solutions of **1** were analyzed using X-ray powder diffraction. The patterns were identical and in good resemblance with that calculated from the single crystal structure. However, analyses using chiral HPLC of individual crystals grown from the racemic solution revealed these crystals to be almost racemic, inconsistent with expectations for a conglomerate.

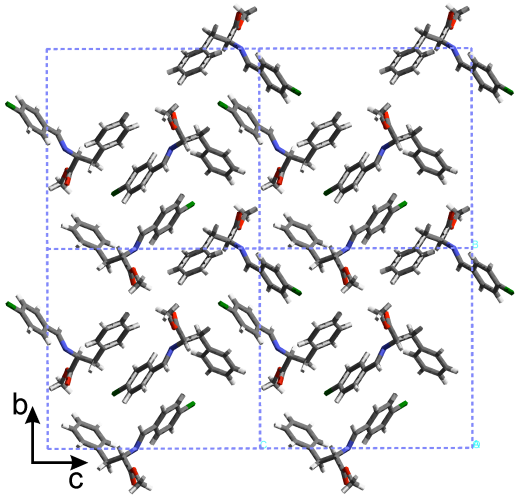

Figure 5.1. Crystal structure of the unit cell of (*S*)-**1**.

This paradoxical situation was further investigated by partial dissolution of the crystals grown from the racemic mixture in a saturated enantiomerically pure solution.[6i,17] Using optical microscopy the enantioselective dissolution of fragments of the crystal was observed (Figure 5.2). This indicates that the crystals are composed of domains of single chirality.

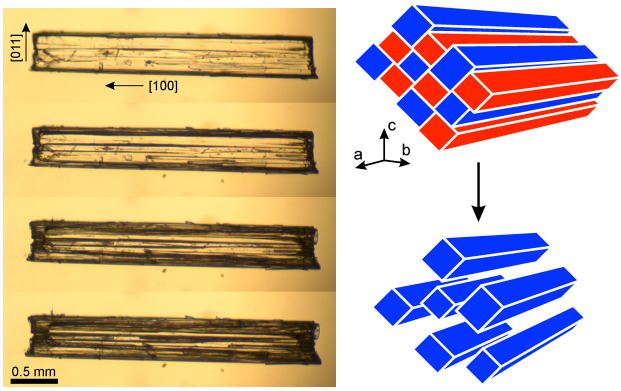

Figure 5.2. Optical microscopy images showing the partial dissolution of (*RS*)-**1** in a saturated solution of (*S*)-**1** in isopropanol (10 min. time interval between images) (left). Schematic representation of the enantioselective dissolution; the enantiomorphs of *R* and *S* are colored red and blue, respectively (right).

Using polarization microscopy and X-ray diffraction, it was observed that these domains were all well ordered as match-shaped crystallites stacked parallel to the crystallographic [100] direction. The morphology of the resulting epitaxial conglomerate is made up of {100} top faces and {011} side faces in terms of the crystallographic axes of the individual domains. Because the enantiomers crystallize epitaxially on each other the technique of resolution by preferential crystallization cannot be applied straightforwardly.

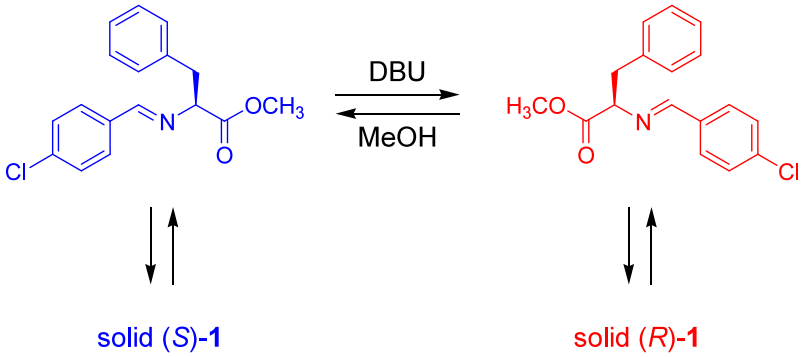

Scheme 5.2. Chemical and physical equilibria in the process of attrition enhanced crystallization/dissolution of **1**.

Intrigued by this challenge we tried to deracemize these epitaxial conglomerate crystals to a single chiral solid phase using the recently developed method of attrition enhanced Ostwald ripening (Scheme 5.2).[9,10] For these near-equilibrium deracemization experiments, scalemic mixtures of **1** (3.2 g) were suspended in MeOH (10.0 g) and ground using a magnetic stirring bar and glass beads (6.0 g). After solution-solid equilibrium had been reached, the solution racemization was initiated by addition of the base DBU (10 mol% based on **1**).[18,19] Samples of the solid were collected over time and the enantiomeric purity was measured using chiral HPLC. We found that even slight initial enantio-imbalances of 0.3% enantiomeric excess *ee* in **1** direct the deracemization within 4-5 days to the enantiomerically pure solid state of the enantiomer initially in excess (Figure 5.3; appendix for opposite enantiomer). As expected, the time evolution of the *ee* in the solid state follows the exponential behavior typical for this process (Figure 5.3, right).[10,13] Although the rate of racemization of **1** in the solution phase is relatively slow ($t_{½}$ = ca. 8 min.), the high solubility of racemic **1** of approximately 20wt% results in a relatively high deracemization rate.[10]

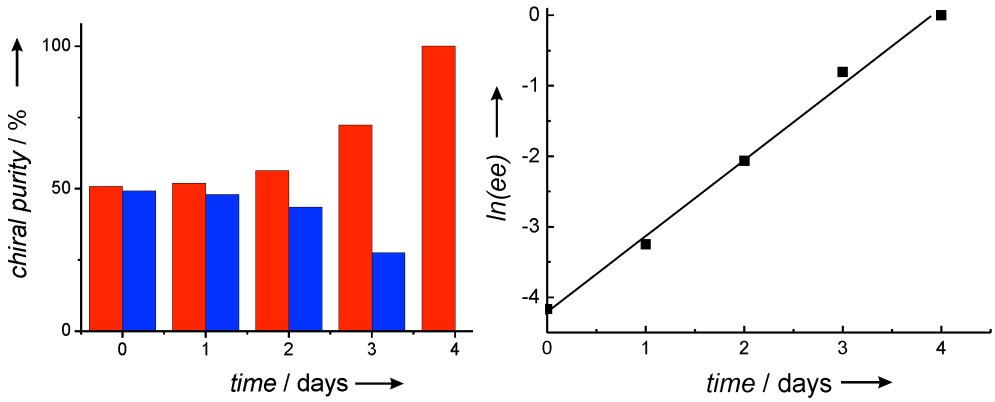

Figure 5.3. Evolution of the solid phase enantiomeric ratio during grinding (left), showing an exponential evolution of the enantiomeric excess in (*R*)-**1** (right). The initial *ee* in the solid phase before dissolution is 0.35%, and increases slightly upon dissolution.

To obtain more insight into Ostwald ripening processes we studied the effect of the crystal size distribution on the deracemization outcome. Enantiopure solution-solid mixtures were combined in which one mixture was ground by glass beads, resulting in many small crystals under racemizing conditions and the other mixture of the opposite enantiomer was only gently stirred under racemizing conditions in the absence of glass beads, so that the crystals remained relatively large. Subsequently, the latter mixture was added to the first one and the deracemization was followed in time. Even mixtures starting with an enantiomeric excess in the enantiomer of small crystals, rapidly evolve to a single chiral solid phase of the enantiomer that initially contained the large crystals (Figure 5.4; see appendix for the opposite direction). These results clearly demonstrate the Ostwald ripening character of this process, in which large crystals grow at the expense of smaller ones.

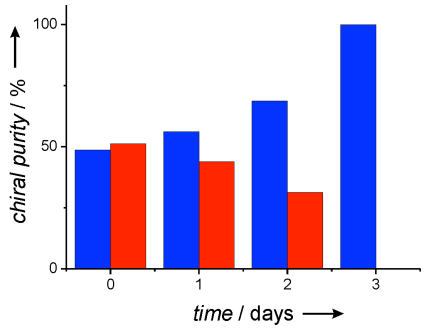

Figure 5.4. Evolution of the enantiomeric excess starting with overabundance of small (*R*)-**1** crystals and a minor population of large (*S*)-**1** crystals. The small crystals rapidly dissolve and nurture the larger (*S*)-crystals until complete symmetry breaking is achieved.

The crystal packing of **1** is mainly determined by weak Van der Waals forces, as the molecule is not able to form any H-bondings. These rather isotropic weak forces are expected to make the crystallization process more sensitive for epitaxial 2D nucleation of the opposite enantiomer. Coquerel *et al.* explained the heterochiral epitaxial nucleation resulting from an oscillating nucleation and growth process of enantiomerically pure crystals with an inversion frequency in the enantiomerically pure layers determined by diffusion limitations in the solution.[6i] The local differences in supersaturation that caused this alternating 2D nucleation were circumvented by applying smooth stirring conditions, resulting in crystals with a significant enantiomeric excess. Although in our near-equilibrium experiments primary nucleation is a rare and probably negligible process, epitaxial heterochiral nucleation cannot be excluded. The vigorous stirring and the solution phase racemization will, however, circumvent the local differences in supersaturation between the two enantiomers.[19,20] Additionally, the continued fragmentation of the crystals will more likely occur on the domain boundaries, thereby separating the enantiomorphous phases and creating a larger surface area for both.

5.3 Conclusions

The mutual epitaxial growth of enantiomers in conglomerate crystals has been frequently reported.[6] Here we use attrition enhanced deracemization to resolve the solid phase in liquid-solid mixtures of **1**. Under near-equilibrium conditions, the complete conversion of a racemic mixture of enantiomers, in the form of epitaxial racemic conglomerate crystals, into a single chiral solid phase of the desired handedness has been achieved. The observation that a population of small crystals, enantiomerically in excess, nurture the population of large

crystals of the opposite handedness supports the fundamental role of Ostwald ripening in this process. The method offers an attractive alternative in situations where the formation of epitaxial racemic conglomerates hampers the resolution by preferential crystallization.

5.4 References and Notes

[1] L. Pasteur, *C.R. Hebd. Séanc. Acad. Sci. Paris* **1848**, *26,* 535.

[2] J. Jacques, A. Collet, S. H. Wilen, *Enantiomers, Racemates and Resolution* (Krieger, Florida, 1994).

[3] L. Addadi, Z. Berkovitch-Yellin, N. Domb, E. Gati, M. Lahav, L. Leiserowitz, *Nature* **1982**, *296*, 21.

[4] L. Addadi, S. Weinstein, E. Gati, I. Weissbuch, M. Lahav, *J. Am. Chem. Soc.* **1982**, *104*, 4610.

[5] G. Coquerel, *Top. Curr. Chem.* **2007**, *269*, 1.

[6] a) S. Furberg, O. Hassel, *Acta Chem. Scan.* **1950,** *4,*1020; b) B. S. Green, M. Knossow, *Science* **1981,** *214,* 795; c) I. Weissbuch, D. Zbaida, L. Addadi, L. Leiserowith, M. Lahav, *J. Am. Chem. Soc.* **1987,** *109,* 1869; c) R. J. Davey, S. N. Black, L. J. Williams, D. M. McEwan, D. E. Sadler, *J. Cryst. Growth* **1990,** *102,* 97; d) G. A. Porter, C. Garcia, R. McCagau, B. Adger, A. Collet, *Angew. Chem.* **1996,** *108,* 1780; *Angew. Chem. Int. Ed. Engl.* **1996,** *35,* 1666; e) M. Berfeld, D. Zbaida, L. Leiserowitz, M. Lahav, *Adv. Mater.* **1999**, *11,* 328; f) D. Zbiada, M. Lahav, K. Drauz, G. Knaup, M. Kottenhahn, *Tetrahedron* **2000,** *56,* 6645; g) R. G. Kostyanovsky, K. A. Lyssenko, A. N. Kravchenko, O. V. Lebedev, G. K. Kadorkina, V. R. Kostyanovsky, *Mendeleev Commun.* **2001,** *11,* 134; h) S. Beilles, P. Cardinael, E. Ndzié, S. Petit, G. Coquerel, *Chem. Eng. Sci.* **2001,** *56,* 2281; i) C. Gervais, S. Beilles, P. Cardinael, S. Petit, G. Coquerel, *J. Phys. Chem.* **2002,** *106,* 646; j) V. Yu. Torbeev, K. A. Lyssenko, O. N. Kharybin, M. Yu. Antipin, R. G. Kostyanovsky, *J. Phys. Chem. B* **2003,** *107,* 13523; k) P. A. Levkin, V. Yu. Torbeev, D. A. Lenev, R. G. Kostyanovsky *Top. Stereochem.* **2006,** *25,* 81-134; l) J. Th. H. van Eupen, W. W. J. Elffrink, R. Keltjens, P. Bennema, R. de Gelder, J. M. M. Smits, E. R. H. van Eck, A. P. M. Kentgens, M. A. Deij, H. Meekes, E. Vlieg, *Cryst. Growth Des.* **2008,** *8,* 71.

[7] Viedma, C. *Phys. Rev. Lett.* **2005**, *94*, 065504.

[8] P. S. M. Cheung, J. Gagnon, J. Surprenant, Y. Tao, H. Xu, L. A. Cuccia, *Chem. Commun.* **2008**, 987-989.

[9] W. L. Noorduin, T. Izumi, A. Millemaggi, M. Leeman, H. Meekes, W. J. P. van Enckevort, R. M. Kellogg, B. Kaptein, E. Vlieg, D. G. Blackmond, *J. Am. Chem. Soc.* **2008**, *130*, 1158.

[10] W. L. Noorduin, H. Meekes, W. J. P. van Enckevort, A. Millemaggi, M. Leeman, B. Kaptein, R. M. Kellogg, E. Vlieg, *Angew. Chem.* **2008,** *120,* 6545.

[11] Viedma, C. *Astrobiol.* **2007**, *7*, 312.

[12] J. H. E. Cartwright, O. Piro, I. Tuval, *Phys. Rev. Lett.* **2007**, *98,* 165501.

[13] W. L. Noorduin, H. Meekes, A. A. C. Bode, W. J. P. van Enckevort, B. Kaptein, R. M. Kellogg, E. Vlieg, *Cryst. Growth Des.* **2008**, *8*, DOI: 10.1021/cg701211a.

[14] Y. Takahashi, K. Arai, Y. Obara, H. Matsumoto, JP 61103852 (Nissan Chem. Industr., Ltd. Japan 1986). (*Chem. Abst.* **105**, 43327)

[15] K. Maruoka, T. Ooi, *Chem. Rev*. **2003**, *103*, 3013-3028.

[16] J. M. Bijvoet, A. F. Peerdeman, A. J. van Bommel, *Nature* **1951,** *168,* 271.

[17] K. Toyokura, K. Mizukawa, M. Kurotani, *Crystal growth of L-SCMC seeds in a DL-SCMC solution of pH 0.5. CGOM3*; A. S. Myerson, D. A. Green, P. Meenan, Eds.; ACS Conference Proceedings Series: Washington DC, 1996; p 72.

[18] It is essential to use new glass wear, beads and stirring bars for each experiment to avoid chiral contamination, see also ref. [9] and; a) D. W. Armstrong, J. P. Kullman, X. Chen, M. Rowe, *Chirality* **2001,** *13,* 153; b) M. Lahav, I. Weissbuch, E. Shavit, C. Reiner, G. J. Nicholson, V. Schurig, *Orig. Life Evol. Biosph.* **2006,** *36,* 151; c) C. Viedma, *Cryst. Growth Des.* **2007,** *7,* 553; d) S. Osuna-Esteban, M.-P. Zorzano, C. Menor-Salván, M. Ruiz-Bermejo, S. Veintemillas-Verdaguer, *Phys. Rev. Lett.* **2008,** *100,* 146102.

[19] This might also explain the successful crystallization induced enantiomeric transformation of **1** and in the system of triazolylketone, which in the absence of solution phase racemization forms an epitaxial racemic conglomerate.[14,6c,20]

[20] S. N. Black, L. J. Williams, R. J. Davey, F. Moffatt, R. V. H. Jones, D. M. McEwan, D. E. Sadler, *Tetrahedron* **1989,** *45*, 2677.

Chapter 6

Fast Attrition Enhanced Deracemization of Naproxen by a Gradual *in-situ* Feed

6.1 Introduction

Routes to create enantiomerically pure compounds starting from prochiral or racemic components are a principal issue in the discussion on the emergence of prebiotic chiral molecules. Such routes to single handedness are also of paramount practical importance today, especially for economical high yielding processes to pharmaceutical compounds that often must be registered in enantiomerically pure form.[1]
Louis Pasteur already demonstrated that enantiomorphous crystals (a racemic conglomerate) of a tartrate salt could be separated manually.[2] Crystallization of a conglomerate is an attractive option to obtain enantiomerically pure materials provided a better means of separation than crystal picking is available. Resolution by crystallization becomes much more attractive if simultaneous racemization of the unwanted enantiomer occurs. This combination of crystallization and racemization in solution results in a so-called total 'spontaneous resolution'.[3] For this, enantiopure seeds are introduced in a clear supersaturated solution in which racemization takes place. These seeds grow further, resulting in an increasing amount of enantiopure solid material, until the solution is depleted of racemate. To reduce the nucleation rate of the undesired enantiomer the supersaturation can be lowered by introducing many secondary nuclei of the desired enantiomer through stirring.[4,5] In principle, all chiral material that crystallizes can be converted into the desired enantiomer. The theoretical yield in enantiopure solid phase is thus 100%, and in practice only limited by the solubility. To prevent the unwanted enantiomer from nucleating, however, the crystallization conditions, in particular the temperature, need to be controlled well.

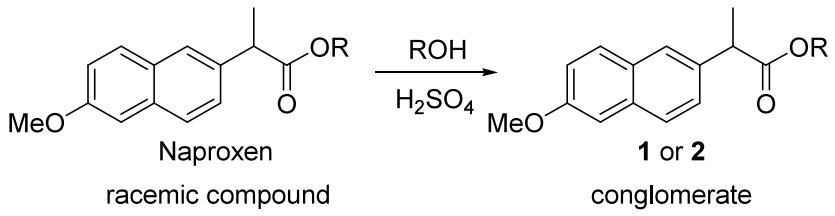

Scheme 6.1. Esterification of Naproxen to the methyl ester **1** (R=Me) or ethyl ester **2** (R=Et).

The recent demonstration of a complete deracemization using crystallization with abrasive grinding under near-equilibrium conditions is a remarkably simple and much more reliable technique to reach an enantiomerically pure end state for these systems.[6] Recently we determined the rate determining parameters for this deracemization process.[6d] In particular, we found that the deracemization time increases linearly with the amount of solids in the slurry. Furthermore, the time needed for the system to overcome the threshold of the autocatalytic process could be minimized by starting from an enantioenriched solid phase.[6c]

Would it therefore be beneficial to start with a small amount of solids having a large enantiomeric excess (*ee*), and then gradually feed the slurry under isothermal conditions with racemic material? In this way, the solid phase can sustain a high *ee*, resulting in a high deracemization rate. Overall this should shorten the time to reach an enantiopure solid phase. Although the gradual feeding can be realized mechanically, alternatively the target molecule can be synthesized *in-situ*, making the practical execution very simple. To show the practical applicability, the nonsteroidal anti-inflammatory drug (*S*)-Naproxen is used as an example.

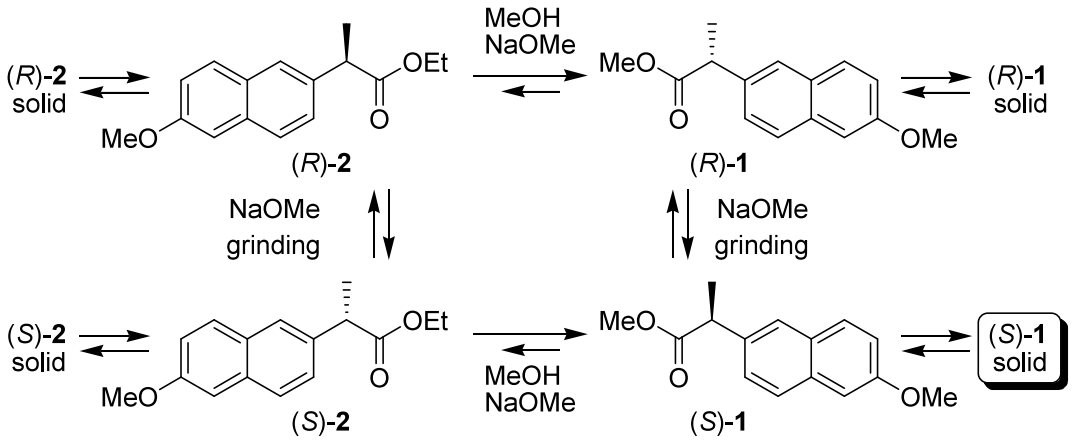

Scheme 6.2. Chemical and physical equilibria during the simultaneous transesterification and deracemization of racemic **2** into enantiopure **1**.

Naproxen itself crystallizes as a racemic compound and is therefore not suitable for a resolution as described above.[7] Remarkably its methyl ester **1** and ethyl ester **2**, both readily prepared by acid catalyzed esterification of Naproxen (Scheme 6.1), do crystallize as racemic conglomerates, i.e. as separate enantiomorphous phases.[7b,8] Both esters can easily be racemized under basic conditions. However, spontaneous resolution as described by Arai *et al.* through seeding of a clear saturated solution of (*RS*)-**1** with (*S*)-**1** and crystallization by cooling gave poor results.[8]

6.2 Results and Discussion

We here describe the complete deracemization of Naproxen methyl ester **1** by abrasive grinding of a nearly racemic crystal suspension by an *in-situ* feed via transesterification of solid racemic ethyl ester **2**. Under the basic racemization conditions compound **2** is converted reversibly into **1** using MeOH as a solvent. The solubility of **1** (7.7 wt%, 20°C) is appreciably lower than that of **2** (11.9 wt%, 20°C) in this solvent (Scheme 6.2). The reversible conversion and the difference in solubilities can be used to generate a supersaturated solution of **1**, starting from a saturated solution of **2** in contact with solid **2**, thereby gradually feeding the slurry with racemic **1**. In this way, there is no necessity to cool the system to induce nucleation.

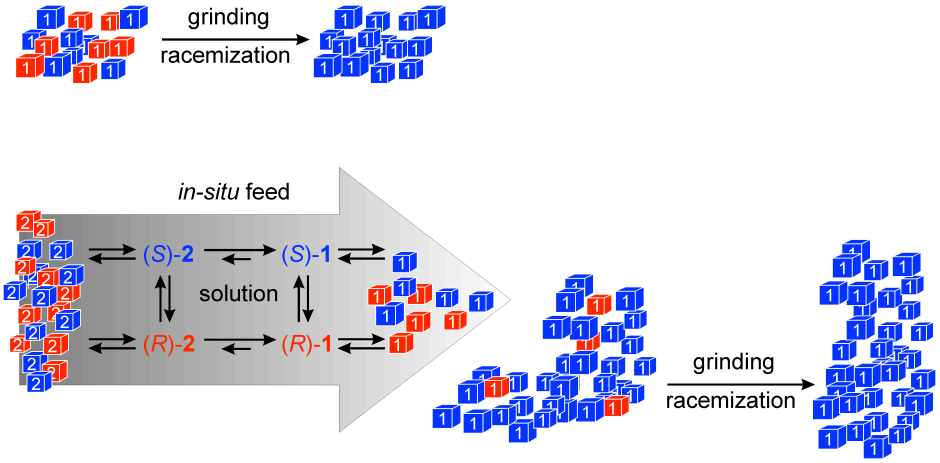

Figure 6.1. Schematic representations of the direct deracemization of **1** (top) and the one-pot deracemization using an *in-situ* gradual feed (below). In the latter process, racemic solid material **2** dissolves and is transformed into (less soluble) racemic **1**. As a result of Dimroth's principle, (*RS*)-**1** precipitates, thereby nurturing an already highly enriched solid phase of **1** which is readily deracemized under abrasive grinding conditions.[10]

We will compare the efficiency of two routes to deracemization of **1**: direct abrasive grinding of **1** and abrasive grinding using **2** as feeding material (Figure 6.1). First, (*RS*)-**1** was deracemized using abrasive grinding without the gradual feed. For that, solution-solid mixtures of methanol and (*RS*)-**1**, containing glass beads, were ground using a thermostated standard ultrasonic cleaning bath. Solution racemization was initiated using sodium methoxide. Figure 6.2 shows that an initial enantiomeric excess as low as 1.5% leads to exponential evolution to an enantiopure (*S*)-**1** solid phase.[9] Under these conditions **1** is completely stable and no decomposition products were observed. As can also be seen from the figure, starting with 20% *ee* results in the complete deracemization in 1.5-2 days. To combine this abrasive grinding deracemization with a gradual feed using the *in-situ* transesterification reaction (Scheme 6.2), a solid mixture of 92 mol% (*RS*)-**2** and 8 mol% (*S*)-**1** was partially dissolved in MeOH/NaOMe and ground using glass beads and magnetic stirring at 700 rpm.[11] Sodium methoxide is initiating both the solution phase racemization, as well as the conversion of compound **2** into **1** via transesterification. As the solubility of **1** is lower and the solvent shifts the esterification equilibrium towards the side of **1**, all solid material of **2** is converted into **1** (Figure 6.3, dashed line), following Dimroth's principle.[10,12] Simultaneously, the crystalline **1** is deracemized as a result of the grinding (Figure 6.3, solid line).]

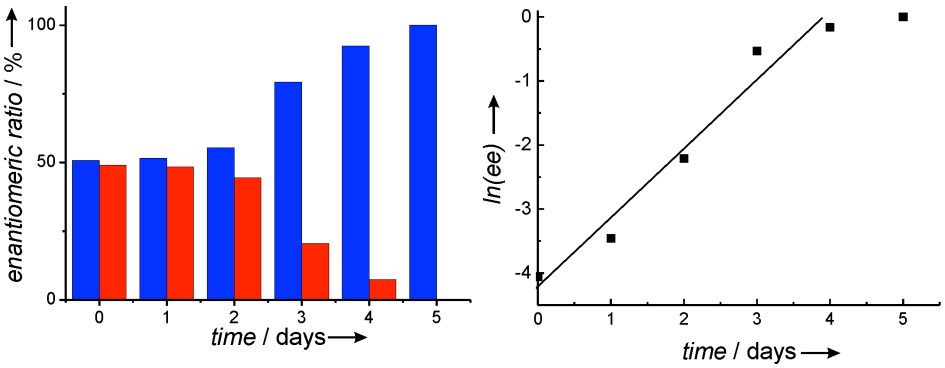

Figure 6.2. Evolution of the solid phase *ee* in the (*S*)-enantiomer (blue) at the cost of the (*R*)-enantiomer (red) of **1** under abrasive grinding (left). The increase in the solid phase *ee* is exponential (right).

Indeed, the result is a complete conversion of racemic **2** in an enantiomerically pure solid phase of (*S*)-**1**, with a deracemization time of **1** that is reduced dramatically in comparison with the results in Figure 6.2, despite that ultrasonic deracemization usually takes less time than in stirred slurries.[6d]
The cascade of events in the present process can be compared with the cooling crystallizations of Kondepudi *et al.*, in which the supersaturation is created by cooling a saturated solution.[4] McBride *et al.* argued that in those experiments the abrasive grinding results in the generation of many small seeds of the same handedness resulting in a high chiral purity.[5] In our process, this supersaturation is created by the *in-situ* synthesis of **1**, which has a lower solubility than **2**. Although the secondary nucleation, as a result of the grinding, will produce many crystals of the same handedness, the racemization of **1** in the solution is not sufficiently fast. Therefore, the unwanted enantiomer also nucleates. The resulting solid, which is still rich in the (*S*)-enantiomer, is however readily deracemized to 100% enantiomeric purity under the grinding conditions. In the precipitation stage, the gradual feeding with racemic **1**, through the *in-situ* transesterification of **2**, avoids too large a drop in the solid state *ee*. Thereby the system remains in the autocatalytic regime, providing a high deracemization rate throughout the process. Paradoxically, relatively slow gradual feeding overall results in a faster evolution to an enantiopure solid **1**.

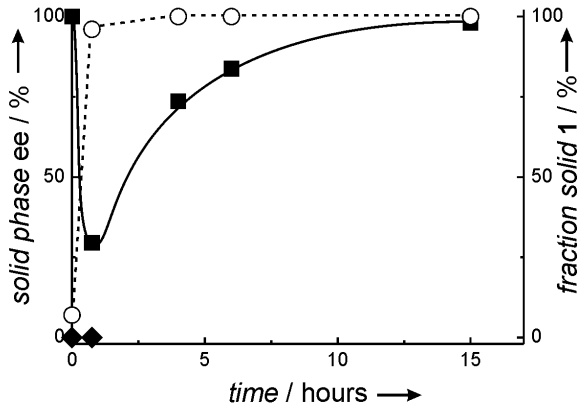

Figure 6.3. Evolution of the solid phase *ee* in the (*S*) enantiomer of **1** (filled squares) and **2** (filled diamonds) during the esterification mediated deracemization. The fraction of **1** in the solid phase (axis right) is depicted by the open circles. Lines are provided as a guide to the eye.

6.3 Conclusions

Various routes have been applied to obtain (*S*)-Naproxen, among which the classical resolution using *N*-alkylglucamine with *ex-situ* racemization of the unwanted enantiomer is currently favored.[1] Using this large volume generic drug as an example, we have demonstrated a novel and fast method to obtain enantiomerically pure material by applying an *in-situ* conversion reaction in combination with attrition enhanced deracemization in a one-pot process. The conversion reaction provides both a gradual feed following Dimroth's principle as well as a supersaturation without the need for cooling.[10] The authors foresee that similar results can be obtained for other molecules, thereby expanding the toolbox for the preparation of pharmaceutical compounds.

6.4 References and Notes

[1] H.-J. Federsel, *Nature Rev.* **2005,** *4,* 685-697.

[2] L. Pasteur, *C.R. Hebd. Séanc. Acad. Sci. Paris* **1848**, *26,* 535.

[3] a) E. Havinga, *Chem. Weekblad* **1941**, *38*, 642; b) E. Havinga, *Biochem. Biophys. Acta* **1954**, *13*, 171. For a review see: R. Yoshioka, in *Topics in Current Chemistry*, Vol. 269, Eds. K. Sakai, N. Hirayama, R. Tamura (Springer-Verlag, Berlin, 2007) 83-132 .

[4] D. K. Kondepudi, R. J. Kaufman, N. Singh, *Science* **1990**, *250*, 975-977.

[5] J. M. McBride, R. L. Carter, *Angew. Chem.* **1991,** *103,* 298; *Angew. Chem. Int. Ed.* **1991,** *30,* 293.

[6] a) C. Viedma, *Phys. Rev. Lett.* **2005**, *94*, 065504; b) P. S. M. Cheung, J. Gagnon, J. Surprenant, Y. Tao, H. Xu, L. A. Cuccia, *Chem. Commun.* **2008**, 987; c) W. L. Noorduin, T. Izumi, A. Millemaggi, M. Leeman, H. Meekes, W. J. P. van Enckevort, R. M. Kellogg, B. Kaptein, E. Vlieg, D. G. Blackmond, *J. Am. Chem. Soc.* **2008**, *130*, 1158; d) W. L. Noorduin, H. Meekes, W. J. P. van Enckevort, A. Millemaggi, M. Leeman, B. Kaptein, R. M. Kellogg, E. Vlieg, *Angew. Chem.***2008,** *120,* 6545; *Angew. Chem. Int. Ed.* **2008,** *47,* 6445; e) B. Kaptein, W. L. Noorduin, H. Meekes, W. J. P. van Enckevort, R. M. Kellogg, E. Vlieg *Angew. Chem.* **2008,** *120,* 7336; *Angew. Chem. Int. Ed.* **2008,** *47,* 7226; f) C. Viedma, J. E. Ortiz, T. de Torres, T. Izumi, D. G. Blackmond, *J. Am. Chem. Soc.* **2008**, *130*, 15274; g) S. B. Tsogoeva, S. Wei, M. Freund, M. Mauksch, *Angew. Chem.* **2009,** *121,* 598; *Angew. Chem. Int. Ed.* **2009,** *48,* 590-594; h) C. Viedma *Astrobiol.* **2007**, *7*, 312; i) J. H. E. Cartwright, O. Piro, I. Tuval, *Phys. Rev. Lett.* **2007**, *98,* 165501; j) W. L. Noorduin, H. Meekes, A. A. C. Bode, W. J. P. van Enckevort, B. Kaptein, R. M. Kellogg, E. Vlieg, *Cryst. Growth Des.* **2008**, *8*, 1675.

[7] a) T. Manimaran, G. P. Stahly, *Tetrahedron Asymm.* **1993**, *4*, 1949; b) J. Jacques, A. Collet, S. H. Wilen, *Enantiomers, Racemates and Resolution* (Krieger, Florida, 1994).

[8] K. Arai, Y. Ohara, Y. Takakuwa, T. Iizumi, U.S. Pat. Appl. 4417070, **1983**.

[9] Surprisingly, the cooling crystallizations of Arai *et al.* only lead to poor enrichments, whereas in the grinding method complete enantiopurity is reached.[8] This can be explained by the relatively slow solution phase racemization ($t_{½} \approx 18$ min). In the case of cooling crystallization, a racemization rate that is slower than the crystallization rate will lead to a supersaturated solution in the undesired enantiomer. This results in the crystallization of the latter, thereby decreasing the enantiopurity of the solid phase. In case of the grinding process the relatively slow rate of the racemization process has no influence on the final *ee*, as in this case the process evolves under near-equilibrium conditions, for which nucleation is rare, if not absent.[6d,i]

[10] O. Dimroth, *Justus Liebigs Ann. Chem.* **1910**, *377*, 127-163.

[11] Grinding using a magnetic stirring bar leads to longer deracemization times as compared to ultrasonic agitation under further identical conditions.[6d]

[12] Moreover, this allows starting with a large excess of solids of **2**.

Chapter 7

Complete Chiral Resolution Using Additive Induced Crystal Size Bifurcation During Grinding

7.1 Introduction

Chiral molecules that crystallize as separate solid phases, i.e. racemic conglomerates, can in principle be resolved by manually sorting the crystals as Louis Pasteur already demonstrated for a tartrate salt.[1] Although enantioselective seeding of a clear supersaturated solution provides the desired enantiomer more readily, careful control of the experimental conditions is required to prevent nucleation of the opposite enantiomer.[2] This resolution process can be improved further by using enantiopure additives that hamper the crystallization of the unwanted enantiomer.[3]

Recently, abrasive grinding has been used to obtain a single chiral solid phase from an initially racemic mixture of conglomerate crystals in contact with a solution in which the molecules racemize or are achiral.[4] Although the execution of this process is remarkably simple, the requirement for an intrinsically chiral molecule that both crystallizes as a conglomerate *and* racemizes in solution can be difficult to fulfil.

Here we demonstrate for a racemic conglomerate of a derivative of the natural amino acid alanine that, even in the absence of racemization, a solid phase of single handedness can be isolated by applying abrasive grinding if the saturated solution contains a well-chosen chiral additive. This provides a robust route to enantiomerically pure materials without depending on the often unpredictable nucleation behaviour of both solid phases and without having to apply (often severe) conditions for racemization.

7.2 Results and Discussion

Second harmonic generation and X-ray powder diffraction experiments recently revealed that the imine of 2-methyl-benzaldehyde and alanine amide **1** (Figure 7.1) crystallizes as a racemic conglomerate.[4h,2] Single crystal X-ray diffraction showed the space group to be $P2_12_12_1$. This crystal structure is suitable for the use of growth inhibitors as the four symmetry related and thus differently oriented molecules ensure that many crystal surface orientations have similar structures on opposite sides of the crystal.

From the crystal structure (Figure 7.2) it follows that the α-position occupied by the methyl group in **1** is a suitable position for the growth inhibiting substituent of the tailor-made additive as it is exposed on virtually all crystal surfaces. We chose a phenyl group as the substituent in a potential inhibitor leading to compound **2**. In Figure 7.1 the process of grinding solution-solid mixtures of **1** using glass beads in the presence of the enantiopure additive **2** is depicted. Samples of the solid phase were collected using filtration followed by a washing step to dissolve the smallest crystals. The enantiomeric excess (ee) of the collected solid phase evolves to the enantiopure state for the system containing the additive (Figure 7.3). Solution-solid mixtures ground in the presence of the additive (*R*)-**2** or (*S*)-**2** were inexorably enriched in the solid phase in (*S*)-**1** and (*R*)-**1**, respectively.[6,7] As expected, in the absence of the additive the solid phase remained racemic (not shown).

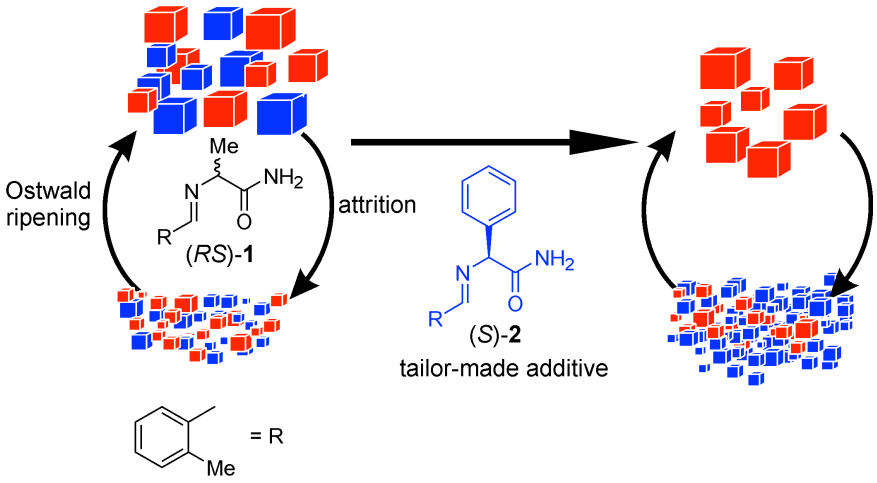

Figure 7.1. Schematic representation of the dissolution and growth of racemic conglomerate crystals during continuous ablation of the crystals. Adding the enantiopure additive (*S*)-**2** stereoselectively hampers the growth of (*S*)-crystals (blue) of the same handedness. Therefore these crystals become smaller and the population of larger crystals becomes monopolized by the unhampered (*R*)-enantiomer (red). The two size populations that are shown separately here are in reality completely mixed.

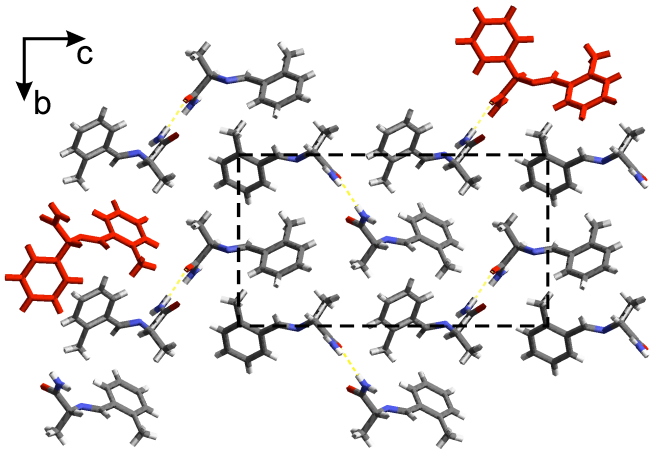

Figure 7.2. Crystal structure of **1** viewed along the [100] direction. The unit cell is indicated by the dashed lines. Two molecules of **1** have been replaced by tailor-made additive molecules **2** (in red) on two crystal surface orientations, indicating hampering of the growth as a result of the protruding phenyl groups at the α-position.

During the ablation of the crystalline phase small fragments dissolve nurturing the growth of the larger crystals, a process called Ostwald ripening (Figure 7.1).[8] The continuous process of growth and ablation results in a steady-state for the crystal size distribution (CSD). In case an additive stereoselectively hampers the growth, the CSD shifts towards smaller sizes for that enantiomer. The enantioselective hampering follows the 'rule of reversal', that is, the additive (*R*)-**2** blocks (*R*)-**1**, resulting in a monopolization of large (*S*)-**1** crystals and *vice versa*.[3b] The effectiveness of the hampering depends, in addition to the additive itself, on its concentration in solution and the total crystal surface area to be blocked.

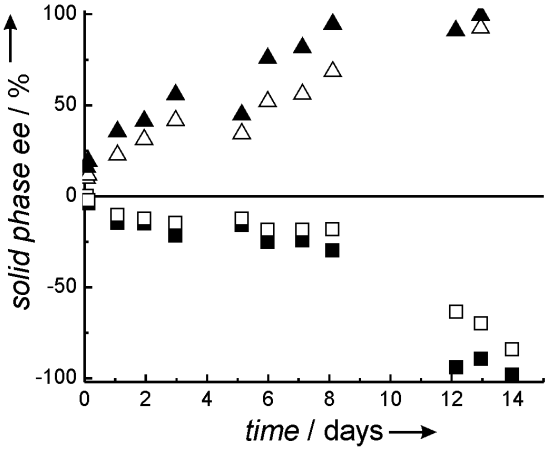

Figure 7.3. Evolution of the solid phase enantiomeric excess during abrasive grinding of racemic **1** in the presence of 16.5 mol% enantiopure **2**. Positive ee values are assigned to (*S*)-**1** (Triangles for flasks containing (*R*)-**2**, squares for flasks containing (*S*)-**2**, open symbols: ee before washing, closed symbols: ee after washing).

It should be noted that in the absence of the washing step, the enantioenrichment is less effective, although the yield in solids would be larger.[9] Not all small crystal fragments of the hampered enantiomer will pass the filter in that case, resulting in a smaller enantiomeric excess in the solid phase. Applying the washing step dissolves the small crystals, leaving the large crystals on the filter.

7.3 Conclusions

Crystallization in combination with tailor-made additives as a route to enantiopure materials has been used before.[3] Here we have merged the use of tailor-made additives with the recently extensively studied technique of abrasive grinding.[4] In summary, we have demonstrated a chiral resolution technique based on additive induced asymmetric bifurcation in the crystal size distribution under near-equilibrium abrasive grinding conditions. In comparison with preferential crystallization, this resolution does not depend on the unpredictable nucleation behaviour of the enantiomers. This easily applicable method may have profound implications for the screening and the separation, even on an industrial scale, of racemic conglomerates that do not racemize in solution. More generally, the authors foresee an increasing scope for near-equilibrium solid-liquid grinding as a versatile tool for solid state chiral purification.

7.4 References and Notes

[1] L. Pasteur, *C.R. Hebd. Séanc. Acad. Sci. Paris* **1848**, *26,* 535.
[2] J. Jacques, A. Collet, S. H. Wilen, *Enantiomers, Racemates and Resolution* (Krieger, Florida, 1994).
[3] a) L. Addadi, Z. Berkovitch-Yellin, N. Domb, E. Gati, M. Lahav, L. Leiserowitz, *Nature* **1982**, *296*, 21; b) L. Addadi, S. Weinstein, E. Gati, I. Weissbuch, M. Lahav, *J. Am. Chem. Soc.* **1982**, *104*, 4610; c) I. Weissbuch, M. Lahav, L. Leiserowitz, *Cryst. Growth Des.* **2003,** *3*, 125.
[4] a) C. Viedma, *Phys. Rev. Lett.* **2005**, *94*, 065504; b) P. S. M. Cheung, J. Gagnon, J. Surprenant, Y. Tao, H. Xu, L. A. Cuccia, *Chem. Commun.* **2008**, 987; c) W. L. Noorduin, T. Izumi, A. Millemaggi, M. Leeman, H. Meekes, W. J. P. van Enckevort, R. M. Kellogg, B. Kaptein, E. Vlieg, D. G. Blackmond, *J. Am. Chem. Soc.* **2008**, *130*, 1158; d) W. L. Noorduin,

H. Meekes, W. J. P. van Enckevort, A. Millemaggi, M. Leeman, B. Kaptein, R. M. Kellogg, E. Vlieg, *Angew. Chem.* **2008,** *120,* 6545; *Angew. Chem. Int. Ed.* **2008,** *47,* 6445; e) B. Kaptein, W. L. Noorduin, H. Meekes, W. J. P. van Enckevort, R. M. Kellogg, E. Vlieg, *Angew. Chem.* **2008,** *120,* 7336; *Angew. Chem. Int. Ed.* **2008,** *47,* 7226; f) C. Viedma, J. E. Ortiz, T. de Torres, T. Izumi, D. G. Blackmond, *J. Am. Chem. Soc.* **2008**, *130*, 15274; g) S. B. Tsogoeva, S. Wei, M. Freund, M. Mauksch, *Angew. Chem.* **2008,** *121,* 598; *Angew. Chem. Int. Ed.* **2008,** *48,* 598; h) M. Leeman, W. L. Noorduin, B. Kaptein, E. Vlieg, H. Meekes, W. van Enckevort, K. Zwaagstra, J.M. de Gooijer, K. Boer, R.M. Kellogg, *submitted*; i) C. Viedma *Astrobiol.* **2007**, *7*, 312; j) J. H. E. Cartwright, O. Piro, I. Tuval, *Phys. Rev. Lett.* **2007**, *98,* 165501; k) W. L. Noorduin, H. Meekes, A. A. C. Bode, W. J. P. van Enckevort, B. Kaptein, R. M. Kellogg, E. Vlieg, *Cryst. Growth Des.* **2008**, *8*, 1675.

[5] G. Coquerel, *Top. Curr. Chem.* **2007,** *269,*1.

[6] The filtrate is enriched in the hampered enantiomer, be it to a lesser extent as it is depending on the solubility.

[7] XRPD measurements showed no polymorphic transitions upon grinding, and HPLC showed no incorporation of **2** in crystals of **1**.

[8] W. Ostwald Lehrbuch der Allgemeinen Chemie, Vol. 2, Part1 (Leipzig, Germany, 1896).

[9] Under the present conditions, including the washing step, the yield of the resolution is approximately 40% based on the pure enantiomer.

Chapter 8

Complete Chiral Symmetry Breaking of an Amino Acid Derivative Directed by Circularly Polarized Light

8.1 Introduction

The reasons for the overwhelming abundance of L-amino acids and D-sugars has intrigued scientists ever since the discovery of molecular handedness.[1-10] Le Bel and Van 't Hoff in the 19th century considered CPL as a possible cause of this asymmetry.[1,2] Circularly polarized light has been observed in star-formation regions,[3,4] and enantioselective photodecomposition of racemic mixtures using CPL has been demonstrated in the 1970s.[5,6] In these examples, however, only a small enantiomeric excess (*ee*) was found in the material remaining after decomposition.

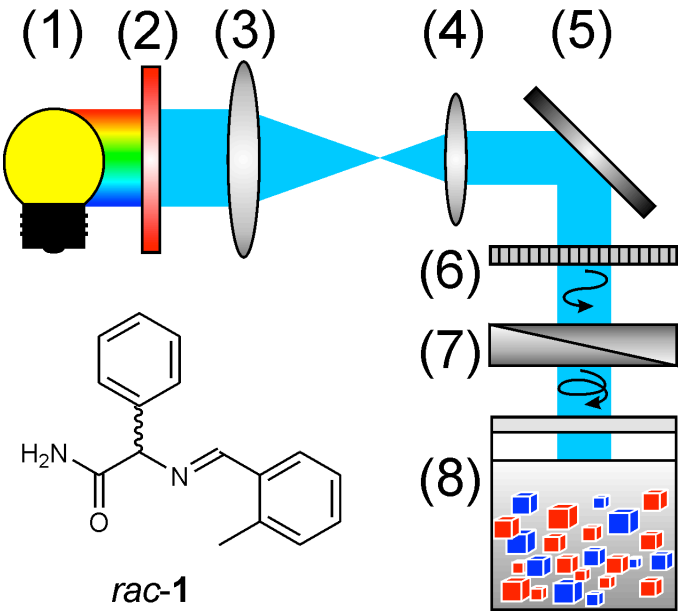

Figure 8.1. Experimental set-up: using an adjustable quarter-wavelength plate either *r*- or *l*-CPL is produced at 310 nm. (1) Hg(Xe) light source (200W), (2) 300-400nm filter, (3) & (4) quartz lenses, (5) UV-mirror, (6) linear polarizer filter, (7) Babinet-Soleil compensator (adjustable ¼λ plate), (8) reaction vessel with quartz window on top. Insert: structure formula of **1**.

Clearly, an amplification mechanism is needed to arrive at an enantiomerically pure end state. One elegant solution to this problem was provided by Soai *et al.*, who demonstrated that a highly enriched pyrimidine alkanol could be synthesized by photolysis of the racemic alcohol using CPL to induce a small amount of enantioselective photodecomposition.[11,12] This method, however, needed several repetitive amplification steps using the material as catalyst in a synthetic reaction that generates the alcohol. An alternative asymmetric amplification method was discovered by Viedma, who used abrasive grinding of enantiomorphous sodium chlorate crystals in contact with a saturated solution to obtain crystals of single handedness.[13]

Recently Viedma's technique was extended by some of us to intrinsically chiral molecules that form a racemic conglomerate in the solid phase.[14] We have reported that the enantioselective symmetry breaking can be directed using small enantiomeric imbalances, tailor-made additives and differences in crystal size distributions.[14,15] We here demonstrate that circularly polarized light causes symmetry breaking in an amino acid derivative, which can be readily amplified by use of the grinding process as a single-step asymmetric amplification method. The handedness of the final enantiopure solid is determined by the rotation sense of the incoming circularly polarized light.

8.2 Results and Discussion

In our experiments, a solid-liquid mixture of the imine **1** (Figure 8.1) in acetonitrile (MeCN) was typically irradiated for 70 hours with circularly polarized UV-light of 0.3 mW intensity. The CPL, centred around the circular dichroism (CD) peak of **1** at 310 nm (Figure 8.2), was produced using a Babinet-Soleil optical compensator. After irradiation, the slurry was transferred to a round bottom flask together with which glass beads and a magnetic stirring bar. The organic base DBU was added to induce racemization in solution. The slurry was stirred at 800 rpm. By means of chiral HPLC analysis it was found that after 5 days of grinding, the solid phase of **1** had become enantiomerically pure, with a configuration depending on the handedness of the CPL irradiation (Table 8.1, experiments 1-2). To speed up the deracemization process, ultrasonic grinding was applied as an alternative in the deracemization step.[16] In this variation, after CPL irradiation, glass beads and DBU were added to the solid/liquid mixture and the reaction vessel was positioned in a thermostated standard ultrasonic cleaning bath. In all cases, *l*-CPL resulted in the emergence of an (*S*) solid phase and *r*-CPL gave an (*R*) solid phase with virtually 100% yield and a deracemization time of less than 16 hours using ultrasonic assisted grinding (Table 8.1, experiments 3-6). In earlier studies, in the absence of CPL irradiation, we performed more than 100 deracemization experiments, starting with racemic **1** that always evolved to (*R*)-**1**.[14,16] Those results were interpreted as being due to minute levels of chiral impurities that overruled the expected randomness of the outcome of the experiments. The present results of *l*-CPL leading to (*S*) solid material therefore demonstrate the strong directing capacity of CPL in the deracemization experiments.

To unravel the mechanism, we tested whether CPL irradiation in the absence of a solid phase would be sufficient for symmetry breaking. Undersaturated clear solutions of racemic **1** in MeCN were irradiated with CPL in the absence of a solid phase. After 70 hours, the irradiation was stopped and the racemization agent DBU was added to ensure complete racemization of the solution. After one additional hour, the reaction mixture was saturated by adding an excess amount of racemic solid **1**, thereby creating a solid-liquid mixture. This mixture was then subjected to abrasive grinding. It was again found that the handedness of the CPL directed the deracemization outcome (Table 8.1, experiments 7-10). Because DBU readily racemizes compound **1** in solution, an asymmetric photo induced enantiomeric inversion of **1** can be ruled out as the determining cause of the symmetry breaking.[17] The effect of the irradiation is therefore likely the formation of a non-racemizable chiral photo-product in the solution. During the abrasive grinding this photoproduct may act as a 'tailor-made' enantioselective crystal growth inhibitor.[18-21]

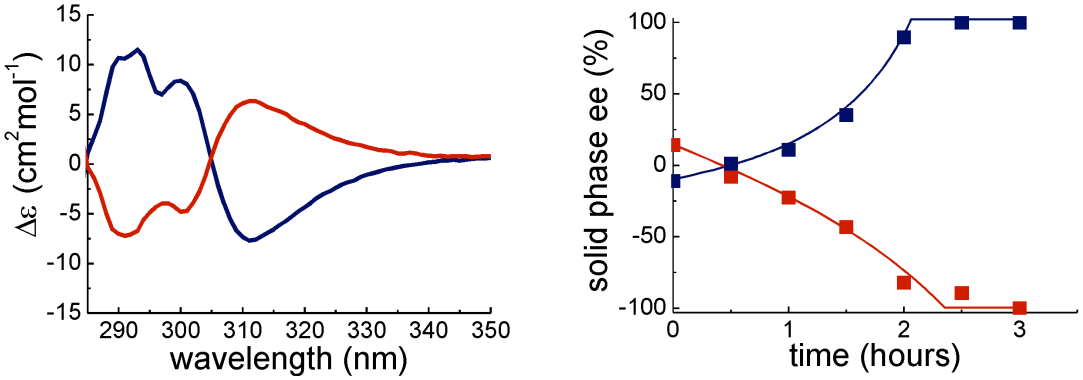

Figure 8.2. CPL absorption spectra and the solid phase deracemisation starting from an initial enantioimbalance. Left, CD spectra of enantiopure (*R*)-**1** (red) and (*S*)-**1** (blue) in MeCN at room temperature. All deracemizations using CPL were performed for wavelengths between 300-400 nm. Right, the evolution of the enantiomeric excess during the deracemisation of **1** starting with an initial enantiomeric excess in the presence of the photochemically formed additive of the same handedness. The directing power of the photoproducts is sufficiently strong to overcome the initial opposite ee (Experiments 15-22, colours as in left panel).

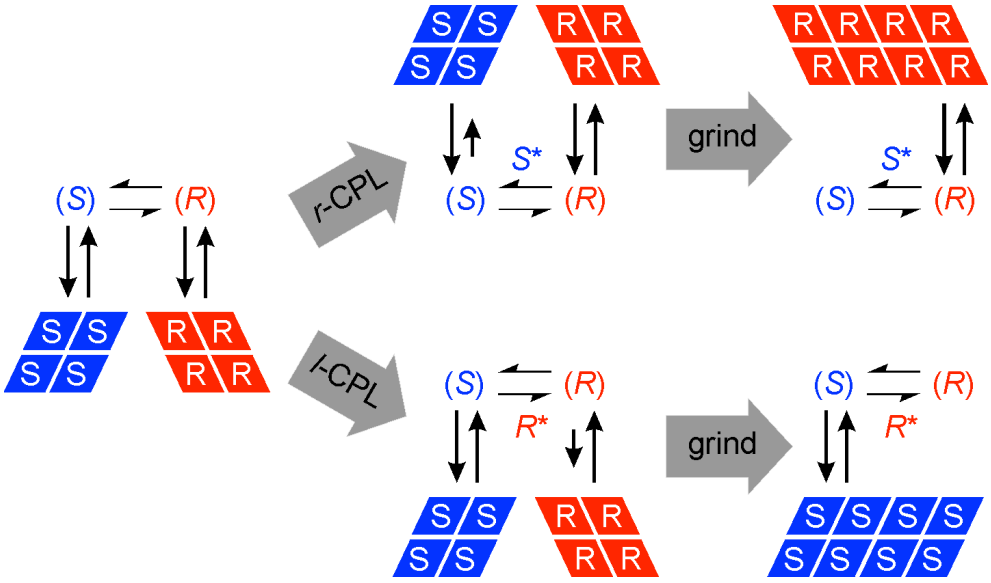

Figure 8.3. Cascade of events during the CPL directed deracemization of racemic **1**. Initially, dissolved enantiomers of **1** are represented by (*R*) and (*S*) and are in equilibrium with the corresponding crystal phase (left panel). During the *l*-CPL irradiation of solution-solid mixture of racemic **1** an enantioselective growth inhibitor *R** is formed (middle panel, lower route). This compound *R** enantioselectively hampers the growth of (*R*)-**1** crystals so that the solid phase enriches in (*S*)-**1**. This chiral imbalance is fully amplified upon abrasive grinding, resulting in a complete deracemization of racemic **1** to a solid phase of (*S*)-**1** (right panel). A similar, but opposite, process occurs upon *r*-CPL irradiation (upper route).

Table 8.1. Circularly polarized light directed deracemization experiments.

exp.[a]	handedness of CPL	irradiation conditions	grinding method	final ee (%)	configuration
1	*r*	*rac*-**1** solid/liquid	stirring	>99.9	*R*
2	*l*	*rac*-**1** solid/liquid	stirring	>99.9	*S*
3,4	*r*	*rac*-**1** solid/liquid	ultrasonic	>99.9	*R*
5,6	*l*	*rac*-**1** solid/liquid	ultrasonic	>99.9	*S*
7,8	*r*	*rac*-**1** clear solution	ultrasonic	>99.9	*R*
9,10	*l*	*rac*-**1** clear solution	ultrasonic	>99.9	*S*
11,12	non-*pol*.	(*S*)-**1** clear solution	ultrasonic	>99.9	*R*
13,14	non-*pol*.	(*R*)-**1** clear solution	ultrasonic	>99.9	*S*
15-18	nonpol.	(*R*)-**1** clear solution ((*R*)-biased solid added)	ultrasonic	>99.9	*S*
19-22	nonpol.	(*S*)-**1** clear solution ((*S*)-biased solid added)	ultrasonic	>99.9	*R*

[a] Table 1, experiments 1-2: abrasive grinding using a magnetic stirring bar. After CPL irradiation of 0.42 g racemic **1** in 6.25 g MeCN, the solid-solution mixture was transferred to a 25 mL round bottom flask containing 8.0 g glass beads and an oval Teflon coated stirring bar (2 cm). Stirring was effectuated at 800 rpm. After 1-2 hours, solution phase racemisation was initiated by adding 0.12 g DBU. Experiments 3-6: abrasive grinding of a solid-liquid mixture of 0.44 g racemic **1** in 6.25g MeCN using an ultrasonic bath [16]. After CPL irradiation, 8.0 g glass beads and 0.12 g DBU were added to the reaction vessel. Experiments 7-10: CPL irradiation of a clear undersaturated solution of 0.12 g racemic **1** in 6.25 g MeCN. After four days, 0.12 g DBU was added. After one additional hour to ensure complete racemisation, 0.32 g racemic **1** and 8.0 g glass beads were added and the solid-liquid mixture was deracemised in an ultrasonic bath. Experiments 11-14: irradiation of enantiopure **1** using a nonpolarized 300W light source: 0.1 g of the irradiated enantiopure sample was dissolved in 6.25 g MeCN and 8.0 g glass beads and 0.12 g DBU were added to the reaction vessel. After 1 hour racemisation time, 0.42 g racemic **1** was added to the solution and grinding was performed using the ultrasonic bath. Experiments 15-22: irradiation of enantiopure **1** using a nonpolarized 300W light source and subsequent deracemisation in the presence of an enantiomeric imbalance in the solid phase: 0.02 g of the irradiated enantiopure sample was dissolved in 5.6 g MeCN and 0.35 g racemic **1**, 0.005 g enantiopure **1** (of the same enantiomer as was used in the irradiation step) and 8.0 g glass beads were added to the reaction vessel. After 40 min. of grinding using the ultrasonic bath, 0.20 g DBU was added to initiate the racemization in the solution.

The correlation between the CPL handedness and the final outcome of the deracemization is rationalized by considering the chiroptical properties of **1**. As follows from the CD spectra in Figure 8.2, the circular dichroism, $\Delta\varepsilon = \varepsilon_l - \varepsilon_r$, of (*R*)-**1** at 310 nm is positive, which means that (*R*)-**1** absorbs *l*-CPL more strongly than *r*-CPL. Thus, the irradiation of *l*-CPL transforms (*R*)-**1** more rapidly than (*S*)-**1**. The resulting excess of chiral *R** additive then stereoselectively hampers the crystal growth of the (*R*) crystals, driving the abrasive grinding process to an enantiomerically pure (*S*) solid phase (Figure 8.3). In this interpretation the stereochemical outcome follows Lahav's "rule of reversal".[18-20]

This hypothesis of the photosynthesis of a 'tailor-made' additive was further supported by examining the effect of irradiation of undersaturated solutions of enantiopure **1** in MeCN using nonpolarized UV light. Samples were irradiated using a 300 W nonpolarized Hg light source for ca. 24 hours. The solution was subsequently racemised by adding DBU and a solution-solid mixture was again created by adding racemic solid **1**. This mixture was then deracemised using ultrasonic grinding. Experiments 11-14 in Table 8.1 show that irradiated

solutions containing initially only enantiopure (*R*)-**1** direct the solid phase deracemisation to enantiopure (*S*)-**1** and (*S*)-**1** irradiated solutions direct the outcome to an enantiopure (*R*)-**1** solid. This confirms that during the irradiation *R** is formed from (*R*)-**1**, thereby directing the deracemisation to (*S*)-**1** and *vice versa*. To further prove that the process is driven by a chiral photoproduct *R** rather than an imbalance of enantiomers we performed experiments initially biased in the unwanted enantiomer. For that we added solid 1 with an initial ee in (*R*) to an irradiated solution containing *R** and subsequently performed the deracemisation experiment (Table 8.1, experiments 15-18). Similar experiments were preformed for the other enantiomer (Table 8.1, experiments 19-22). Kinetic data for these latter experiments are presented in Figure 8.2. Even an initial enantiomeric excess of 14% could be fully overcome by the additive, thus driving the process to an enantiopure solid phase in the opposite enantiomer.

8.3 Conclusions

The origin of the single handedness of biomolecules is a fundamental scientific issue. Various deterministic scenarios for the prebiotic evolution of biological homochirality, as found in left-handed amino acids and right-handed sugars, have been proposed. Circularly polarized light is one of the possible actors for this process.[1-9,22] Using circularly polarized light, we have achieved the complete deracemization of an amino acid derivative directed by the rotation sense of the light. Abrasive grinding was applied as a single-step asymmetric autocatalysis mechanism. For a small fraction of the molecules the light induces the formation of enantioselective crystal growth inhibitors that direct the deracemization process deterministically. Our observations provide a scenario for the hypothesis that the formation of enantiomeric excess in prebiotic organic molecules in the early days of the earth could have been induced by the action of CPL, either extraterrestrial or earth based.[4] The subsequent amplification of the extremely small initial enantiomeric excess may have proceeded through the combined process of attrition and racemization. Even if in nature these processes are very slow, single chirality will ultimately be achieved over eons of time.[23,24] As such, the results support a scenario for the deterministic evolution of biomolecular handedness, a feature that is considered as a signature of life.

8.4 References

[1] J. A. Le Bel, *Bull. Soc. Chim. Fr.* **1874,** *22,* 337-347.
[2] J. H. Van ‘t Hoff, Voorstel tot uitbreiding der tegenwoordig in de scheikunde gebruikte structuur-formules in de ruimte: benevens een daarmee samenhangende opmerking omtrent het verband tusschen optisch actief vermogen en chemische constitutie van organische verbindingen. (Utrecht, September 3, 1874).
[3] J. Bailey, A. Chrysostomou, J. H. Hough, T. M. Gledhill, A. McCall, S. Clark, F. Menard, M. Tamura, *Science* **1998,** *281,* 672-674.
[4] J. R. Cronin, S. Pizzarello, *Science* **1997,** *275,* 951.
[5] G. Balavoine, A. Moradpour, H. B. Kagan, *J. Am. Chem. Soc.* **1974,** *96,* 5152-5158.
[6] J. J. Flores, W. A. Bonner, G. A. Massey, *J. Am. Chem. Soc*. **1977,** *99,* 3622-3625.
[7] N. P. M. Huck, W. F. Jager, B. de Lang, B. L. Feringa, *Science* **1996,** *273,* 1686-1688.
[8] G. L. J. A. Rikken, E. Raupach, *Science* **2000,** *46,* 932-935.
[9] R. J. Cave, *Science* **2009,** *323,* 1435-1436.
[10] L. D. Barron, *J. Am. Chem. Soc.* **1986,** *108,* 5539–5542.
[11] K. Soai, T. Shibata, H. Morioka, K. Choji, *Nature* **1995,** *378,* 767-768.
[12] T. Kawasaki, *et al. J. Am. Chem. Soc.* **2005,** *127,* 3274-3275.
[13] C. Viedma, *Phys. Rev. Lett.* **2005,** *94,* 065504.
[14] W. L. Noorduin, *et al. J. Am. Chem. Soc.* **2008,** *130,* 1158–1159.
[15] B. Kaptein, *et al. Angew. Chem. Int. Ed.* **2008,** *47,* 7226–7229.
[16] W. L. Noorduin, *et al. Angew. Chem. Int. Ed.* **2008,** *47,* 6445–6447.
[17] B. Norden, *Nature* **1977,** *226,* 566-567.
[18] L. Addadi, *et al. Nature* **1982,** *296,* 21-26.
[19] I. Weissbuch, L. Addadi, M. Lahav, L. Leiserowitz, *Science* **1991,** *253,* 637-645.

[20] L. Addadi, S. Weinstein, E. Gati, I. Weissbuch, M. Lahav, *J. Am. Chem. Soc.* **1982,** *104,* 4610-4617.
[21] A. Guijarro, M. Yus, *The origins of chirality in the molecules of life* (RCS, Cambridge, 2008).
[22] W. L. Noorduin, *et al. Cryst. Growth Des.* **2008,** *8,* 1675-1681.
[23] M. J. McBride, J. C. Tully *Nature* **2008,** *452,* 161-162.

Appendix

Supporting Information

Supporting Information Chapter 2

Preparation of the starting material (*RS*)-1

Racemic *N*-(2-methylbenzylidene)-phenylglycine amide ((*RS*)-**1**) was prepared from commercially available (*RS*)-phenylglycine ((*RS*)-Phg).

Step 1: A suspension of 1 mol of (*RS*)-Phg, originally produced commercially by DSM Pharmaceutical Products from benzaldehyde by means of a Strecker reaction with NH_3/HCN and subsequent acidic hydrolysis*, in 1 L of MeOH was cooled to 0°C and 1.2 mol of $SOCl_2$ was slowly added over a period of several hours in order to keep the temperature below 20°C. The clear solution was stirred for 18 h at ambient temperature and subsequently refluxed for 1 h in order to remove the SO_2. The volume was then reduced to 350 mL by evaporation under reduced pressure and 1.5 L of MTBE was added to crystallize the (*RS*)-Phg methyl ester HCl salt. The crystals were filtered and dried under reduced pressure and were used as such in the next step.

* Note: Phg forms a very stable racemic compound and has a eutectic composition with 97% *ee*.

Step 2: The crystals described above were added in portions to a stirred solution of 750 mL of concentrated ammonia. During the addition (*RS*)-Phg amide started to precipitate and stirring was continued for a few hours until all the methyl ester was converted (tested by TLC on silica, eluent: $CHCl_3$, MeOH, conc. ammonia 60:45:20). The racemic amide was filtered, washed with cold water (note, solubility 5 wt%) and dried. Overall yield approximately 80%.

Step 3: To a stirred solution of 68.6 g of (*RS*)-Phg amide in a mixture of 150 mL of water and 300 mL of MeOH at ambient temperature was added 55.9 g of 2-methylbenzadehyde over a period of 1 hour (after addition of 20% of the aldehyde crystallisation usually starts spontaneously; if not it is better to add racemic seed crystals for a controlled crystallisation). The thick suspension was stirred for 20 h at ambient temperature and then filtered. The crystals were washed with 100 mL of MeOH/water 2:1 and 200 ml of MTBE, dried under reduced pressure, thus yielding 110 g (95%) of NMR and HPLC pure (*RS*)-**1** as colorless needles. M.p. 153°C. ^{1}H NMR (200 MHz, $CDCl_3$) δ 8.61 (s, 1H), 7.95 (dd, 1H, J=8.0 and 1.7 Hz), 7.19-7.53 (m, 8H), 7.01 (br s, 1H), 5.91 (br s, 1H), 4.99 (s, 1H) and 2.52 (s, 3H). ^{13}C NMR (50 MHz, $CDCl_3$) δ 171.61 (s), 160.26 (d), 139.42 (s), 137.00 (s), 132.44 (s), 129.80 (d), 129.67 (d), 127.23 (d), 126.73 (d) 126.26 (d), 124.95 (d), 76.36 (d) and 17.94 (q). Calculated for $C_{16}H_{16}N_2O$: C, 75.16%; H, 6.39%; N, 11.10%. Found: C, 75.78%; H, 6.37%; N, 11.09%. MS(CI): m/z = 253 (M+1).

(*RS*)-**1** may be further purified by several recrystallisations from MeOH (2.5 L for 100 g, crystallisation yield 75-80%). However, this had no effect on the deracemization experiments described in this paper.

Care should be taken not to heat the methanolic solution of (*RS*)-**1** for longer period of time, in order to prevent formation of the cyclization product 2-(2-methylphenyl)-5-phenyl-imidazolidin-4-one (racemic 1:1 diastereomeric mixture).

Analogously to the method above also (*R*)-**1** and (*S*)-**1** were prepared from commercially available (*R*)-phenylglycine amide and (*S*)-phenylglycine, respectively. M.p. 180°C. (*R*)-enantiomer; $[\alpha]^{25}_D$ -29.9 (c = 0.5, MeOH).

The virgin deracemization experiments

In 100 mL round bottom flask with an oval PTFE-coated magnetic stirring bar (L 20mm, Ø 10mm) were weighed in 4.0g of (*RS*)-**1**, 36g of MeOH (PA quality) and 10g Ø 2-2.5 mm glass pearls

(Aldrich). The flask was sealed and stirred for 24 hours at 1250 rpm magnetic stirrer to equilibrate the solvent and solute. Furthermore, the possible memory effect of the crystal size distribution is overcome by grinding all the crystals. From this suspension the t = 0 sample was taken. To the suspension was then added 200 mg (200 µL) of 1,8-diazabicyclo[5.4.0]undec-7-ene (DBU) (5 mol%) and stirring was started at 1200-1300 rpm. Samples were taken every 3 days. The chiral purity was measured using chiral HPLC as described below, and confirmed by polarimetry.
Further analysis was performed using ^{1}H-NMR, DSC and XRPD.
After prolonged stirring in the solid **1** samples 2-(2-methylphenyl)-5-phenyl-imidazolidin-4-one can be detected as a racemic 9:1 diastereomeric side-product. Both diastereomers of the side-product are racemic within the HPLC detection limits (*fide infra*).

Experiments with initial enantiomeric imbalances
In the case MeOH was used as a solvent, a total of (*R*/*S*)-**1** (c.a. 2.0 g), glass pearls (5 g) and MeOH (18 g) were placed in a 100 ml round bottom flask with a magnetic stirring bar. The mixture was stirred overnight at room temperature in order to crush solid particle size. To the suspension, DBU (100 µL, 5 mol%) was added and stirring was started at 1000 rpm. The flask was manually shaken daily and samples were taken before addition of DBU (t = 0) and 7, 14, 21 and 35 days after the addition of DBU. Four experiments with 2% *ee*, 5% *ee*, 7% *ee* and 10% *ee* (*S*) were carried out in MeOH (Figure 2.1). When using MeCN as a solvent, (*RS*)-**1** + appropriate amounts of (*R*)-**1** or (*S*)-**1** (total c.a. 4.0 g), glass pearls (10 g) and MeCN (36 g) were placed in a 100 mL round bottom flask. After stirring overnight (1250 rpm), the t = 0 sample was taken and DBU was added (200 µL,5 mol%). Samples were taken every 3 days. Further analysis was performed as described for the virgin experiments. No side product formation was observed in MeCN.

Experiments with (*R*)- and (*S*)-phenylglycine as additive
In a 100 mL B24 round bottom flask with magnetic stirring bar were weighed in 10 gram of glass pearls, 4.0 g of (*RS*)-**1** and 36 g of MeOH or MeCN. The mixture was stirred at 1250 rpm at room temperature for 15 min. Thereafter, 2.5-200 mg of (*R*)-Phg was added using a weighing paper. Stirring was continued for 1-24 h to reach equilibrium. From this suspension the t = 0 sample was taken. To the suspension was then added 200 mg (200 µL) of DBU (5 mol%) and stirring was continued at 1200-1300 rpm. For high concentrations of Phg additional DBU has to be added to overcome the effect of reduced basicity as a result of salt formation between the DBU and Phg. After addition of DBU the pH should be approximately 12 to ensure that racemization occurs.

Sampling
For sampling, 2-3 mL of the slurry was taken with a pipette and filtered on a P3 or P4 glass filter (Ø 10 mm). The residue was washed with 1 mL of MeOH or MeCN, respectively, and 2 mL of MTBE to remove mother liquid and DBU, and dried in a vacuum stove overnight at 40 ºC.

Dissolution enrichment experiments
Small enantioimbalances can already be amplified to single chirality. Although the starting material is prepared from (*RS*)-Phg, which is a very stable racemic compound, we checked the enantiopurity by dissolution. Conglomerates which are enriched in one enantiomer enrich in the solid phase upon dissolution. To check if **1** was racemic, ca. 0.4 g **1** was partially dissolved in 12 ml MeCN. After stirring the suspension overnight, the solid material was collected on a P3 glass filter and dried in a vacuum stove. Chiral HPLC analysis and polarimetry showed no chiral enrichment, confirming that the starting material was racemic within the detection limits.

Determination of the ee by chiral HPLC analysis of the solids samples
Sample preparation 0.5 mg solid in 1.5 mL eluent, injection volume 20µL, HPLC column Chiralcel-OJ (250x4.6 mm ID), eluent n-hexane/2-propanol 80/20 v/v%, flow 1mL/min, r.t., detection λ=254 nm. Retention times (*S*)-**1** 11.4 min, (*R*)-**1** 17.4 min, (*2R**,*5R*)-2-(2-methylphenyl)-5-phenyl-imidazolidin-4-one (cyclic side-product) 8.8 min, (*2S**,*5S*)-side-product 9.8 min, (*2S**,*5R*)-side-product 11.2 min, (*2R**,*5S*)-side-product 11.9 min. The response factor of **1** is 25 times higher than of the cyclic side-products at 254 nm, whereas at 213 nm the response factor is 1.5 times higher.

Control of ee determination

As a check of the *ee* determination by the chiral HPLC method described above, an independent *ee* analysis has been performed on some of the samples.

Therefore 50-60 mg of enantiomerically enriched **1,** isolated from various deracemization experiments, was dissolved in 3 mL of 0.25M HCl solution. The solution was extracted two times with 3 mL of $CHCl_3$. The remaining aqueous solution of phenylglycine amide HCl salt was used as such for the *ee* determination by the following HPLC method. Column; Crownether Cr(+) 150 x 4.6 mm ID, eluent; aqueous $HClO_4$ pH=1.2 / Methanol 90/10 v/v%, flow; 1 mL/min, temperature; 25 °C, detection: UV 220 nm, detection limit: 0.01 area%.

The results of this control *ee* determination were in agreement with the values obtained by the standard HPLC method described above.

Supplementary Information Chapter 4

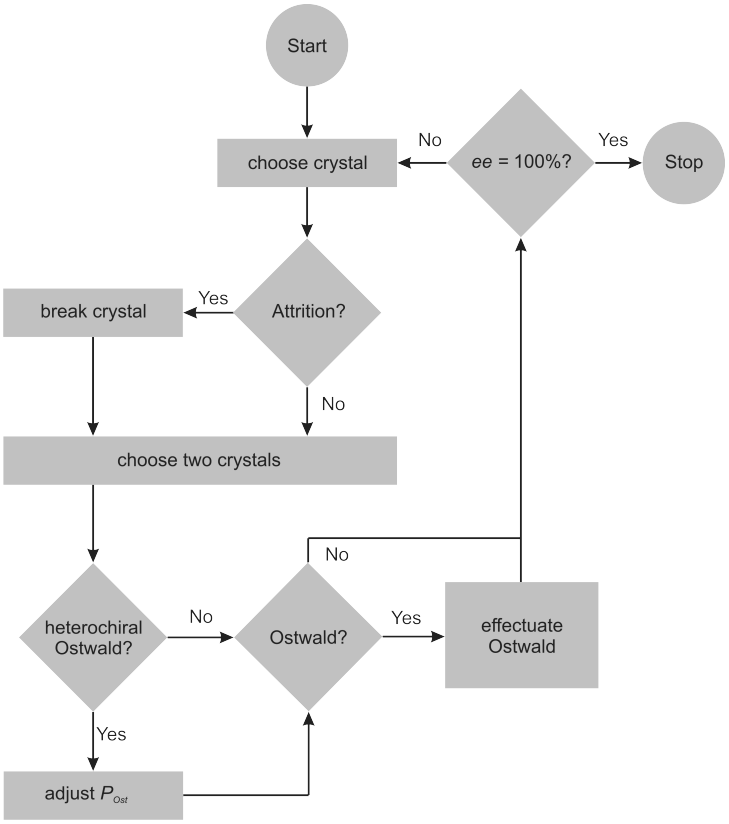

Figure SI-4.1. Flow diagram of the Monte Carlo simulation modeling the processes of Ostwald ripening and attrition as independent processes.

Monte Carlo simulation

Monte Carlo simulations showed that two processes are responsible for the deracemization process: continuous attrition of crystals and Ostwald ripening for which large crystals grow at the cost of smaller ones.[20]

In the model, these two competing processes were parameterized by the attrition-ripening ratio, ξ, defined as the ratio of the probability for an attrition and an Ostwald ripening effect, $\xi = P_{attr}/P_{Ost}$. A second parameter, the racemization efficiency, χ, was introduced to cover the racemization rate in the solution. For the process of Ostwald ripening a distinction between a homochiral and a heterochiral mechanism was made. In the homochiral event, a molecule is transported via the solution from a small crystal to a large one of the same chirality. In the heterochiral step the dissolved molecule is converted

in solution to the opposite chirality and then attached to a crystal with a handedness opposite to that of the small crystal. The model shows that for instantaneous racemization, the deracemization time increases with the size of the system whereas for relatively slow solution racemization this deracemization time is independent of the system size. In the present simulations the Ostwald ripening events and the attrition events has been treated as independent processes in time in order to arrive at an expression for the deracemization rate that is more readily interpreted in terms of experimental parameters. For that the ratio ξ has been replaced by a parameter ζ, which represents the probability of an attrition event. Using the parameters ζ and χ during each time interval in the simulations both an attrition event and an Ostwald ripening event can be probed. The results of the simulations with this new parameter set are in essence the same as those of the former simulations. Consistent with the former simulation study, both these parameters have an optimal value that results in a minimal deracemization time.

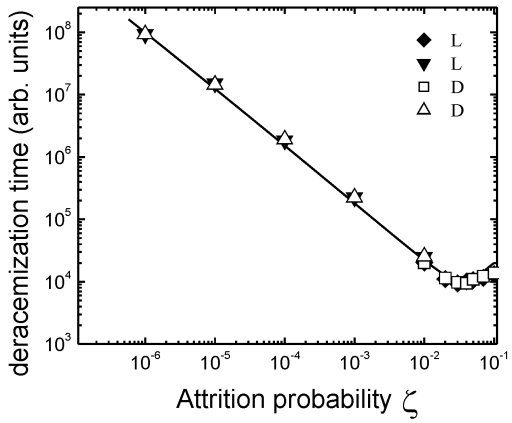

Figure SI-4.2. The average deracemization time t_{derac} as a function of the attrition probability ζ for a compound racemizing in solution (χ = 0.1), with either D (open symbols) or L (full symbols) crystals in the final state. The initial *ee* = 0. Results are averaged over 100 simulation runs and are shown for two system sizes: $N = 2 \cdot 10^4$ (square symbols), $N = 2 \cdot 10^5$ (triangle symbols). The line is drawn as a guide to the eye.

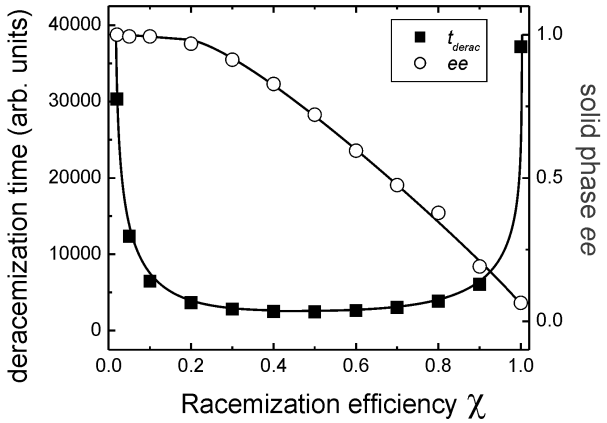

Figure SI-4.3. The deracemization time as well as the percentage of the deracemizations ending in pure L averaged over 1600 simulations as a function of the racemization efficiency χ for ξ = 0.04 and an initial *ee* = 5% in L. Lines are a guide to the eye.

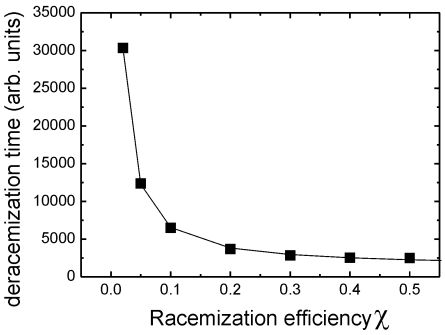

Figure SI-4.4. Fit of data in Figure SI-4.3 of the deracemization time being inverse by proportional to the racemization efficiency χ.

Ostwald ripening probability

The Ostwald ripening probability κ will depend on the solute exchange frequency between the solution and the crystallites which in turn depends on the surface free energy of the crystallites in the solution. Nielsen has shown that a linear relation exists between the surface free energy γ of the crystals in solution and the solubility b_{solute} according to:[23]

$$\gamma \propto \ln b_{solute} . \tag{SI 4.1}$$

The Gibbs free energy of a crystal of n molecules is:

$$G(n) = -n\Delta\mu + \gamma(n) , \tag{SI 4.2}$$

where $\Delta\mu$ is the difference in chemical potential for a molecule in the bulk solution and in the bulk crystal, i.e. $\Delta\mu = \mu_f - \mu_s$. The surface free energy $\gamma(n)$ depends on the shape of the crystal. To keep the model simple we assume that all crystals are perfect spheres, for which the surface area can be expressed in terms of the number of molecules as:

$$A(n) = 4\pi\left(\frac{3n\Omega}{4\pi}\right)^{2/3} , \tag{SI 4.3}$$

with Ω the molecular volume. The surface free energy can then be written as:

$$\gamma(n) = A(n)\cdot\gamma , \tag{SI 4.4}$$

where γ is the specific surface free energy. The driving force per molecule for an Ostwald event for which a molecule is transformed from a crystal with n_i molecules to a crystal with n_j molecules thus becomes:

$$\Delta\Delta\mu = \Delta\mu_{n_i} - \Delta\mu_{n_j} = \left(\frac{\partial G(n)}{\partial n}\right)_{P,T,n=n_i} - \left(\frac{\partial G(n)}{\partial n}\right)_{P,T,n=n_j}$$

$$= \frac{\gamma 8\pi}{3}\left(\frac{3\Omega}{4\pi}\right)^{2/3}\left[\left(\frac{1}{n_i}\right)^{1/3} - \left(\frac{1}{n_j}\right)^{1/3}\right] \tag{SI 4.5}$$

where Ω is the molecular volume and n_1 and n_2 are the number of molecules in the spheriacly shaped crystals involved in the Ostwald ripening event. The rate for the Ostwald ripening process will then be determined by

$$J_{Ost} \propto b_{solute} \exp\left[\frac{\Delta\Delta\mu}{RT}\right] = b_{solute} \exp\left\{\frac{\gamma 8\pi}{3RT}\left(\frac{3\Omega}{4\pi}\right)^{2/3}\left[\left(\frac{1}{n_1}\right)^{1/3} - \left(\frac{1}{n_2}\right)^{1/3}\right]\right\} \quad \text{(SI 4.6)}$$

Combining equations (SI 4.1) and (SI 4.6) leads to:

$$J_{Ost} \propto b_{solute}^{S}, \quad \text{(SI 4.7)}$$

where,

$$S = 1 + \frac{8\pi}{3RT}\left(\frac{3\Omega}{4\pi}\right)^{2/3}\left[\left(\frac{1}{n_1}\right)^{1/3} - \left(\frac{1}{n_2}\right)^{1/3}\right]. \quad \text{(SI 4.8)}$$

Substituting some typical values for the various parameters in S leads to the conclusion that one can make the approximation $S = 1$. Thus, we can write for the Ostwald probability:

$$\kappa = \alpha_{Ost} b_{solute}. \quad \text{(SI 4.9)}$$

Racemization rates in solution

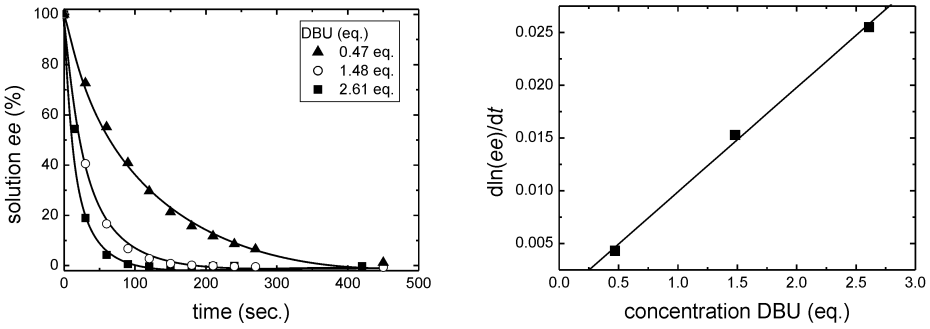

Figure SI-4.5. Racemization of (*R*)-**1** in saturated solutions of MeCN for various concentrations of racemizing catalyst DBU (left). Plotting the racemization rate as a function of time shows a linear dependence of the racemization rate as a function of the concentration racemizing agent **1** (right).

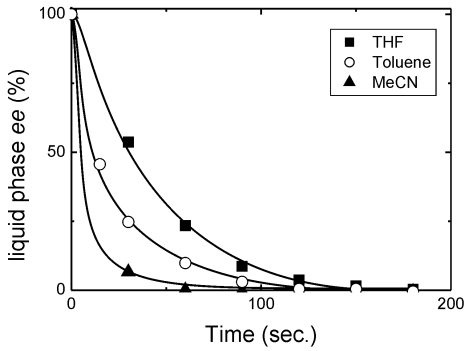

Figure SI-4.6. Racemization of saturated solutions of (*R*)-**1** in 0.456 mol/kg DBU for different saturated solvents.

Ultrasonic experiments
Experiments were performed using an Elma Transsonic T470/H ultrasonic bath. The bath was kept at a constant temperature of 23 °C using a cooling spiral that was attached to a Julabo F25 thermostat bath.

Supporting Information Chapter 5

Scheme SI 5.1. Synthesis of compound **1**.

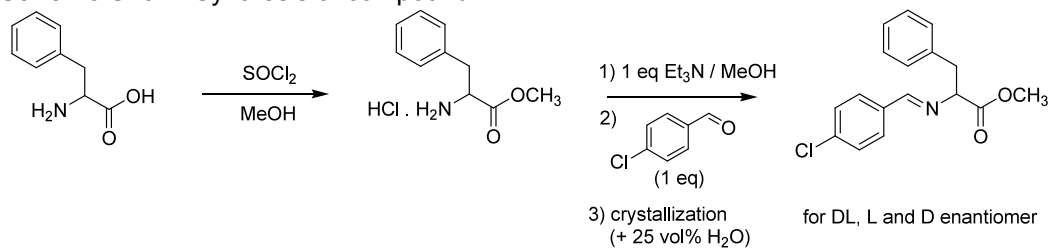

Synthesis of (*RS*)-*N*-(4-chlorobenzylidene)phenylalanine methyl ester
(*RS*)-Phenylalanine methyl ester HCl-salt:
To a suspension of 83 g (0.50 mol) of (*RS*)-phenylalanine in 550 ml of MeOH at 5°C was added drop-wise 47 ml (0.65 mol) of $SOCl_2$ over a 3 hours period. During the addition the mixture was cooled in an ice-bath in order to keep the temperature <10°C. The clear solution was stirred for 20 h and subsequently for 2 h at 50°C. After evaporation of the solvent under reduced pressure 108 g (100%) of (*RS*)-phenylalanine methyl ester HCl-salt was obtained as a white solid. ^{1}H NMR (300 MHz, DMSO-d6) δ 8.89 (br s, 3H, NH3), 7.34-7.24 (m, 5H, Ph), 4.21 (dd, 1H, α-H), 3.64 (s, 3H, OCH_3), 3.25 (dd, 1H, β-H) and 3.11 (dd, 1H, β-H).

Synthesis of (*RS*)-*N*-(4-Chlorobenzylidene)phenylalanine methyl ester
A solution of 108 g (0.50 mol) of the (*RS*)-phenylalanine methyl ester prepared as above in 300 ml of MeOH was neutralized with 80 ml (0.51 mol) of triethylamine to pH 8. To the clear solution at ambient temperature was added 70 g (0.50 mol) of 4-chlorobenzaldehyde in small portions over 30 min. The clear solution was stirred for 1 h and then seeded to induce crystallization. After the crystallization 100 ml of water was added and the mixture was cooled to 0°C. The crystalline product was filtered, washed with 200 ml MeOH:H_2O 2:1, 200 ml MeOH:H_2O 1:1 and 30 ml MeOH. After drying 140 g (0.464 mol, 93%) of (*RS*)-*N*-(4-chlorobenzylidene)phenylalanine methyl ester was obtained as a white crystalline solid. Melting point: 65.1°C. ^{1}H NMR (300 MHz, CD_2Cl_2) 7.96 (s, 1H, CH=N), 7.68 (d, 2H, Ar-H), 7. 43 (d, 2H, Ar-H), 7.31-7.20 (m, 5H, Ph), 4.22 (dd, 1H, α-H), 3.76 (s, 3H, OCH_3), 3.38 (dd, 1H, β-H) and 3.15 (dd, 1H, β-H). ^{13}C NMR (75 MHz, CD_2Cl_2) δ 172.49 (s), 162.94 (d), 138.31 (s), 137.72 (s), 135.12 (s), 130.50(d) , 130.35 (d), 129.62(d) , 129.04 (d), 127.32(d) , 75.38 (d), 52.80 (q) and 40.49 (t).

Synthesis of (*S*)-*N*-(4-chlorobenzylidene)phenylalanine methyl ester
This compound was prepared as described above in 94% yield from commercially available (*S*)-phenylalanine methyl ester HCl-salt (Across). Melting point: 87.4°C. $[\alpha]^{25}_D$ -281 (c=1, MeOH). HPLC, e.e. ≥ 99.5% (column Chiralpak AD 150 x 4.6 mm, eluent n-heptane/iPrOH 97.5:2.5 vol%, flow 1.0 ml/min, detection UV 254 nm).

Synthesis of (*R*)-*N*-(4-chlorobenzylidene)phenylalanine methyl ester
This compound was prepared as described above in 93% yield from commercially available (*R*)-phenylalanine methyl ester HCl-salt (Bachem). Melting point: 87.4°C. $[\alpha]^{22}_D$ +285 (c=1, MeOH). HPLC, e.e. ≥ 99.5% (column Chiralpak AD 150 x 4.6 mm, eluent n-heptane/iPrOH 97.5:2.5 vol%, flow 1.0 ml/min, detection UV 254 nm).

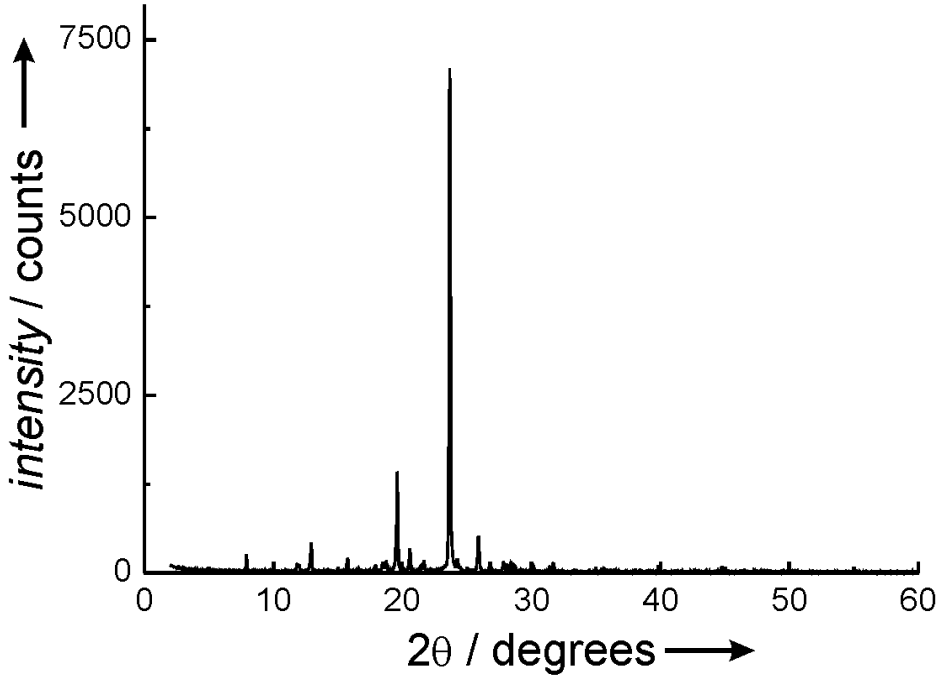

Figure SI-5.1. X-ray powder pattern of **1**.

Morphology
The morphology of the crystals grown form the enantiomerically pure and racemic solutions was analyzed using two circle optical goniometry and a CCD camera attached on the single crystal diffractometer.

Deracemization experiments
In a 100 mL round bottom flask with an oval PTFE-coated magnetic stirring bar (L 20mm, Ø 10mm) were weighed in 3.2 g of (*R/S*)-**1**, 10.0 g of MeOH (dried and distilled from CaH_2) and 6.0 g Ø 2-2.5 mm glass pearls (Aldrich) under Schlenck conditions. The flask was sealed and stirred for 2 hours at ca. 600 rpm using a magnetic stirrer to equilibrate the solvent and solute. To the suspension 0.24 g (10 mol%) of 1,8-diazabicyclo[5.4.0]undec-7-ene (DBU) was added. After 10 minutes, the t = 0 sample was taken from this suspension. Additional samples were taken daily. The enantiomeric purity was measured using chiral HPLC as described below. The chemical purity was monitored using ^{1}H-NMR, DSC and XRPD (Figure SI-5.1).

Sampling
For sampling, 0.2 mL of the slurry was taken using a syringe and filtered on a P4 glass filter (Ø 10 mm). The residue was washed with 0.5 mL of 2-propanol and 0.1 mL of methyl tert-butyl ether (MTBE) to remove the mother liquid and DBU, and dried overnight at 40 ºC in a vacuum stove.

Determination of the ee by chiral HPLC analysis of the solid samples
Sample preparation 0.5 mg solid in 1.5 mL eluent, injection volume 20µL, HPLC column Chiralpak-AD-H (250x4.6 mm ID), eluent n-hexane/2-propanol 80/20 v/v%, flow 1mL/min, r.t., detection λ=254 nm. Retention times: (*S*)-**1** 5.3 min, (*R*)-**1** 5.7 min.

Determination of the ee by chiral HPLC analysis of individual crystals of racemic 1
The *ee* determination of five individual crystals by the HPLC method described above revealed that each crystal was virtually racemic: 6, 2, 1, -2 and 5% *ee*, respectively.

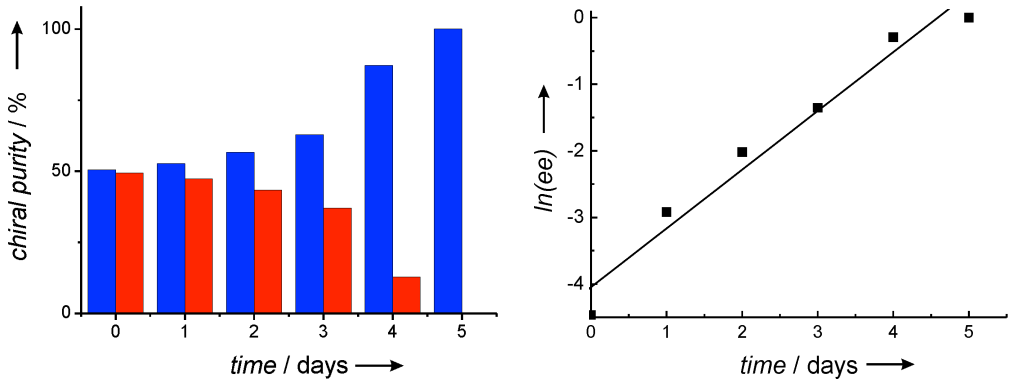

Figure SI-5.2. Typical evolution of the solid phase chiral purity during grinding (left), showing an exponential evolution of the enantiomeric excess in (*S*)-**1** (right). The initial ee in the solid phase before dissolution was 0.35%, and increases upon dissolution to approximately 1%.

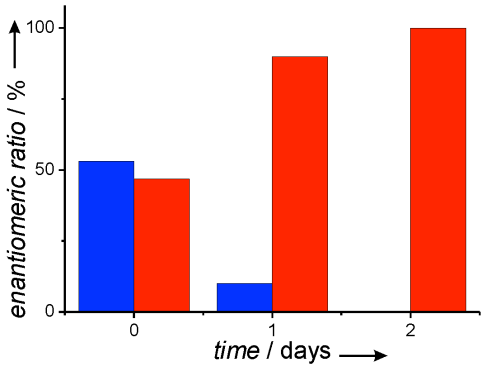

Figure SI-5.3. Evolution of the enantiomeric ratio starting with an excess of small (*S*)-**1** crystals and a minor population of large (*R*)-**1** crystals. The small crystals rapidly dissolve and nurture the larger (*R*)-crystals until complete symmetry breaking is achieved.

Deracemization experiments with different crystal sizes

Typically, in 100 mL round bottom flasks with an oval PTFE-coated magnetic stirring bar (L 20mm, Ø 10mm) were weighed in 1.6 g of (*S*)-**1**, 5.0 g of MeOH (dried and distilled from CaH_2) and 6.0 g Ø 2-2.5 mm glass pearls (Aldrich) under Schlenck conditions. The flask was sealed and stirred for 2 hours at ca. 600 rpm using a magnetic stirrer to equilibrate the solvent and solute. In another 100 mL round bottom flask with an rod-like PTFE-coated magnetic stirring bar (L 20mm, Ø 5mm) were weighed in 1.5 g of (*R*)-**1**, and 5.0 g of MeOH (dried and distilled from CaH_2) under Schlenck conditions. No glass beads were added. The flask was sealed and stirred for 2 hours at ca. 100 rpm using a magnetic stirrer to equilibrate the solvent and solute. After this, to both flasks was added 0.11 g DBU and stirring was maintained. After 5 hours, the contents of the both flasks were combined (without the rod-like PTFE-coated magnetic stirring bar) and stirring was maintained at 500 rpm. From this mixture the t=0 sample was collected. Additional samples were taken daily.

Supporting Information Chapter 6

Methyl (*RS*)-2-(6-methoxynaphthalen-2-yl)propanoate (methyl ester of naproxen) 1

To a methanol solution (250 mL) of (*RS*)-2-(6-methoxynaphthalen-2-yl)propanoic acid (naproxen, 2.0 g, 8.81 mmol) was added 0.4 g of conc. H_2SO_4 and the reaction mixture was stirred for overnight before it was diluted with CH_2Cl_2 (ca. 50 mL), washed with sat. $NaHCO_3$ aq. solution and dried over sodium sulfate. Solvent evaporation gave the title methyl ester quantitatively.

^{1}H NMR (400 MHz, $CDCl_3$): δ = 7.62 (s, 1H), 7.57 (d, 1H, J = 8.5 Hz), 7.48-7.45 (m, 2H), 7.18 (d, 1H, J = 2.6 Hz), 6.89 (d, 1H, J = 2.4 Hz), 3.71 (q, 1H, J = 7.1 Hz),3.36 (s, 3H), 3.28 (s, 3H), 1.52 (d, 3H, J = 7.1 Hz).

Methyl (*S*)-2-(6-methoxynaphthalen-2-yl)propanoate (methyl ester of naproxen) 1
To a methanol solution (250 mL) of (*S*)-2-(6-methoxynaphthalen-2-yl)propanoic acid (naproxen, 6.13 g, 27.0 mmol) was added 1.0 g of conc. H_2SO_4 and the reaction mixture was stirred for overnight before it was diluted with CH_2Cl_2 (ca. 50 mL), washed with sat. $NaHCO_3$ aq. solution and dried over sodium sulfate. Solvent evaporation gave the title methyl ester quantitatively.
^{1}H NMR (400 MHz, $CDCl_3$): δ = 7.62 (s, 1H), 7.57 (d, 1H, J = 8.5 Hz), 7.48-7.45 (m, 2H), 7.18 (d, 1H, J = 2.6 Hz), 6.89 (d, 1H, J = 2.4 Hz), 3.71 (q, 1H, J = 7.1 Hz),3.36 (s, 3H), 3.28 (s, 3H), 1.52 (d, 3H, J = 7.1 Hz).

Ethyl (*RS*)-2-(6-methoxynaphthalen-2-yl)propanoate (ethyl ester of naproxen) 2
Following the procedure of (*RS*)-**1**, however with ethanol instead of methanol, (*RS*)-2-(6-methoxynaphthalen-2-yl)propanoic acid (naproxen, 5.74 g, 27.0 mmol) in 250mL ethanol with ca. 1.2 g concentrated H_2SO_4 was converted to the title product quantitatively.
^{1}H NMR (300 MHz, $CDCl_3$): δ = 7.72-7.67 (m, 3H), 7.41 (dd, 1H, J = 1.8 Hz, J = 8.4 Hz), 7.16-7.12 (m, 2H), 4.21-4.05 (m, 2H), 3.91 (s, 3H), 3.83 (q, 3H, J = 7.2 Hz), 1.55 (d, 2H, J = 3.0 Hz), 1.20 (t, 3H, J = 8.1 Hz).

Ethyl (*S*)-2-(6-methoxynaphthalen-2-yl)propanoate (ethyl ester of naproxen) 2
Following the procedure of (*S*)-**1**, however with ethanol instead of methanol, (*S*)-2-(6-methoxynaphthalen-2-yl)propanoic acid (naproxen, 10.25 g, 48.2 mmol) in 350 mL ethanol with ca. 2.0 g concentrated H_2SO_4 was converted to the title product quantitatively.
^{1}H NMR (300 MHz, $CDCl_3$): δ = 7.72-7.67 (m, 3H), 7.41 (dd, 1H, J = 1.8 Hz, J = 8.4 Hz), 7.16-7.12 (m, 2H), 4.21-4.05 (m, 2H), 3.91 (s, 3H), 3.83 (q, 3H, J = 7.2 Hz), 1.55 (d, 2H, J = 3.0 Hz), 1.20 (t, 3H, J = 8.1 Hz).

Deracemization of methyl (*RS*)-2-(6-methoxynaphthalen-2-yl)propanoate 1
In a standard 10 mL sample vial were added 8.7 g glass beads, 0.7553 g (*RS*)-**1**, 0.0030 g (*S*)-**1** and 6.302 g of a 13.6 wt% solution of NaMeO in MeOH (from stock: 2.2g Na dissolved in 45 mL MeOH). The sample vial was closed with a septum, and placed on an Elma Transsonic T470/H ultrasonic bath. The bath was kept at a constant temperature of 23 °C using a cooling spiral that was attached to a Julabo F25 thermostat bath. For sampling, 0.3 mL of the slurry was taken using a syringe, filtered on a P4 glass filter and washed with ca. 2mL MeOH. The chemical and enantiomeric purity was measured using chiral HPLC, ^{1}H-NMR and XRPD. HPLC analysis was performed on Chiralcel-OJ (250x4.6 mm ID) column, eluent n-hexane/2-propanol 98/2 v/v%, flow 1mL/min, r.t., detection λ=254 nm. Retention times (*S*)-**1** 11.5 min, (*R*)-**1** 12.8 min.

Transesterification mediated deracemization of methyl (*RS*)-2-(6-methoxynaphthalen-2-yl)propanoate
Under Schlenck conditions, to a standard 25 mL roundbottom flask were added 8.7 g glass beads, 0.6120 g (*RS*)-**2**, 0.050 g (*S*)-**1** and 6.502 g of a 13.8 wt% solution NaOMe in MeOH (from a stock containing 10mL MeOH and 0.5g Na) and an oval magnetic stirring bar. The flask was agitated at 700rpm and watches were synchronized. For sampling, 0.3 mL of the slurry was taken using a syringe, filtered on a P4 glass filter and washed with ca. 2mL MeOH. The chemical and enantiomeric purity was measured using chiral HPLC, ^{1}H-NMR and XRPD. HPLC analysis was performed on Chiralcel-OJ (250x4.6 mm ID) column, eluent n-hexane/2-propanol 98/2 v/v%, flow 1mL/min, r.t., detection λ=254 nm. Retention times (*S*)-**2** 10.2 min, (*R*)-**2** 10.8 min, (*S*)-**1** 11.5 min, (*R*)-**1** 12.8 min.

Supporting Information Chapter 7

Typically, 1.0 g (*RS*)-**1**, 0.2 g enantiopure **2** (16.5 mol%), 8.0 g glass beads (2.5mm) and 20.0 g MeCN were added to a 50 mL round bottom flask and stirred at 600 rpm using a magnetic bar. For sampling, ca. 0.2 mL of the slurry was filtrated on a P3 glass filter and washed 1-2 sec. with 0.2 mL Toluene. Samples were analyzed using H-NMR, XRPD and HPLC (chiralcel AD-H column (250x4.6 mm), eluent n-hexane/2-propanol, 90/10 v/v%, flow 1ml/min, retention times: (*S*)-**1** 7.5 min., (*R*)-**1** 8.2 min., (*R*)-**2** 13.6 min., (*S*)-**2** 15.2 min.).

Supporting Information Chapter 8

Circularly polarized light irradiation set-up
A 200W Xenon Mercury lamp was used to generate a broad spectrum of UV-Vis light. An optical train consisting of a 300-400nm filter, two lenses and a UV-mirror provided a vertical light beam. The circular polarisation was generated using a polarizer followed by a Babinet-Soleil compensator. The circularity of the light was checked using a polarisation filter and a power meter behind the Babinet-Soleil compensator. In this work, all the irradiations were carried out using circularly polarized light of 310nm wavelength. The power of the resulting CPL is approximately 0.35 mW.

CPL irradiation experiments
For the irradiation experiments reaction vessels with a quartz window were used. The vessel containing 0.44g racemic **1** and 6.25g MeCN was irradiated for 3 to 5 days with CPL. After the irradiation the quartz window was removed and 8.0g glass beads and 0.12 g DBU were added, after which the reaction vessel was closed with a septum. Then the slurry was ground for 16-30 hours using a thermostated ultrasonic cleaning bath at 25°C. X-ray powder diffraction patterns of the solids obtained showed no polymorphism as a result of the CPL irradiation.[1]

Check experiment using linearly polarized light
To confirm that the directed symmetry breaking was caused by the sense of the incoming CPL, experiments were carried out using linearly polarized light. For this, the same experimental setup was used as for the CPL experiments, but without the Babinet-Soleil compensator. Following the procedure for the CPL irradiation experiments, a vessel containing 0.44g racemic **1** and 6.25g was irradiated for 3 days. After the irradiation 8.0g glass beads and 0.12 g DBU were added after which the reaction vessel was closed with a septum. The slurry was ground for 16-30 hours using a thermostated ultrasonic cleaning bath at 25°C. HPLC analysis revealed that all these experiments evolved to an enantiopure (*R*)-**1** solid phase, as is also observed in experiments without irradiation.

Sampling and HPLC analysis
For sampling, 0.3 mL of the slurry was taken using a syringe and filtered on a P3 or P4 glass filter (Ø 10 mm). The residue was washed with 1 mL of MeOH or MeCN and 2 mL of MTBE to remove mother liquid and DBU, and dried overnight in a vacuum stove at 40 ºC.
For *ee* determination using HPLC analysis, about 0.5 mg solid was dissolved in 1.5 mL eluent, injection volume 20µL, HPLC column Chiralcel-OJ (250x4.6 mm ID), eluent n-hexane/2-propanol 80/20 v/v%, flow 1mL/min, detection λ=254 nm. Retention times (*R*)-**1** 7.9 min, (*S*)-**1** 8.5 min.

HPLC analysis of the solution phase after irradiation
HPLC analysis of the solution phase shows the formation of low concentrations of several products upon irradiation (Figure SI 2). The complex mixture of photoproducts formed in low yield after long irradiation was analysed extensively. Only one photo-oxidation product *N*-benzoyl-2-methylbenzamide could be isolated and identified but this compound can not be involved as a directing agent in the deracemisation process since it is achiral.

2-(2-methylphenyl)-5-phenyl-imidazolidin-4-one as directing agent

Chiral cyclic products of **1** are known to be formed easily and the retention times of these products correspond to minute peaks in the HPLC traces of the irradiated solutions (Figure SI 3). Therefore we expect these products to be present in the solutions. To test their directing activity in the deracemisation process of **1** we synthesised such cyclic products and subsequently used them as additives in the deracemisation experiment. Indeed, these cyclic products direct the outcome of the deracemisation reaction. The handedness of the outcome follows 'the rule of reversal', in line with the overall effect of the impurities we observed.

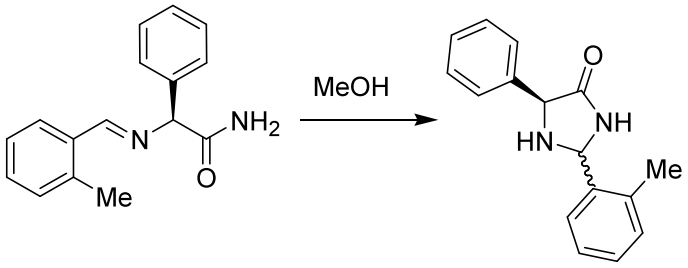

Figure SI 8.1. The formation of the diastereomeric cyclic products 2-(2-methylphenyl)-5-phenyl-imidazolidin-4-one **2** and **2'** from **1** as observed in protic solvents.

Synthesis of 2-(2-methylphenyl)-5-phenyl-imidazolidin-4-one 2

In a 10 mL round bottom flask equipped with a reflux cooler 0.17 g enantiopure **1** was dissolved in 2.0 g MeOH. The solution was heated overnight at 50 °C yielding a mixture of the diastereomeric mixture of the cyclisation product 2-(2-methylphenyl)-5-phenyl-imidazolidin-4-one (enantiopure 1:1 diastereomeric mixture). This mixture of diastereoisomers could be separated using flash chromatography.

First fraction **2**: ^{1}H NMR (300 MHz, DMSO) δ 8.72 (d, 1H), 7.6-7.15 (m, 9H), 5.83 (d, 1H), 4.52 (d, 1H), 3.73 (t, 1H), 2.4 (s, 3H).

Last fraction **2'**: ^{1}H NMR (300 MHz, DMSO) δ 8.63 (s, 1H), 7.6-7.15 (m, 9H), 5.83 (d, 1H), 4.62 (d, 1H), 4.03 (t, 1H), 2.4 (s, 3H).

HPLC retention times: (*R*)-**2**: 9.6 min, (*R*)-**2'**: 10.0 min, (*S*)-**2**: 11.1 min, (*S*)-**2'**: 11.8 min.

Testing of 2-(2-methylphenyl)-5-phenyl-imidazolidin-4-one as chiral additive

In a standard reaction vial 1.04 g of the diastereomeric mixture of 2-(2-methylphenyl)-5-phenyl-imidazolidin-4-one **2** was dissolved in 3.00 g MeCN. To the clear solution was added 0.15 g DBU to racemise possible traces of enantiopure **1**. After 3 hours 8.5 g glass beads and 0.55g (*RS*)-**1** were added to create a solution-solid mixture. The mixture was deracemised in an thermostated ultrasonic cleaning bath overnight. The deracemisations containing the cyclic diastereomeric mixture of (*S*)-**1** evolved to (*R*)-**1** and *vice versa*.

References Supporting Information

[1] Garetz, B. A.; Aber, J. E.; Goddard, N. L.; Young, R. G.; Myerson, A. S. Nonphotochemical, polarization-dependent, laser-induced nucleation in supersaturated aqueous urea solutions. *Phys. Rev. Lett.* **77,** 3475-3476 (1996).

Summary

The properties of chiral molecules can be different in living organisms for left- and right handed molecules. Therefore, ways to produce molecules of single handedness are of paramount practical importance today, especially for economical, high yielding processes to synthesize pharmaceutical compounds that often must be registered in enantiomerically pure form. Recently a surprisingly simple way to achieve complete chiral resolution for the conglomerate forming salt $NaClO_3$ was discovered. Viedma demonstrated the inexorable transformation of a racemic solid phase into a solid phase of single chirality by simply grinding the crystals in a saturated solution. Although the exact mechanism was not understood, the conversion relies on the fact that the chiral identityin the solid phase of the intrinsically achiral $NaClO_3$ is lost upon dissolution (Figure 1). This intriguing result formed the starting point of this PhD research.

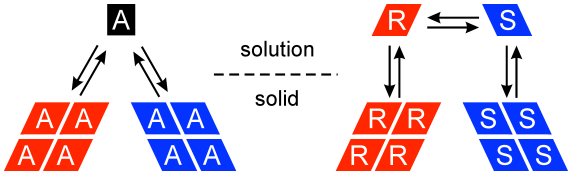

Figure 1. Analogy between solid-solution equilibrium for an intrinsically achiral molecule and a chiral molecule undergoing solution-phase racemization.

The results of Viedma inspired us to apply the technique of abrasive grinding to genuine chiral, consisting of chiral molecules like many pharmaceutical products and their intermediates. To achieve this, a system is needed that first of all forms a conglomerate, and secondly racemizes in solution, in order to maintain a racemic solution during the deracemization process. In Chapter 2 we demonstrate the proof of principle for this method using the imine **1** as a chiral compound, as it is easily racemized in a solution by adding the base DBU (Figure 2). In a series of experiments, showing a complete deracemization of the solid phase in approximately 30 days, the concept was proven. Furthermore, we were able to direct the outcome either by starting from a small enantioimbalance in the solid phase or by adding enantiopure additives.

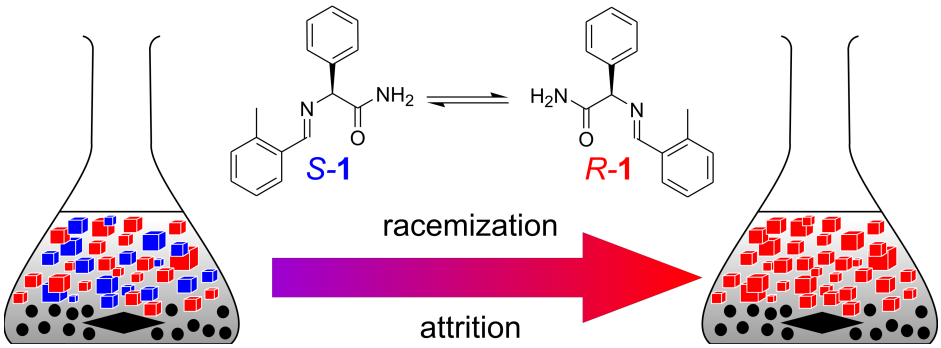

Figure 2. Schematic representation of the deracemization process using abrasive grinding.

We noticed that in the absence of grinding, Ostwald ripening always leads to a solid of single chirality for $NaClO_3$ (Figure 3, left). Ostwald ripening is a process in which under near equilibrium conditions the larger crystals grow at the cost of the smaller ones. This is a

consequence of the Gibbs-Thomson effect, which arises from the fact that large crystals have a lower free energy because of their smaller surface-to-volume ratio. Ostwald ripening, therefore, always leads to a final state consisting of one single crystal that by necessity has a single handedness. This process takes, however, a very long time, up to months, or even years.

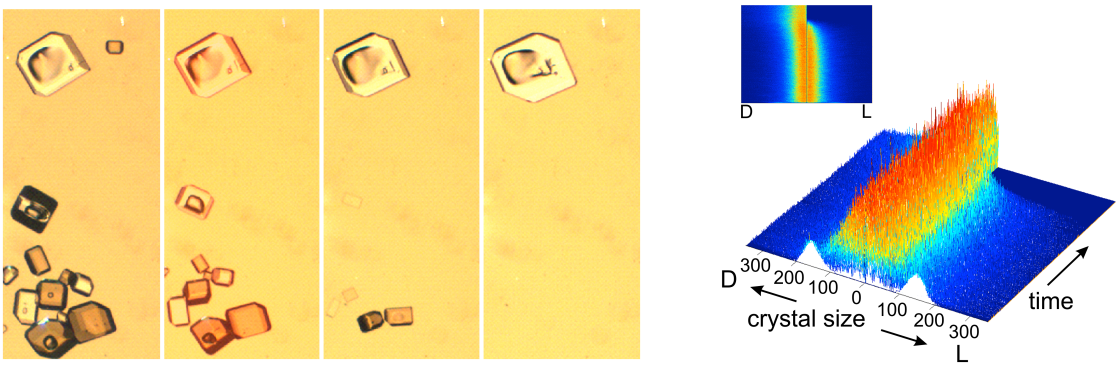

Figure 3. Left: Ostwald ripening of $NaClO_3$ crystals as observed under a microscope. By using polarizers, the crystals of one handedness are dark and the other light. The end result is a single crystal with single chirality. Right: the result of a computer simulation in which an initial racemic mixture of crystals evolves towards chiral purity.

To further elucidate the accelerating mechanism behind the grinding technique we performed a computer simulation study (Chapter 3). The continuous abrasion of the crystals to small fragments in the deracemization experiments turned out to indeed accelerate the deracemization process. The computer simulations showed that an excess in one of the enantiomers as a result of stochastic fluctuations or of chiral additives, will force the deracemization process to a 100% chiral purity of the solid state (Figure 3). Moreover, the simulations revealed the relevant parameters for the optimization of the deracemization process. In further experiments, choosing suitable conditions inspired by the simulation results, we were able to decrease the deracemization time from approximately 30 days to less than one day, making this a practical route to enantiomerically pure materials (Chapter 4).

Next the research focussed on finding different molecules to show the general applicability of this method. First, a derivative of the natural amino acid phenyl alanine was deracemized (Chapter 5). However, for this compound, the two enantiomeric solids exhibit mutual epitaxial growth, leading to crystals that consist of several blocks of each enantiomer. Such a growth mode inhibits direct resolution by entrainment. We were pleased to observe, however, that under abrasive grinding conditions a mixture of enantiomers was still converted completely into a single chiral solid phase of the desired handedness.
Using the nonsteroidal anti-inflammatory drug Naproxen as an example of commercially interesting molecule we demonstrated that the commercially relevant (*S*)-enantiomer could be obtained by applying the technique of grinding under racemizing conditions (Chapter 6).

We realized that if we could enantioselectively hamper the growth of one of the two enantiomers using a chiral additive, these crystals could not recover from the grinding, thereby remaining small. This would allow a resolution of the enantiomers without the necessity of the racemization reaction in the solution. In Chapter 7 this idea was tested using a derivate of the amino acid alanine. In case an additive stereoselectively hampers the crystal growth, the crystal size distribution shifts towards smaller sizes for that enantiomer. The

enantioselective hampering follows the 'rule of reversal', that is, the additive (*R*)-**1** blocks (*R*)-**2**, resulting in a monopolization of large (*S*)-**2** crystals and *vice versa*. The large crystals can then be separated by applying a simple washing step in which the small crystals of the undesired handedness are washed away, yielding an enantiopure solid phase of large crystals.

The findings so far also touch on the fundamental scientific issue of the origin of the single handedness of biomolecules in the prebiotic world. Various deterministic scenarios for the evolution of biological homochirality, as found in left-handed amino acids and right-handed sugars, have been proposed. Circularly polarized light (CPL), a phenomenon that is also observed during star formation, is one of the possible actors for such mechanisms. As we knew that the grinding deracemization technique is extremely sensitive to chiral influences, we decided to investigate the use of CPL to direct the final outcome. Indeed, in Chapter 8 we demonstrate that it is possible to transform under grinding conditions a racemic mixture of left- and right-handed crystals into crystals of single chirality hand, with a handedness depending on the rotation sense of the circularly polarized light. The observed deterministic deracemization is attributed to the enantioselective photochemical formation of a chiral crystal growth inhibitor.

Routes to enantiomerically pure molecules are of cardinal importance in the pharmaceutical and food industry. Compared to asymmetric synthesis and separation of enantiomers, the near equilibrium deracemization method is a promising technique with virtually 100% yield. Although the technique is limited to racemic conglomerates that racemize in solution, screening of derivatives on that property broadens the general applicability. From another perspective, the deracemization method outlines a possible pathway to the homochirality found in nature, thereby contributing to the discussion on the emergence of prebiotic chiral molecules.

Samenvatting

De eigenschappen van chirale moleculen kunnen in levende organismen verschillend zijn voor hun links- en rechtshandige variant. Economisch rendabele routes met een hoge opbrengst om moleculen van één hand te maken zijn daarom van groot belang, vooral voor medicijnen die in toenemende mate enantiomeer zuiver worden geregistreerd. Kort geleden werd een verbazingwekkend eenvoudige methode gevonden om het conglomeraat vormende chirale zout natriumchloraat ($NaClO_3$) te transformeren naar kristallen van één hand. Viedma liet zien dat een mengsel van links- en rechtshandige kristallen in een verzadigde oplossing, door het malen van de kristallen, volledig werd omgezet in kristallen van slechts een enantiomorf. Alhoewel het onderliggende mechanisme niet helemaal begrepen werd, berust de omzetting op het feit dat de chirale identiteit van het intrinsiek niet chirale $NaClO_3$ verloren gaat tijdens het oplossen van de kristallen (Figuur 1). Deze intrigerende resultaten vormden het startpunt van dit promotieonderzoek.

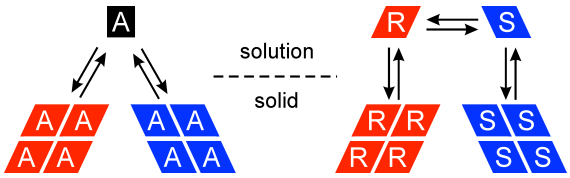

Figuur 1. De analogie tussen het vaste stof-vloeistof evenwicht voor intrinsiek achirale moleculen en voor chirale moleculen die racemiseren in de vloeistoffase.

Viedma's resultaten inspireerden ons om deze techniek van verpulverend malen toe te passen op intrinsiek chirale moleculen en in het bijzonder op farmaceutisch relevante verbindingen. Om dit te bewerkstelligen is allereerst een systeem nodig dat kristalliseert in de vorm van een conglomeraat. Daarnaast moeten de moleculen ook racemiseren in de oplossing om zo een racemische oplossing te behouden tijdens de deracemisatie. In hoofdstuk 2 laten we zien dat de methode werkt. Daarbij gebruiken we een imine **1** als chiraal molecuul omdat dit eenvoudig racemiseert in de oplossing door de base DBU toe te voegen (Figuur 2). Het concept werd bewezen in een serie experimenten waarbij de vaste stof volledig werd gederacemiseerd in 30 dagen. Verder konden we de uiteindelijke uitkomst sturen met kleine entiomere overmaten in de vaste stof en door enantiomeer zuivere additieven.

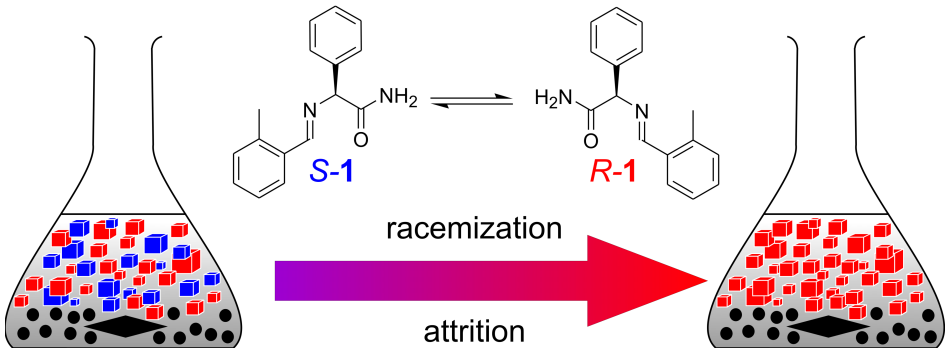

Figuur 2. Schematische weergave van het deracemisatieproces via verpulverend malen.

Het viel ons op dat Ostwald ripening in de afwezigheid van malen ook altijd leidt tot een vaste stof die uit slechts een hand bestaat (Figuur 3, links). Ostwald ripening is een proces waarbij onder condities die dicht bij evenwicht liggen, grote kristallen groter worden ten koste van de kleinere. Dit in een gevolg van het zogenaamde Gibbs-Thomson effect dat voortkomt uit het feit dat grotere kristallen een lagere vrije energie hebben omdat hun oppervlak in verhouding tot hun volume kleiner is. Daardoor resulteert Ostwald ripening altijd in een vaste stof die bestaat uit een enkel kristal en dus uit slechts één hand. Dit proces kan echter heel lang duren, maanden en soms zelfs jaren.

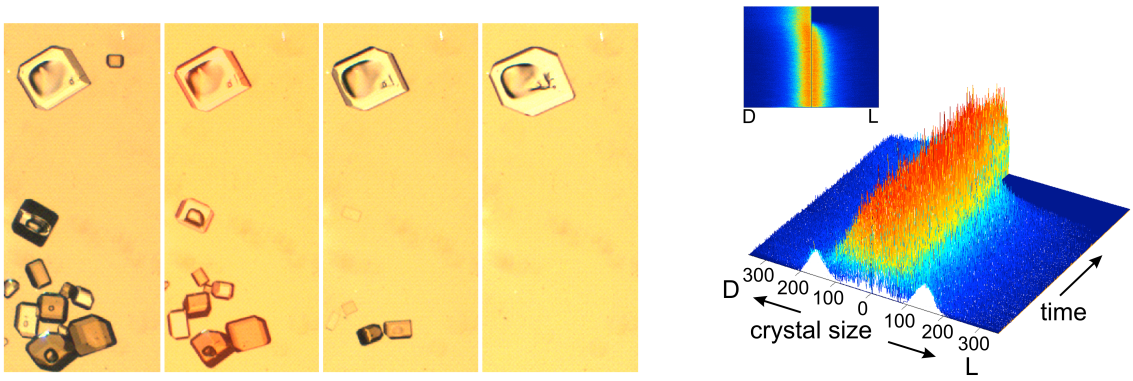

Figure 3. Links: Ostwald ripening van $NaClO_3$ kristallen gezien door een microscoop. Met behulp van polarisatiefilters blijven de kristallen van een hand donker en die van de andere hand lichten op. Het eindresultaat is één enkel kristal van één hand. Rechts: de resultaten van een computersimulatie waarbij een aanvankelijk racemisch mengsel van kristallen evolueert naar een enantiomeer zuivere vaste stof.

Om het versnellende mechanisme van het malen beter te begrijpen hebben we vervolgens een computersimulatiestudie uitgevoerd (Hoofdstuk 3). De simulaties lieten zien dat het voortdurend breken van kristallen in kleine fragmenten inderdaad het deracemisatieproces versnelt. Ook bleek dat kleine fluctuaties in de enantiomere overmaat als een gevolg van stochastische fluctuaties of chirale additieven de deracemisatie naar 100% chirale zuiverheid in de vaste stof sturen (Figuur 3, rechts). Verder onthulden de simulaties ook de snelheidsbepalende parameters van het proces. In daaropvolgende praktische experimenten konden we hierdoor de deracemisatietijd terugbrengen van ongeveer 30 dagen tot minder dan een dag, waardoor dit een in de praktijk toepasbare route werd om enantiomeer zuivere materialen te maken (Hoofdstuk 4).

Hierna richtte het onderzoek zich op andere verbindingen om zo de algemene toepasbaarheid aan te tonen. Allereerst werd een afgeleide van het natuurlijke aminozuur fenylalanine gederacemiseerd (Hoofdstuk 5). Het bleek echter dat voor deze stof de twee enantiomorfen onderling epitaxiaal op elkaar groeien in de vorm van dunne balken. Een dergelijke groei maakt een klassieke resolutie onmogelijk. Toch konden deze min of meer racemische kristallen worden omgezet in een enantiomeer zuivere vaste stof door de techniek van verpulverend malen toe te passen. Een volgende stap was het ontwikkelen van een route om het enantiomeer zuivere niet-steroïdale anti-inflammatoire middel Naproxen te maken, om te laten zien dat het proces ook gebruikt kan worden voor commercieel interessante moleculen. Door het toepassen van het maalproces onder racemiserende condities kon hierdoor de commercieel belangrijke (*S*)-enantiomeer worden gemaakt.

We realiseerden ons dat als we in staat waren om de groei van kristallen van een hand selectief te blokkeren met een additief dat deze kristallen dan niet zouden kunnen herstellen van het fijnmalen en klein zouden blijven. Hierdoor zou het mogelijk zijn om de enantiomeren van elkaar te scheiden zonder dat de racemisatie in de oplossing vereist was. In Hoofdstuk 7 wordt dit idee getest voor een afgeleide **2** van het aminozuur alanine. Als een additief stereoselectief de kristalgroei blokkeert, verschuift de kristalgrootte verdeling voor die enantiomeer naar kleinere afmetingen. De stereoselectieve blokkering volgt de 'rule of reversal'. Dat betekent dat het additief (*R*)-**1** de kristalgroei van (*R*)-**2** blokkeert waardoor er alleen grote (*S*)-**2** kristallen over blijven en *vice versa*. Deze grote kristallen kunnen dan verzameld worden door een simpele wasstap waarbij de kleine kristallen van de ongewenste hand oplossen. Hierdoor blijft een enantiomeer zuivere vaste stof achter die alleen bestaat uit grote kristallen.

De bovengenoemde resultaten raken ook aan de fundamentele discussie over het ontstaan van de enantiomeer zuiverheid van biomoleculen in de prebiotische wereld. Verschillende deterministische scenario's zijn al voorgesteld om de evolutie van biologische homochiraliteit te verklaren zoals gevonden wordt in linkshandige aminozuren en rechtshandige suikers. Circulair gepolariseerd licht is een mogelijk sturende kracht in een aantal van die hypotheses. Omdat we wisten dat de maaltechniek zeer gevoelig is voor chirale invloeden, besloten we om de invloed van circulair gepolariseerd licht te testen. Inderdaad vonden we dat het mogelijk is om onder malende condities een racemisch mengsel van links- en rechtshandige kristallen om te zetten in kristallen van één hand waarbij de draaiing van het licht bepaalt welke hand wordt gevormd. De waargenomen deterministische deracemisatie wordt verklaard door de enantioselectieve fotochemische omzetting van een fractie van de moleculen in additieven die de kristalgroei blokkeren.

Routes naar enantiomeer zuivere moleculen zijn van groot belang voor de farmacie en de voedselindustrie. Vergeleken met asymmetrische synthese en scheiding van enantiomeren is deze deracemisatietechniek een veelbelovende methode met 100% opbrengst. Alhoewel de techniek gelimiteerd is tot racemische conglomeraten die racemiseren in de oplossing kan screening van derivaten op deze eigenschappen de algemene toepasbaarheid vergroten. Vanuit een ander perspectief beschrijft deze deracemisatietechniek ook een mogelijke route naar homochiraliteit zoals die wordt aangetroffen in de natuur, zodat deze resultaten bijdragen aan de discussie over het ontstaan van prebiotische chirale moleculen.

Dankwoord

De afgelopen jaren heb ik veel geleerd van alle enthousiaste mensen om me heen. Allereerst wil ik Elias bedanken. Ik heb een supertijd gehad op de afdeling vaste stof chemie, de heel gezellige barbecues bij jullie thuis, de spoedcursus overleven in Amerika, ik vond het allemaal prachtig. Willem, de fabricage van "Duitse wijn" van druivenstruiken die door de versnipperaar gingen, maakte als klein buurjongetje, al grote indruk. Ook op de universiteit heb ik van jou nog een hoop geleerd over wijn, microscopie, kristalgroei en nog veel meer. Hugo, aanvankelijk zat je natuurlijk helemaal niet in het project. Maar vanaf het moment dat je een paar nachten met Grolsch in de pijpdampen het computermodel maakte dat ons overtuigde dat het malen geen complete onzin was, zat ik voortdurend bij jou op de "gastenstoel". De schrijfacties waarbij we met een kop koffie de manuscripten bijschaafden vond ik altijd heel gezellig.

Tijdens het onderzoek is voortdurend samengewerkt met Syncom B.V. en DSM. Een speciaal woord van dank voor Prof. Kellogg die onder de ambitieuze naam Ultimate Chiral Technology deze promotie mogelijk maakte. Ik waardeer het zeer dat u altijd nauw betrokken was bij het onderzoek. Ook het afsluitende symposium met het etentje waren zeer geslaagd en heel gezellig.
Bernard, ik denk met veel plezier terug aan onze samenwerking maar ook heel onderhoudend. Onze vele en lange telefoongesprekken waren absoluut belangrijk voor het onderzoek. Ik heb veel geleerd van al je kennis over kristallen en organische chemie en genoten van het wielrennen in zuid Limburg en het wandelen in de Alpen.
Ook Peter Quaedflieg, Rinus Broxterman, Hans de Vries en Hans Schoemaker wil ik graag bedanken voor hun bijdragen aan het UCT project. Verder wil ik Edith Gelens bedanken voor alle hulp. Michel Leeman en Maarten van der Meijden wil ik graag bedanken voor de goede samenwerking die tot meerdere publicaties heeft geleid. I also would like to thank Donna Blackmond, Toshiko Izumi and Alessia Millemaggi. It was very exciting to work with you on the first publication that gave a boost to my PhD project. Prof. Meir Lahav has been an inspiring person for me. I would like to thank you for giving me the opportunity to present our results during the 'Origins of Homochirality' meeting in Stockholm. There I also met Cristobal Viedma, the founding father of the grinding method, with whom I shared many ideas in an open-hearted atmosphere.

Ook alle mensen van organische chemie wil ik graag bedanken voor hun hulp bij het onderzoek of als ik weer eens mijn pasje kwijt was. Floris Rutjes, heel erg bedankt dat ik altijd kon binnenlopen voor adviezen en dat ik jullie apparatuur kon gebruiken. Jorge: we hadden echt eerder moeten beginnen met etentjes en fietstochtjes.
Verder wil ik graag Ad Swolfs bedanken voor de NMR, Rene Aben voor de fijne kneepjes van de organische chemie, Floris van Delft voor de tips die ik kreeg (jammer dat die suikers zo'n plakbende gaven) en Desiree en Jacky voor alle administratieve dingetjes en het altijd weer weten waar iedereen uithing. Kasper Koch en Pieter Nieuwland wil ik graag bedanken voor de hulp bij de chirale HPLC. Heel veel succes met jullie bedrijf.

Ook Theo Rasing en Peter Christianen wil ik bedanken. Het enorme enthousiasme en jullie kennis was absoluut essentieel om het laatste hoofdstuk te kunnen maken. Albert van Etteger en Tonnie Toonen: volgens mij moeten jullie veel lol hebben gehad met die chemici die stuntelen met optica. Bedankt voor jullie geduld en alle uitleg.

Jan Smits, heel veel bedank voor het meten van alle kristalstructuren die terug te vinden zijn in het proefschrift.

Geert Deroover en alle medewerkers van AGFA-Gevaert wil ik ook graag danken voor hun hulp bij de maalproeven en voor de Vlaamse gastvrijheid.

Zjak, jou wil ik heel graag bedanken voor je enorme enthousiasme. Het was heel mooi dat we een paar keer bij Synthon langs konden komen om jullie apparatuur te gebruiken.

Aan dit promotieonderzoek hebben ook meerdere studenten meegeholpen. Koen (mijn eerste student), Anne (sjaaltjes), Annelies (voetbal), Arno ('the Dedicated Unit DEvise'), Pim (vinyl), Bas (toeteren) en Dirk (live action role playing) zeer bedankt voor jullie hulp.

De heel goede sfeer op de afdeling was absoluut belangrijk voor mij. Alle koffiepauzes, gezellige etentjes, tafelvoetbalcompetities en de discussies over werkelijk alle mogelijke onderwerpen maakten het al met al een mooie boel. Daarom heel erg bedankt Jan van Kessel, Wiesiek, Fieke, Alaa, Elizabeth, René, Natalia (en daarmee ook Martijn), Paul P., Maurits (lepelen tegen onze Angstgegner John), Jan Los, Menno, Edwin, Sander, Zjak, Carmen, Cristina en Ismail. En natuurlijk moeten ook mijn kamergenoten worden genoemd, Paul T. (gedeelde culinaire interesses, wijncolloquia, alle projectjes), Rienk (ook voor de medische begeleiding als ik in de kreukels lag, het was toch wel lachen op de EHBO in Park City) en Vedran (Deutschmeister).

Ook de groep van AMS moet natuurlijk niet vergeten worden vanwege de voetbaltafel, tourkamer en al jullie gereedschap. Daarom wil ik ook graag John, Paul, Gerard, Peter, Harry, Erik, Gerbe, Ton, Hina, Ine, Tim en Günther bedanken. Wil, erg bedankt voor het maken van onderdelen die essentieel waren voor het onderzoek (koffiestamper, onderdelen voor de voetbaltafel, cannoli buizen).

Iedereen van het fietsen en hardlopen, speciaal Mart en Theo, heel erg bedankt. Patrick, ik ken niemand met wie ik zo kan ouwehoeren over werkelijk alles, bij een gestaag gemiddelde van 33 km/h (oh, zitten we al onder Sittard...). De vakantie in Portugal was echt zwaar relaxed en absoluut essentieel voor de laatste 'cartouche' om het proefschrift af te ronden. Ik vind het mooi om te zien hoe Luciënne en jij alles aanpakken en er echt iets van maken. Scarlett, je bent een supermeid en ik ben heel blij dat ik je ontmoet heb.
Tenslotte wil ik mijn ouders en broertjes graag bedanken.

Curriculum Vitae

Name:	Willem Lieuwe Noorduin
Date of birth:	31-12-1980

Education:

1993-1999:	Secondary school "Collegium Marianum", Venlo
1999-2005:	Study Chemistry at Radboud University Nijmegen
Major thesis	Solid state chemistry (Prof. E. Vlieg)
Subject	Epitaxial vapor growth crystallization of anthraquinone on inorganic substrates
Minor thesis	Organic chemistry (Prof. F.P.J.T. Rutjes)
Subject	A chemoenzymatic route towards febrifugine and epiquinamide
2005-2009:	PhD research at Radboud University Nijmegen at the department of Solid state chemistry
Subject	Single chirality through crystal grinding
Supervisor	Prof. dr. E. Vlieg

List of Publications

W. L. Noorduin, A. A. C. Bode, M. van der Meijden, H. Meekes, A. F. van Etteger, W. J. P. van Enckevort, P. C. M. Christianen, B. Kaptein, R. M. Kellogg, T. Rasing, E. Vlieg
Complete Chiral Symmetry Breaking of an Amino Acid Derivative Directed by Circularly Polarized Light
Nature Chemistry **2009,** in press.

W. L. Noorduin, E. Vlieg, R. M. Kellogg, B. Kaptein
From Ostwald Ripening to Single Chirality
Angewandte Chemie International Edition, **2009,** *48*, in press.

W. L. Noorduin, P. van der Asdonk, H. Meekes, W. J. P. van Enckevort, B. Kaptein, M. Leeman, R. M. Kellogg, E. Vlieg
Complete Chiral Resolution Using Additive-Induced Crystal Size Bifurcation During Grinding
Angewandte Chemie International Edition, **2009,** *48*, 3278-3280.

W. L. Noorduin, B. Kaptein, H. Meekes, W. J. P. van Enckevort, R. M. Kellogg, E. Vlieg
Fast Attrition-Enhanced Deracemization of Naproxen by a Gradual In Situ Feed
Angewandte Chemie International Edition, **2009,** *48,* 4581-4583.

B. Kaptein, W. L. Noorduin, E. Vlieg
Method for the Synthesis of Chiral Alpha-Aryl Propionic Acid Derivatives
EP Patent Application, filed February 6, **2009** (DSM depot # 27115EPO).

B. Kaptein, W. L. Noorduin, H. Meekes, W. J. P. van Enckevort, R. M. Kellogg, E. Vlieg
Attrition Enhanced Deracemization of a Natural Amino Acid Derivative That Forms an Epitaxial Racemic Conglomerate
Angewandte Chemie International Edition, **2008,** *47*, 7226-7229.

W. L. Noorduin, H. Meekes, W. J. P. van Enckevort, A. Millemaggi, M. Leeman, B. Kaptein, R. M. Kellogg, E. Vlieg
Complete Deracemization by Attrition-Enhanced Ostwald Ripening Elucidated
Angewandte Chemie International Edition, **2008**, *47,* 6445-6447.

W. L. Noorduin, H. Meekes, A. A. C. Bode, W. J. P. van Enckevort, B. Kaptein, R. M. Kellogg, E. Vlieg
Explanation for the Emergence of a Single Chiral Solid State during Attrition-Enhanced Ostwald Ripening: Survival of the Fittest
Crystal Growth & Design, **2008**, *8,* 1675-1681.

W. L. Noorduin, T. Izumi, A. Millemaggi, M. Leeman, H. Meekes, W. J. P. van Enckevort, R. M. Kellogg, B. Kaptein, E. Vlieg, D. G. Blackmond
Emergence of a Single Solid Chiral State from a Nearly Racemic Amino Acid Derivative
Journal of the American Chemical Society, **2008,** *130,*1158-1159.

M. A. Wijdeven, R. Wijdmans, R. J. F. van den Berg, W. L. Noorduin, H. E. Schoemaker, T. Sonke, F. L. van Delft, R. H. Blaauw, R. W. Fitch, T. F. Spande, J. W. Daly, F. P. J. T. Rutjes
N,N-Acetals as N-Acyliminium Ion Precursors: Synthesis and Absolute Stereochemistry of Epiquinamide
Organic letters, **2008**, *10,* 4001-4003.